UNIVERSITÀ
DI PAVIA

PhD IN BIOMEDICAL SCIENCES

DEPARTMENT OF BRAIN AND BEHAVIORAL SCIENCES

UNIT OF NEUROPHYSIOLOGY

DEVELOPMENT OF AN EXPERIMENTAL WOUND MODEL ON *EX-VIVO* HUMAN SKIN CULTURE WITH EXTENDED VIABILITY

PhD Supervisor: Prof. Giovanni Nicoletti

PhD Co-Supervisor: Prof. Gianluigi Marseglia

PhD dissertation of
Dr. Marco Saler

a.y. 2024 - 2025

Summary

CHAPTER 1

INTRODUCTION

1.1. The historical evolution of animal experimentation concept

The concept of experimentation in the biomedical sector was born in ancient history. Aristotele, Erasistrato (4th century B.C.) and Galeno (2th century A.C) were the first to conduct *in-vivo* experiments on animals to increase knowledge of anatomy, physiology, pathology and pharmacology. In the 12th century, Zuhr, an Arab doctor, introduced animal experimentation as a method of testing surgical procedures before applying them to humans. However, the first ethical debates on animal experimentation began in the 17th century: public opinion was divided between those against and those favourable. The first said that the benefit to the human species didn't justify the suffering of animals. Furthermore, the results of the experiments could not be applied to humans due to the differences with animal species. Instead, those favourable said that animal experiments were important for the progression of biological and medical knowledge (Hajar R., 2011). Although the debate on the use of animals continued, the failure of some drugs in the 1950s favored a significant increase in the pharmacological trials on animals in many countries.

However, the progress of knowledge and the development of cell and tissue cultures, as an alternative to the use of animals, has favored the development of regulations for their protection. In particular, the principles proposed by Russel and Burch in 1959 were of fundamental importance for the approval of the European directive on the protection of animals used for scientific purposes (Directive 2010/63/EU). This directive has been accepted and adopted by various Member States. Italy has included it in its legislation through the Legislative Decree 26/2014 but providing for more restrictive integrations (Barletta M., 2021).

In the book “The Principles of Human Experimental Technique”, Russell and Burch (Figure 1) proposed a new research method with the aim of improving the treatment of laboratory animals and at the same time promoting the quality of tests and research.
In particular, they identified three key words:

- *replacement*: that is to say the substitution of animals in the experimental phase with alternative methods (*in-vitro* models, *ex-vivo* models, computerized models) of comparable validity;
- *reduction:* meaning the development of an experimental design using the smallest possible number of animals but aiming to maximize the quantity and quality of data;
- *refinement:* that is to say the improvement of experimental procedures to minimize stress and suffering.

These key words called 3R were enunciated to help scientists in their research but also to promote the development of new methods and tools (Tannenbaum J., Taylor Bennett B., 2015).

Figure 1 - William Russell & Rex Burch (https://en.3rcenter.dk/)

The promotion of the principles of replacement, reduction and refinement led to the creation, in December 2017, of the Interuniversity Centre for the Promotion of the Principles of the 3Rs in Teaching and Research. This centre, together with other European 3R centres, institutions and foundations, is part of the EU3RNet.

The main objectives of the 3R Center are:

- to promote courses on the principles of the 3Rs;
- to promote the scientific and cultural debate on the 3Rs;
- to promote, develop and coordinate studies and researches in collaboration with universities, research centers, public and private departments both at national and at international scope;
- to increase and promote the development and use of new methods in basic and applied research;
- to cooperate with associations responsible for animal welfare.

1.2. Skin Anatomy

1.2.1. Epidermidis

The skin is the largest organ of the body, measuring up to 2 m^2 and it's the first physical barrier that divides the body from the external environment. Furthermore, the skin weighs 4-5 kg in an average adult (about 12-15% of body weight). Other functions performed are: protection from ultraviolet (UV) lights, anti-microbial action, protection from mechanical, chemical and physical trauma, vitamin D synthesis, immune activity through Langerhans cells and antigen-presenting cells (at the epidermal layer), secretory function and sensory organ (Napolitano et al., 2023; Lotfollahi Z., 2024). Finally, the skin is responsible for thermoregulation processes through vasoconstriction and vasodilation mechanisms, sweating or through the erection of the hair follicle muscle. For these reasons, due to its continuous interactions with the endocrine, nervous and immune systems, the skin forms a "neuro-immuno-cutaneous-endocrine" network (Lebonvallet et al., 2010).

Anatomically, the skin is composed of 3 layers: the epidermis, the dermis and the hypodermis or subcutaneous tissue (Figure 2). Each tissue is characterised by a specific embryonic lineage, which determines different structural and cellular compositions. In particular, the epidermis derives from the ectoderm, while the dermis and hypodermis derive from the mesoderm, with the exception of the face and neck, which have a neuroectodermal origin (neural crests). The epidermis is mainly composed of keratinocytes, while a small part is represented by dendritic cells, for example: melanocytes, Langerhans cells and Merkel cells. Instead, in dermis the cellular population is represented by fibroblasts; however, in this tissue the collagen fibers, the elastic fibers and the extracellular matrix are greater than in the cellular one.

Finally, the hypodermis represents the deepest layer and is mainly formed by adipose cells and a connective tissue network (Gartner et al., 2006, Gilaberte et al., 2016).

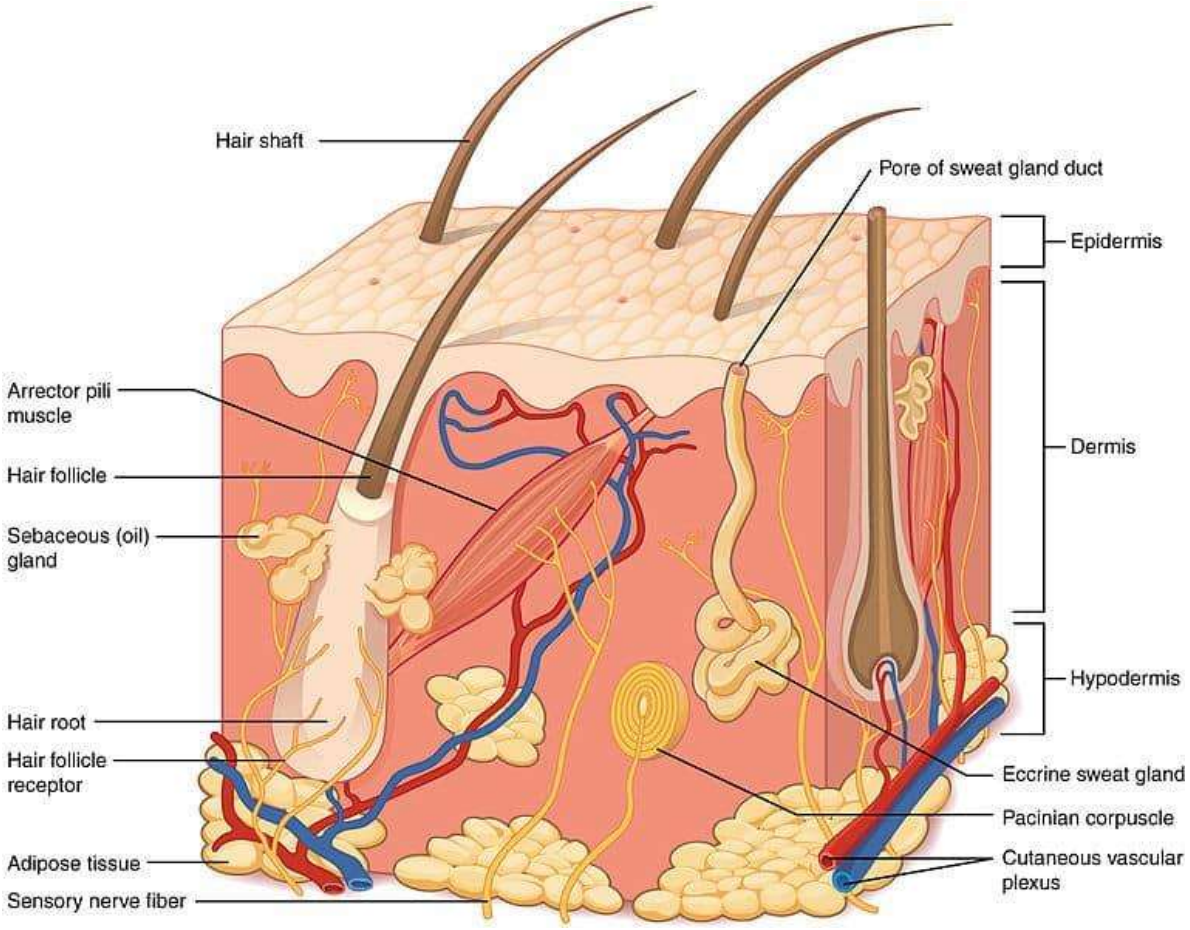

Figure 2 – Layers of skin (Biga et al., 2019)

The epidermis is a stratified keratinized squamous epithelial tissue and its thickness varies depending on the region of the body. The epidermis is composed of five layers of cells: the basal layer (*Stratum basale*), the spinous layer (*Stratum spinosum*), the granular layer (*Stratum granulusum*), the lucid layer (*Stratum lucidum*) and the corneum layer (*Stratum corneum*). However, the stratum lucidum is exclusive to the palm of the hand and to the sole of the foot (Figure 3).

A main characteristic of the epidermis is its capacity of self-renewal that allows the migration of keratinocytes from the basal layer to the corneum layer (in about three weeks) and at the same time a morphological and functional differentiation.

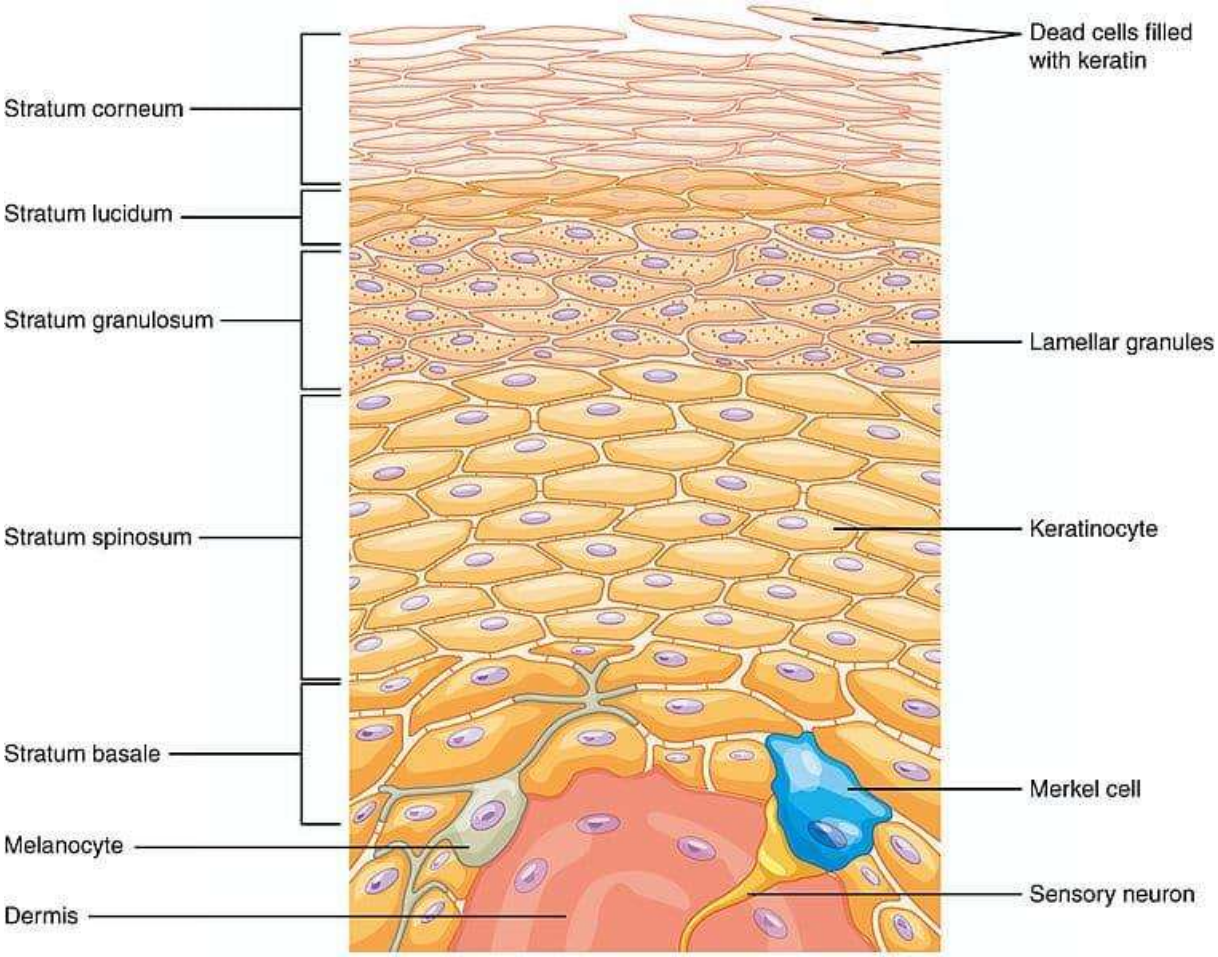

Figure 3 – Skin histology (Lotfollahi, 2024)

In the *basal layer*, keratinocytes have a cubic shape, are distributed in a single layer and anchored by hemidesmosomes to the basal membrane that regulates metabolic exchanges also. Keratinocytes are undifferentiated cells (unipotent stem cells) with an intense mitotic but asymmetric activity; in fact at the end of mitosis a cell will maintain the characteristics of stemness, while the other cell will begin a process of migration and differentiation towards the superficial layers. In addition, in the basal layer there are melanocytes that synthesize melanin, a brown pigment that is accumulated in

vesicles and transferred to keratinocytes. Melanin is responsible for the brown colour of healthy skin and provides for ultraviolet light protection.

In the *spinous layer*, keratinocytes have a polyhedral shape, are organized in 8-10 layers of cells and decrease with age. These cells are linked to adjacent cells through desmosomes. Furthermore, among the keratinocytes there are Langerhans cells and Merkel cells. Langerhans cells are able to phagocytose any pathogens and through the presentation of the antigen at the surface level interact directly with the immune system (Neagu et al., 2022). Instead, Merkel cells are mechanoreceptors, which are sensitive to light pressure stimuli and interact with the afferent somatosensory nerve fibers (Abraham et al., 2019).

In the *granular layer*, keratinocytes have a spindle and elongated shape, and are organized in 3-5 layers of cells. These cells are rich in keratohyaline granules, that contain keratin precursors. Inside these structures there are also glycolipids that bind cells, creating a hydrophobic barrier.

In the *stratum lucidum*, keratinocytes have a flat shape, are organized in 2-3 layers, and filled with keratin. This layer is only present in thick skin, such as the palm of the hand, the sole of the foot, and the fingerprints.

In the *stratum corneum*, keratinocytes have a flat shape, without a nucleus and organized in 25-30 layers of cells. Keratin and other structural proteins are linked and form a rigid and waterproof layer. Furthermore, these cells are surrounded by an acid hydrolipidic film (pH 5.6) with a bactericidal function. This substance derives from the sebum produced by the sebaceous glands attached to the hair follicles. However, the acidic nature of this substance derives from the metabolism of saprophytic bacteria and in particular of *Staphilococcus epidermidis* and *Propionibacterium acnes*, present

in the infundibulum of the hair follicle. This layer is continuously renewing and the entire layer is replaced by new keratinocytes in four weeks. The turnover rate of keratinocytes is reduced but thickness increases in older skin. Some studies suggest that the thickness increasing is a response by body to protect itself from ultraviolet light (Bonham et al., 2020).

1.2.2. Basament membrane, Dermis and Hypodermis

The basement membrane is located underneath the basal layer and separates the epidermis from the dermis. The molecules present in the basement membrane are organized in tight junctions allowing the adhesion of these two tissues. However, in old skin the molecules present in the basement membrane are modified, resulting in a lower adhesiveness between the dermis and the epidermis.

The dermis (Figure 2) is a connective tissue of mesenchymal origin and separated from epidermidis by the basament membrane. However it is highly vascularized, innervated and characterized by a cellular component, fibroblasts and an extracellular matrix. The dermis is organized in papillary and reticular layers, which are structurally different.

The papillary dermis is located near the basement membrane and is 300-400 microns thick, although its thickness decreases with aging (Mine et al., 2008). This region is characterized by the presence of dermal papillae, between which the epidermal ridges sink into the dermis. These structures are rich in nerve endings and microvascular vessels, which are essential for the capture of extracorporeal stimuli (for example, changes in pressure and temperature) and for the oxygen and nutrients diffusion to the avascular epithelial tissue. Compared to the reticular dermis, the papillary dermis is thinner and composed of loose connective tissue characterized by type I collagen

fibers, thin elastic fibers, proteoglycans, and a high presence of fibroblasts and lymphoplasma cells (Smith et al., 2015).

The reticular dermis is separated from the papillary dermis by a vascular plexus, and is composed of dense fibrous connective tissue characterized by type III collagen fibers. These fibers are thick, give strength, and are oriented parallel to the skin surface. Furthermore, the presence of elastic fibers confers elasticity to the tissue.

As previously described, with aging, the papillary dermis becomes progressively thinner and is gradually replaced by the reticular dermis (Napolitano et al., 2023).

Fibroblasts have a mesenchymal origin and they are the most represented cell type in connective tissue. These cells have an elongated spindle or stellate shape with a multitude of cytoplasmic projections. At the ultrastructural level the fibroblast's cytoplasm has an abundance of rough endoplasmic reticulum and a large Golgi apparatus. These cells produce: collagen type I and III, proteoglycans, fibronectin, laminins, glycosaminoglycans (GAG), metalloproteinases and prostaglandins. The most important GAG is hyaluronic acid, a macromolecule formed by alternating equimolecular residues of acid D-glucuronic and N-acetyl-glucosamine. This macromolecule is very polar and therefore retains large quantities of water, promoting an increase in the viscosity of the extracellular matrix, performing a scavenger function (Chunlin et al, 2011) and promoting the wound healing process. In homeostatic conditions, fibroblasts are quiescent cells, however, interaction with the extracellular matrix can promote the activation or reorganization of the matrix itself. Matrix reorganization occurs through enzymes, produced by fibroblasts, which are activated and regulated by inflammatory cytochemistry and growth factors, such as: *transcription growth factor-alpha* and *beta* (TGF-α and TGF-β), *platelet-derived growth factor* (PDGF), *granulocyte-macrophage colony-stimulating factor* (GM-CSF), *epidermal*

growth factor (EGF), and *tumor necrosis factor* (TNF) (Tripoli et al., 2016; desJardins-Park et al., 2018).

These cells synthesize the extracellula matrix, while the metalloproteinases influence its remodeling. Furthermore, some markers, such as pan-fibroblast CD90, PDGFR-alpha and beta, small proteoglycans that influence collagen fiber assembly, have allowed us to characterize different subpopulations of fibroblasts. However, they are a heterogeneous population, and their specificity is determined by their localization within the dermal layers. In the papillary layer, fibroblasts show greater enzymatic activity than in the reticular layer (Harper et al., 1979). A first study conducted by Tabin et al. (2018) highlighted the presence of two subpopulations positive for SFRP2/DPP4 and FMO1/LSP1. In particular, SFRP2+ cells were smaller, elongated, and located between collagen fibers; whereas FMO1+ cells were larger and distributed in the interstitial space and perivascular areas.

A second study conducted by Korosec et al. (2019) allowed the differentiation of papillary and reticular fibroblasts using other markers. Papillary fibroblasts were negative for CD90 and positive for CD26, PDPN and NTN1, they did not differentiate into adipocytes, and showed a high replication rate; while reticular fibroblasts were positive for CD90, ACTA2, COLL11A1, PPARgamma, CNN1 and CD36, and they differentiated into adipocytes, but their replication rate was lower (Figure 4).

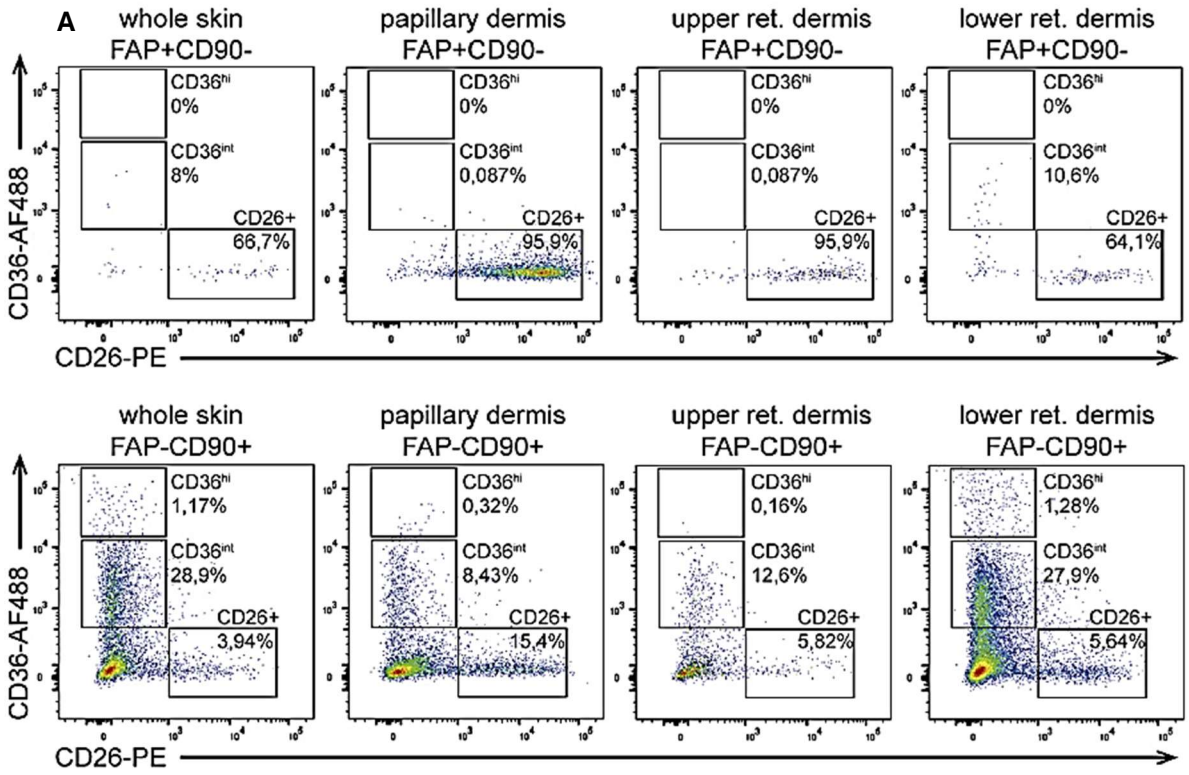
A
whole skin
FAP+CD90-
papillary dermis
FAP+CD90-
upper ret. dermis
FAP+CD90-
lower ret. dermis
FAP+CD90-
CD36hi
0%
CD36int
8%
CD26+
66,7%
CD36hi
0%
CD36int
0,087%
CD26+
95,9%
CD36hi
0%
CD36int
0,087%
CD26+
95,9%
CD36hi
0%
CD36int
10,6%
CD26+
64,1%
CD36-AF488
CD26-PE
whole skin
FAP-CD90+
papillary dermis
FAP-CD90+
upper ret. dermis
FAP-CD90+
lower ret. dermis
FAP-CD90+
CD36hi
1,17%
CD36int
28,9%
CD26+
3,94%
CD36hi
0,32%
CD36int
8,43%
CD26+
15,4%
CD36hi
0,16%
CD36int
12,6%
CD26+
5,82%
CD36hi
1,28%
CD36int
27,9%
CD26+
5,64%
CD36-AF488
CD26-PE

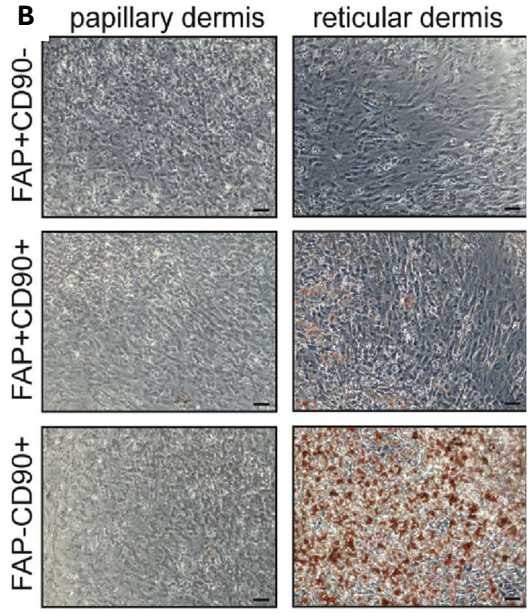
B
papillary dermis
reticular dermis
FAP+CD90-
FAP+CD90+
FAP-CD90+

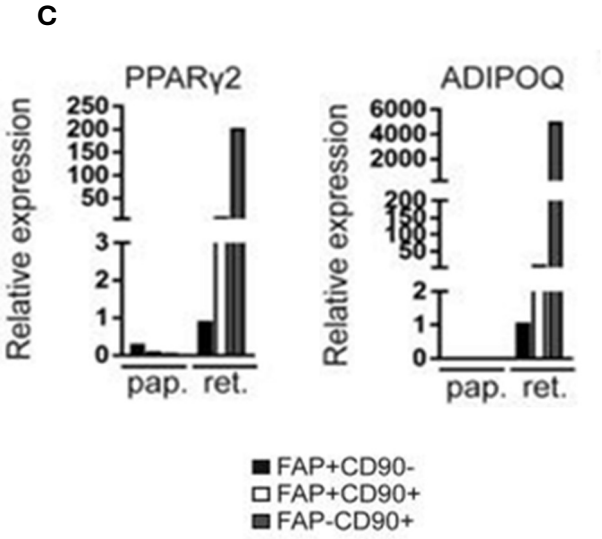
C
PPARγ2
ADIPOQ
Relative expression
250
200
150
100
50
3
2
1
0
6000
4000
2000
200
150
100
50
2
1
0
pap.
ret.
FAP+CD90-
FAP+CD90+
FAP-CD90+

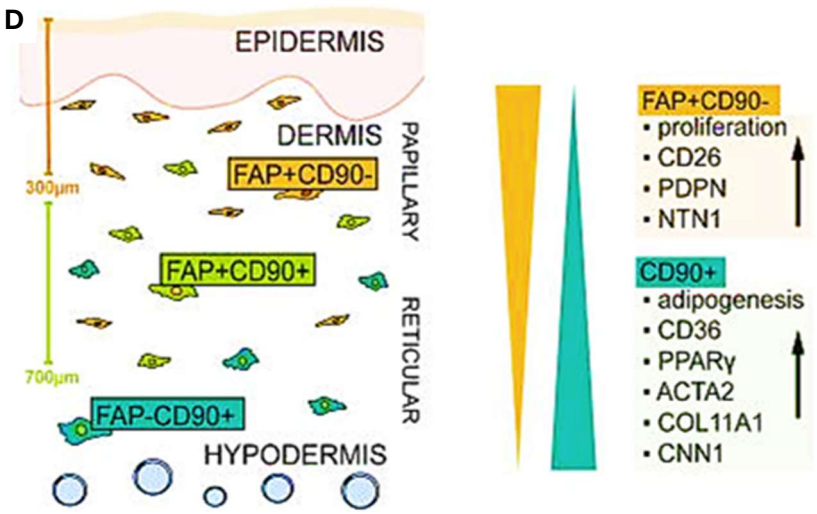

Figure 4 - Dermal cytology. (A) FACS plots showing the expression of surface antigens in fibroblast subpopulations of the skin, papillary dermis, upper reticular dermis, and lower reticular dermis. (B) Microscopic evaluation of intracellular lipid droplets by Oil Red O staining in fibroblasts isolated from the papillary and reticular dermis (scale bars: 500 µm). (C) Plots showing gene expression in fibroblast subpopulations isolated from the papillary and reticular dermis. Values normalized to the FAP+CD90- subset obtained from the reticular dermis. (D) Distribution and expression patterns of fibroblast subpopulations in the papillary and reticular dermis. Pap., papillary; ret., reticular. (Edited imagines - Korosec et al., 2019)

The hypodermis is composed mainly of adipose tissue, but also contains loose and areolar connective tissue with good vascularization. Its function is to cushion significant pressure stimuli and insulation from extreme temperatures; however, in old age the lipid quantity decreases and therefore the cushioning function decreases (Biga et al., 2019) (Figure 2).

1.3. Wound healing process

As described in previous chapters, the skin is the organ with the largest surface area and it is subject to mechanical damage, infections, ultraviolet radiation and high temperatures. These factors make the skin highly susceptible to homeostatic alterations, with a consequent impact on individuals but also on healthcare costs.

The skin regeneration process, after an injury, is inserted in the macro-area of tissue regeneration. However, the capacity for tissue regeneration is inversely proportional to the evolutionary level of the species. In mammals and particularly in humans, this regenerative capacity is almost completely absent and the loss of tissue is usually compensated by a newly formed paraphysiological tissue, called scar, which has a filling function.

Our organism hosts many processes, but the regeneration one is the most complex. In fact, after an injury, numerous intra- and intercellular biochemical pathways acting together to restore tissue integrity and homeostasis are activated. This process involves different cell types, the coagulation cascade and inflammatory pathways. The cellular elements present in greater quantities are immune cells, such as neutrophils, monocytes, macrophages, lymphocytes and dendritic cells but also endothelial cells, fibroblasts and keratinocytes. These cells undergo a gene expression modification close to the injury site that will favor the activation of proliferation, differentiation and/or migration processes and subsequently gene silencing (Pastar et al., 2014; Gurtner et al., 2018).

In summary, six phases can be identified in this complex process: hemostasis, inflammation, angiogenesis, growth, re-epithelialisation and remodelling.

Phase I: hemostasis

Hemostasis is the first stage and occurs in three steps: vasoconstriction, primary and then secondary hemostasis. Following skin injury resulting in microcirculatory haemorrhage, blood vessels rapidly undergo vasoconstriction to reduce bleeding. This process occurs with the contraction of vascular smooth muscle induced by endothelin and prostaglandins, released by damaged endothelial tissue, but also by adrenaline, noradrenaline and catecholamines present in the circulation. In addition, smooth muscle contraction is also promoted by the release of *platelet derived growth factor* (PDGF). The vasoconstriction process is temporary because hypoxia and acidosis in the wound cause passive relaxation of the muscular layer (Godo et al., 2017). However, several molecules, such as bradykinin, fibrinopeptide, serotonin and thromboxane A_2, which result from the activation of the coagulation cascade, resolve the haemorrhagic process (Strecker McGraw et al., 2007) (Figure 5).

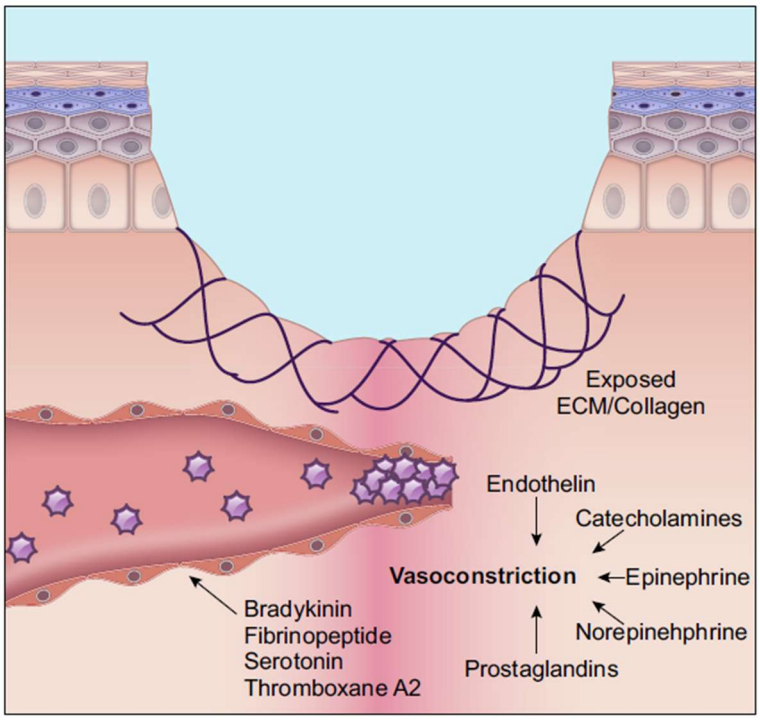

Figure 5 - Vasoconstriction Mechanism: (Rodrigues et al., 2019)

The injury to microcirculation vessels exposes the subendothelial matrix to platelet surface receptors which, through signal transduction, activate integrin, increasing the adhesion processes between platelets and the extracellular matrix (Pradhan et al., 2017). *Integrin αIIbβ3* promotes platelet adhesion to fibrinogen, fibronectin and von Willebrand factor (vWF), while *integrin α2β1* promotes adhesion to collagen fibres. Subsequently, the activation of actin filaments in the platelet cytoplasm causes a morphological change from a discoidal to a spherical shape. The activated platelet shows a large surface area due to the fusion of intracellular granules to the plasma membrane, whose secretion is essential for haemostatic processes (Golebiewska et al., 2015). In addition, glycoprotein Ib-IX-V and glycoprotein VI promote platelet aggregation processes by binding to vWF and collagen in the subendothelial matrix. Finally, the presence of pseudopods and the contraction of actin filaments promote adhesion to the cell matrix and the formation of the platelet plug (Sorrentino et al., 2015) (Figure 6).

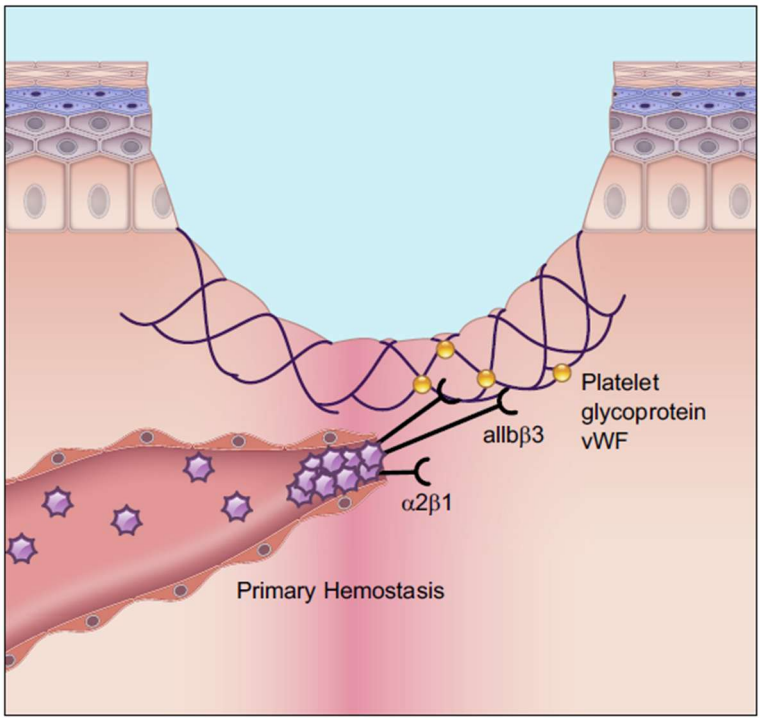

Figure 6 - Primary hemostais (Rodrigues et al., 2019)

The activation of platelets cascade through the intrinsic and extrinsic pathways determines the activation of factor X, which converts prothrombin into thrombin. Subsequently, thrombin converts fibrinogen into fibrin, and interaction with factor XIII promotes the formation of cross-links between fibrin molecules. This interaction forms the secondary haemostatic plug or thrombus, which acts as a temporary matrix for the recovery process (Rodrigues et al., 2019) (Figure 7).

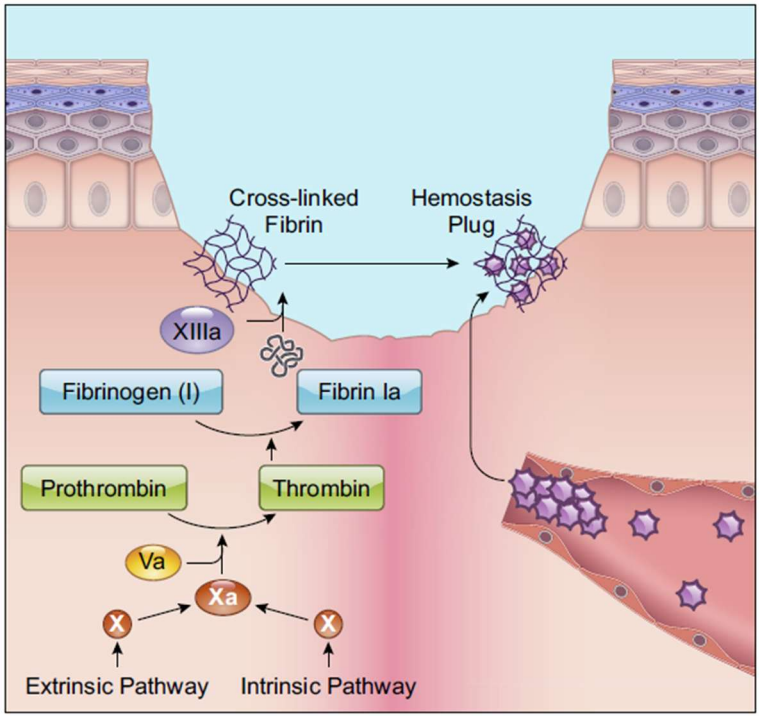

Figure 7 - Seconadry hemostais (Rodrigues et al., 2019)

Phase II: inflammation

The transcriptional processes involved in wound healing are not immediate, so independent pathways are activated in the wound to attract inflammatory cells. The main molecules with chemotactic function are: *damage-associated molecular patterns* (DAMPs), hydrogen peroxide (H_2O_2), lipid mediators, chemokines, calcium ions and reactive oxygen species (ROS) (Figure 8).

Chemokines are particularly important. These are small protein molecules (8–10 kDa) that contain cysteines. The most important are CXC chemokines, in which the two cysteines are separated by one amino acid. Furthermore, CXC chemokines can be ELR-positive if they contain glutamic acid (E), leucine (L) or arginine (R) before the first cysteine, or ELR-negative if they do not contain one of these amino acid residues. In particular, ELR-positive chemokines have a chemotactic function towards neutrophils and show angiogenic properties, while ELR-negative chemokines are chemotactic for lymphocytes. However, chemokine synthesis is promoted by the presence of bacteria, fibrin fragments or pro-inflammatory factors (e.g. TNF-alpha) in the wound and it is time- and dose-dependent (Martins-Green et al., 2013). Finally, Oskeritzian (2012) highlighted the importance of the mast cell degranulation process in the injury. In particular, the release of inflammatory cytokines, vasodilators, vascular permeability factors and proteases allows for better recruitment of immune cells.

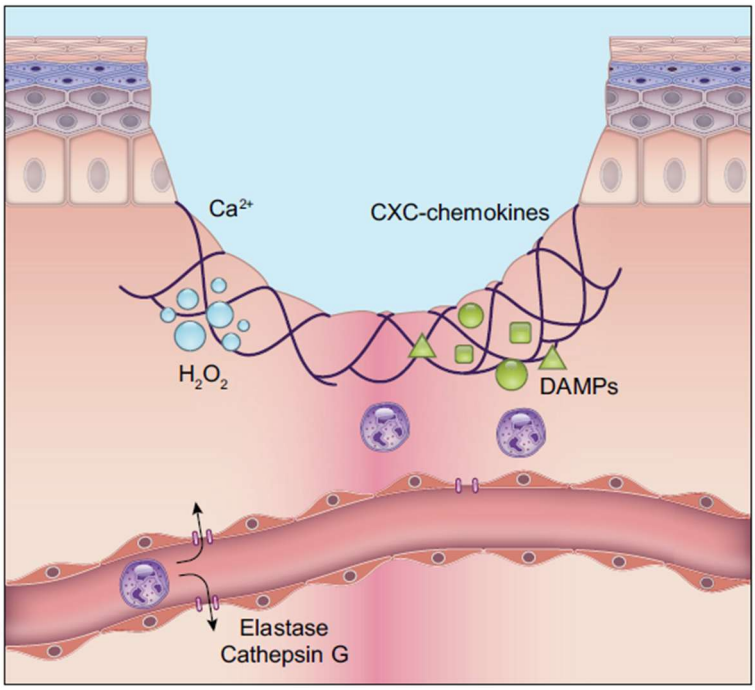

Figure 8 - Mechanisms of inflammatory cell recruitment (Rodrigues et al., 2019)

Neutrophils are the ‘first responders’ that arrive at the site of injury, attracted by the molecules mentioned in the previous paragraph, and after 24 hours they represent over 50% of the cell population. These cells release other molecules capable of amplifying the leukocyte infiltration process, and their degranulation process secretes molecules with bactericidal action. The most important molecules are myeloperoxidase, azurocidin, lysozyme, proteases and human cationic antimicrobial protein (hCAP-18), which increase the permeability of the bacterial membrane, but also lactoferrin, which limits bacterial metabolic activity (Rodrigues et al., 2019).

In addition to the degranulation process, neutrophils synthesise NETs, chromatin filaments bound to histones, cytosolic proteins and proteases, with bactericidal, virucidal and antifungal action. NETs can be released in two ways: cell lysis by myeloperoxidase (suicidal NETosis) or nuclear budding of NETs (vital NETosis) (Jorch et al., 2017) (Figure 9).

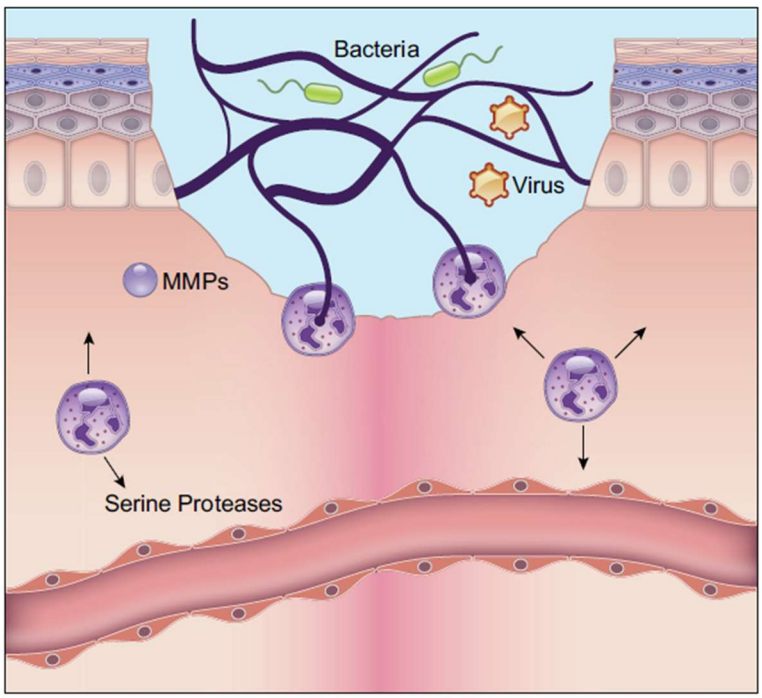

Figure 9 - Mechanism of action of neutrophils by protease and NETosis (Rodrigues et al., 2019)

Finally, neutrophils can phagocytose and destroy bacteria and cellular debris, but they are more selective than macrophages. However, the phagocytosis process leads to the formation of the phagosome and subsequently the phagolysosome through the fusion of granules containing antimicrobial agents and proteases (Borregaard et al., 1997) (Figure 10).

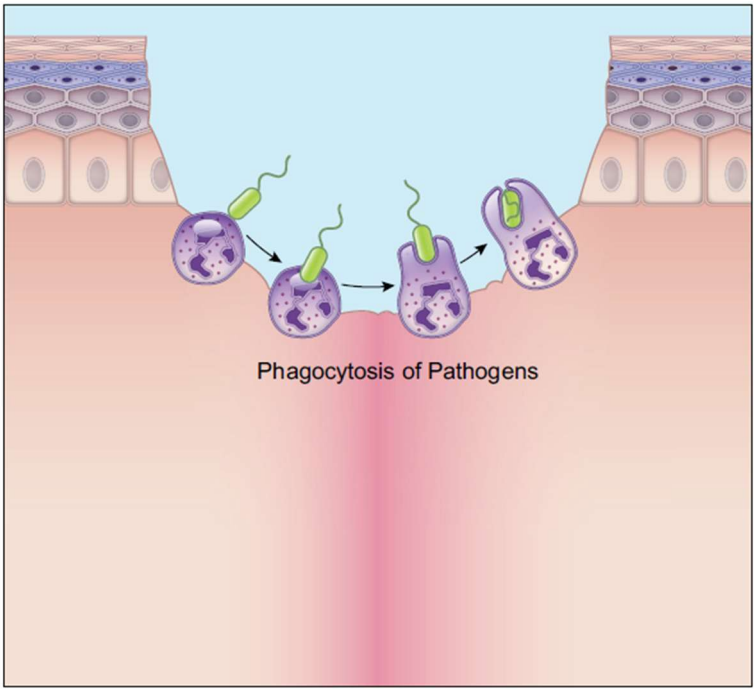

Figure 10 - Mechanism of action of neutrophils by phagocytosis (Rodrigues et al., 2019)

Macrophages are positive cells to markers CD45, CD11b and CD66 and represent another leukocyte population that increases at the wound site within 24-48 hours. The cause is due to an increase in macrophages residing in tissue but also to the recruitment of monocytes from the bone marrow. However, the presence of resident macrophages in the skin is still being studied, but it seems likely that it begins at the embryonic level, while monocyte differentiation process into macrophages in the wound has been yet demonstrated. Monocyte recruitment is due to platelet degranulation and hypoxia-inducible factors. Near the wound site, macrophages can recruit other monocytes and increase the inflammatory response through the synthesis

and release of chemoattractant molecules, such as *monocyte chemoattractant protein* (MCP-1) (Yanez et al., 2017).

In the early stages of healing, these cells, called M1, release pro-inflammatory molecules such as TNF-alpha, interleukin-6 (IL-6) and interleukin-1beta (IL-105). They phagocytose pathogens, which are killed inside the phagosomes by reactive oxygen species (ROS) (Slauch, 2011), and synthesise certain metalloproteinases (MMPs) that degrade the extracellular matrix to promote cell migration. In addition, through phagocytosis, they also remove senescent neutrophils (Figure 11).

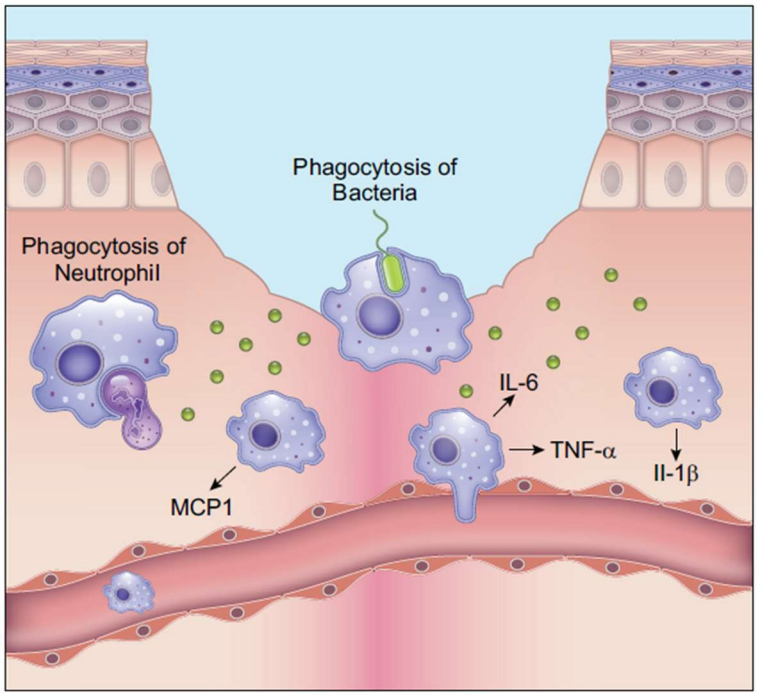

Figure 11 - Mechanism of action of macrophages M1 (Rodrigues et al., 2019)

At the end of the inflammatory process, M1 macrophages transform themselves into M2 macrophages. These cells participate in the angiogenesis process by releasing VEGF, but surface expression of the Tie2 marker, typical of endothelial cells and of some haematopoietic cells, has also been observed. In particular, M2 macrophages

participate in the anastomosis between newly formed vessels and the systemic vasculature through a process called vascular mimicry (Galli et al., 2011) (Figure 12).

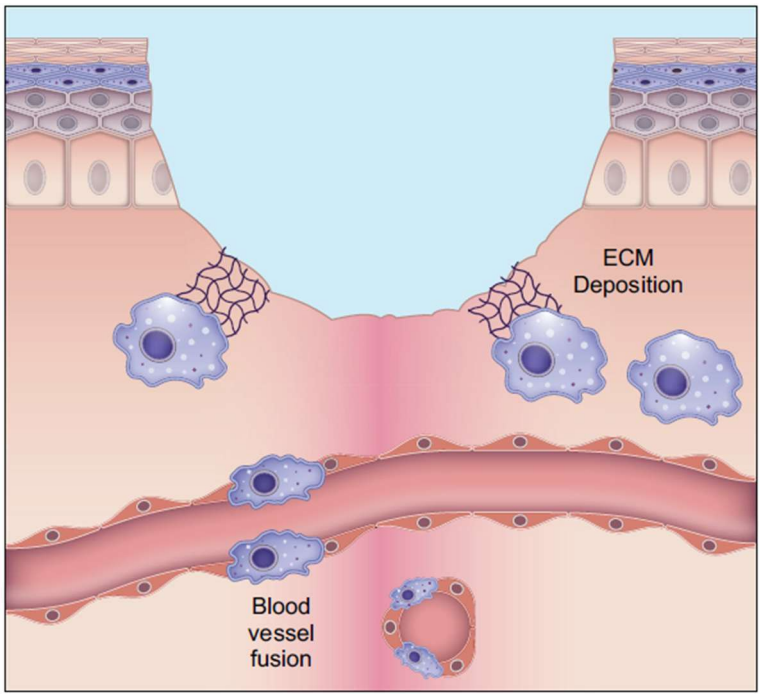

Figure 12 - Mechanism of action of macrophages M2 (Rodrigues et al., 2019)

Subsequently, during the proliferation phase, macrophages enhance the phenotypic transition of fibroblasts into myofibroblasts by promoting the synthesis of α-smooth muscle actin (Zhu et al., 2017). In addition, macrophages can transform themselves into fibrotic cells and consequently synthesise and deposit extracellular matrix (ECM) components in the wound. These macrophages are called M2a macrophages and participate in scar formation (Wong et al., 2011). However, studies have not yet demonstrated whether M2 and M2a macrophages belong to the same group or to distinct subgroups, because the process of neovascularisation and extracellular matrix (ECM) deposition in the wound is simultaneous (Rodrigues et al., 2017)

At the end of the re-epithelialisation phase, the wound undergoes a remodelling process. In this phase, macrophages regain their phagocytic characteristics. In particular, these macrophages, called M2c, release proteases that degrade the excess

extracellular matrix (ECM) that is phagocytosed. In these phases, alterations in macrophage function cause excess of extracellular matrix, deposition with fibrosis and keloids formation. (Lech et al, 2013; Sindrilaru et al., 2013).

Mast cells, another cell population present in the skin, are mainly involved in allergic reactions and helminth infections. Although their role is still being studied, researchers have observed their interaction with other cells during the wound healing process. In the early stages, mast cells produce and release antimicrobial peptides, enzymes for the degradation of the extracellular matrix (ECM) and molecules that promote vascular permeability and the influx of neutrophils (Younan et al., 2010). In addition, histamine released by mast cells promotes keratinocyte proliferation and collagen synthesis by fibroblasts (Weller et al., 2006).

The last cell population is represented by T cells, which comprise two subgroups: γδ+ T cells, also called DETCs, and αβ+ T cells (Bos et al., 1990). DETCs differentiate in the foetal thymus and then migrate and proliferate in the basal layer of the epidermis to reach homeostatic levels. At this phase, these cells are not migratory, but with their extensions, they can capture ligands derived from epidermal stress, such as infections or transformed cells and migrate to the lymph nodes present in the connective tissue, enhancing the immune response (Chodaczek et al., 2012; Xiong et al., 2007). Currently, the scientific community is paying particular attention to these cells as they are the only ones to release cytokines and growth factors that promote the re-epithelialisation process (Jameson et al., 2002).

Following epithelial tissue injury, keratinocytes release two ligands: SKINT and CD100. These molecules activate DETC cells, which change their morphology from dendritic to spheroidal to migrate towards the lymph nodes (Keyes et al., 2016). At the same

time, these cells release some growth factors, such as *keratinocyte growth factor 1* and *2* (KGF-1 and KGF-2) and *insulin-like growth factor 1* (IGF-1), which promote keratinocyte proliferation (Havran et al., 2010).

The αβ+ cells are characterised by memory and include CD4+ helper cells, CD8+ killer cells and regulatory cells (Treg). These cells are able to leave the bloodstream or reside permanently in the skin (Heath et al., 2013). The CD4+ helper cells are mainly located in the dermis while CD8+ helper cells are present in the epidermis (Zhu et al., 2013). In infections or lesions, CD8+ helper cells can migrate to the dermis and remain for a month after the skin alteration has resolved. Subsequently, these cells return to the epidermis (Gebhardt et al., 2011).

Finally, regulatory T lymphocytes (Treg) synthesise and release interleukin 10 (IL-10) and *transforming growth factor-β* (TGF-β), modulating the inflammatory response. (Heath et al., 2013).

Phase III: formation of granulation tissue

During the proliferative phase, granulation tissue forms at the site of injury, but other healing processes occur simultaneously, such as re-epithelialisation, neovascularisation and immunomodulation. This tissue consists of a cellular component and a fibrillar component. These two components are not independent, as one is essential for the other. At the end of the healing process, the granulation tissue is replaced by physiological connective tissue. Neovascularisation or angiogenesis is essential for a correct healing process and involves endothelial cells and pericytes. This process is indispensable for nutrients and oxygen supply because it promotes cell proliferation and tissue regeneration (Gurtner et al., 2008).

The skin microcirculation consists mainly of a dense network of capillaries, and endothelial cells play an important role in the formation of new vessels. However, their activation requires several elements: hypoxic environment, growth factors, proteolytic enzymes and interaction between endothelial cells and perivascular cells. The proliferation and migration of endothelial cells occurs in response to hypoxia and the release of VEGF. In addition, proteolytic enzymes partially degrade the extracellular matrix to promote the development of the new vessel. However, during angiogenesis, two subsets of endothelial cells have been identified: tip cells and stalk cells. Tip cells, with chemotactic activity, emit filopodia towards pro-angiogenic growth factors. This characteristic allows for controlled and organised vessel development (Gerhardt et al., 2003). Stalk cells replicate and simultaneously follow tip cells, maintaining the existing vascular structure. When two tip cells from different vascular structures anastomose, an endothelial tubule is formed, which carries blood flow and, consequently, an adequate supply of oxygen to the tissue (Figure 13) (Blanco et al., 2013; Rodrigues et al., 2017).

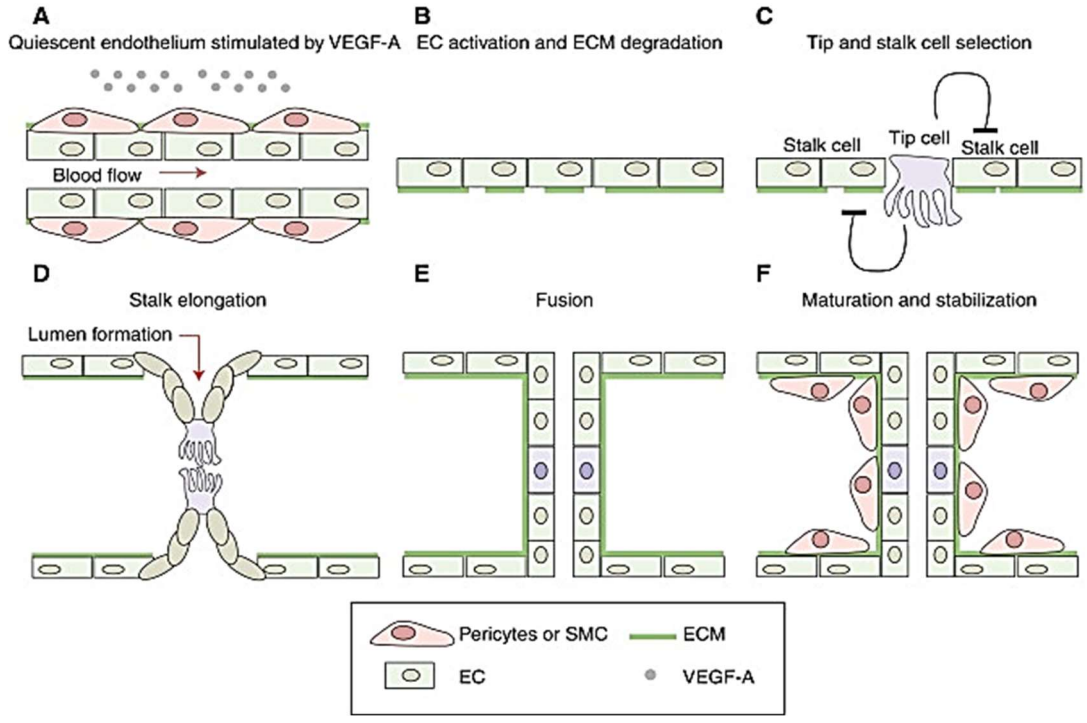

Figure 13 - Schematic model of angiogenesis (Blanco et ak., 2013)

The phenotypic acquisition of tip or stalk endothelial cells is regulated by the Notch pathway and its ligand VEGF, which is produced by subcutaneous adipocytes, macrophages and proliferating keratinocytes in the wound microenvironment (Gerhardt et al., 2003). In addition, these cells express chemokine receptors (Table 1) (Bodnar, 2015) and receptors that are activated exclusively in pathological and/or traumatic conditions (Table 2), promoting angiogenesis (Nagaoka et al., 2000).

Chemokine receptors	Ligands	Function
CCL2R	CCL2 (MCP-1)	● Stimulate angiogenic activity
CXCR4, CXCR7	CXCL12 (SDF-1)	
CCR1, CCR3, CCR5	CCL5	
CXCR1, CXCR2	CXCL1	
CXCR1, CXCR2	CXCL2	
CXCR1, CXCR2	CXCL8 (IL-8)	

Table 1 : Chemokines directly regulating angiogenesis (Edited table – Bodnar, 2015)

Other receptors	Ligands	Functions
P-selctin	P-selectin glycoprotein ligand-1 (PSGL-1)	● Promote leukocyte adhesion ● Stimulate angiogenic activity
E-selectin	E-selectin ligand-1 (ESL-1)	
ICAM1	Lymphocyte function associated antigen-1 (LFA-1)	
Integrin α4β1	Vascular cell adhesion molecule-1 (VCAM1)	

Table 2 : Ligands directly or indirectly regulating angiogenesis (Rodrigues et al., 2017)

Pericytes, discovered by Rouget and Zimmermann (19th century), are located along the axis of the blood vessel and surround the endothelial cells. For this reason, they are incorporated into the vascular basement membrane. These cells perform various

functions, such as destabilising and stabilising the microvasculature, regulating blood flow, creating a physical barrier against bacteria, and participating in the healing process (Armulik et al., 2011). However, identifying pericytes in the perivascular space is complex because other cells, such as vascular smooth muscle cells, fibroblasts, and macrophages, are also present in the same location.

Furthermore, studies have not yet been able to demonstrate whether the presence of pericytes in neovascular structures derives from the presence of pre-existing and resident pericytes or whether they are recruited from a common niche/reservoir (Crisan et al., 2008). However, researchers have hypothesised that, thanks to their proximity to blood vessels, their interactions with endothelial cells and their ability to synthesise extracellular matrices, pericytes play an important role in wound healing.

Fibroblasts are the cells that characterise connective tissues. These cells are a heterogeneous population with variable functions in the wound healing process, such as the deposition and organisation of the extracellular matrix (ECM), the secretion of growth factors and cytokines, and immunomodulation. However, thanks to scientific advances, the scientific community is gaining a detailed understanding of the cytology and cytophysiology of these cells. In particular, studies have shown that fibroblasts are composed of different cell lines, are plastic cells, and are capable of responding to signals from the epidermis or other dermal cells (Driskell et al., 2013).

Heterogeneity of fibroblasts is correlated to their spatial arrangement in the dermis and their interactions with the epithelium. Some studies have shown that dermal repair is due to reticular fibroblasts that express myofibroblastic markers (e.g. alpha-SMA). These cells synthesise large amounts of extracellular matrix that promotes healing. In contrast, fibroblasts located at the base of the hair follicle can promote or reduce follicle

regeneration (Rinkevich et al., 2015; Rognoni et al., 2016). Finally, epidermal stem cells present in the hair follicle, through a paracrine mechanism, can promote the differentiation of fibroblasts into myofibroblasts or smooth muscle cells (Fujiwara et al., 2011).

Another cell population that plays an important role in the healing process are myofibroblasts. The ability of fibroblasts to differentiate into myofibroblasts seems to be limited to some subpopulations (Fujiwara et al., 2011). However, this differentiation ability also seems to be possessed by other cells: fibrocites (Galligan et al., 2013), mesenchymal stem cells (Barbosa et al., 2010) and pericytes (Schrimpf et al., 2011). Myofibroblasts are responsible for the contraction of the wound that needs to be re-epithelialised. After interacting with fibronectin molecules present in the wound, these cells produce α-SMA protein (alpha-smooth muscle actin) (Serini et al., 1998). Subsequently, these cells also produce type I and III collagen (Tomasek et al., 2002). At this stage, the interaction between myofibroblast actin-fibronectin and myofibroblast actin-collagen fibres causes a perpendicular reorganisation of collagen fibres at the wound margins. This new arrangement allows the wound to contract (Tomasek et al., 2002) and increases the mechanical strength of the tissue (Schultz et al., 2011).

Other factors, such as hyaluronic acid, osteopontin, periostin, vitronectin, endothelin, angiotensin and MMPs, are able to promote myofibroblast differentiation (Mirastschijski et al., 2004; Simpson et al., 2009; Leask et al, 2010). However, high concentrations of inflammatory mediators, such as TNF-α, can inhibit the differentiation process and cause a delay in wound healing (Goldberg et al., 2007).

Finally, when tissue regeneration is at an advanced stage, the myofibroblasts present in the injured area die by apoptosis, while others seem to de-differentiate and reacquire

the fibroblast phenotype. However, in many types of fibrosis, such as in the process of hypertrophic scarring, myofibroblasts do not undergo apoptosis. This anomaly causes a progressive increase in the quantity of scar tissue (Van der Veer et al., 2009).

Phase IV: re-epithelialization

The process of re-epithelialisation by stem cells has been studied through lineage tracing experiments. This process has been described using two models: the *epidermal proliferative unit* (EPU) and the *interfollicular epidermis* (IFE). In the first model, the basal layer of the epidermis is formed by stem cells expressing high levels of K14 and beta-1 integrin on their surface (Mascré et al., 2012). These cells are characterised by constant asymmetric cell replication (Mackenzie, 1970).

In the second model, the basal layer of the interfollicular epithelium does not contain stem cells, but all cells can generate a differentiated or progenitor cell (Doupé et al., 2012). However, this model is influenced by two factors: the average rate of cell replication and the proportional rate of asymmetric division (Jones et al., 2008).

The presence of progenitor cells in the lesion would explain the ability of keratinocytes to organise themselves into a multi-layered epithelium and promote superficial healing processes. However, in presence of full-thickness wounds, the absence of keratinocytes in the lesion is compensated for by the recruitment of stem cells from the *interfollicular epidermis* (IFE) that migrate centripetally. These cells will subsequently begin to proliferate and differentiate (Mascré et al., 2012). This characteristic could explain the ability of keratinocytes to organise themselves into a multi-layered epithelium and heal superficial wounds.

Finally, the sebaceous glands and hair follicles show good replicative capacity, while the sweat glands remain in a state of quiescence. However, the presence of a skin

lesion can activate the stem cells of the epidermal appendages, promoting multilinear differentiation (Blanpain et al., 2014) and migration to the lesion site (Ito et al., 2005).

The stem cells present in the stem cell niche of the interfollicular epidermis respond to different microenvironment tissue molecules, such as growth factors and extracellular matrix (ECM) factors. In homeostatic conditions, these factors promote adhesion and a state of quiescence in cell replication. However, the wound exposes the basal and suprabasal keratinocytes present at the wound margins, inducing a change in the three-dimensional conformation of integrins (Ito et al., 2005). In addition, other molecules such as protein kinase C (PKC) and transcription factors promote keratinocyte motility. Cell motility is further promoted by epidermal growth factors, such as EGF and TGF-alpha, and fibroblast growth factors, such as FGF2. These protein molecules, through the signal transduction cascade, promote an increase in the expression of keratins 6, 16 and 17 responsible for cell motility. However, the expression of TNF-alpha must be finely regulated to prevent the formation of a fibrotic condition (Savagner et al., 2005; Pastar et al., 2014).

At the end of the re-epithelialisation process, fibroblasts synthesise and secrete TGF-beta, which promotes the expression of keratins K5 and K14 and a reduction in the replication rate in keratinocytes (Pastar et al., 2014).

The pilo-sebaceous unit can also participate in the re-epithelialisation process thanks to the presence of *interfollicular epithelial* (IFE) stem cells. In presence of full-thickness skin lesions, deep hair bulb stem cells, positive for the LRG marker and Gli1 transcription factor, respond to dermal stimuli, with consequent activation mechanisms to compensate for skin homeostasis alteration (Rompolas et al., 2013). The stem cells of the middle bulb, positive for CD34, Sox9 and keratin 15, are activated only during

the healing process of the *interfollicular epithelium* (IFE). Finally, LRIG1-positive cells in the upper bulb participate in the re-epithelialisation process but also in the formation of new sebaceous glands and hair follicles (Ito et al., 2005) (Figure 14).

Skin lesions have an impact on melanocytes also. These cells are present within the wound on the 4th/6th day but they are unable to produce melanin, while cells at the margins of the wound have been shown a replicative and proteosynthetic capacity. This is due to the presence and activation of the melanocortin 1 receptor (Mc1r) expressed by melanocyte stem cells (McSCs) located in the stem cell niche of the hair follicle. The activation of these cells pushes them to migrate to the injured site, where they subsequently acquire the ability to synthesise melanin (Costin et al., 2007; Rodigrues et al., 2019).

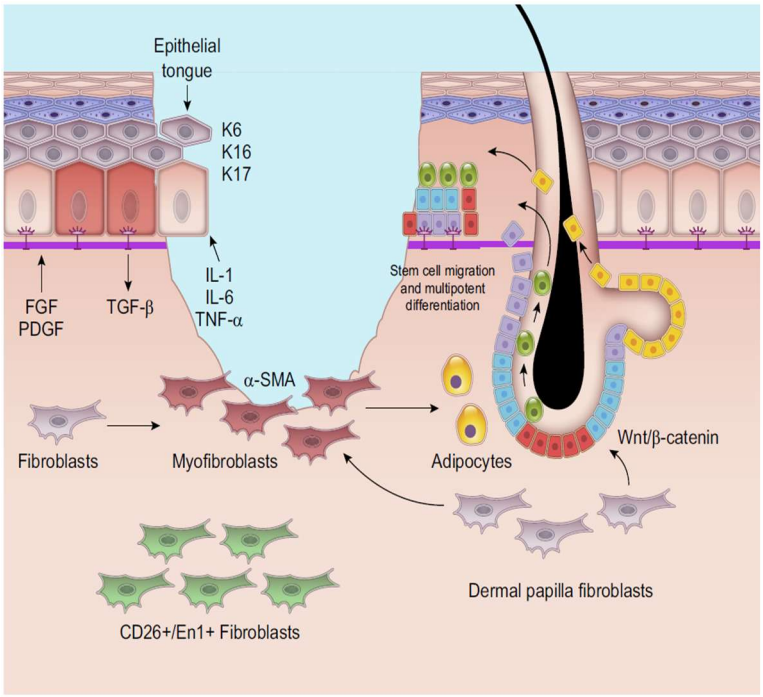

Figure 14 - Re-epithelialization and fibroblast-epidermal cell interactions during re-epithelialization (Rodrigues et al., 2019)

Phase V: remodeling wound healing

The final phase begins two to three weeks after the injury, but the timing varies. This process is called remodelling because all the mechanisms activated in the previous phases are inactivated. In particular, macrophages, isolated endothelial cells and myofibroblasts undergo apoptosis or migrate from the wound. The tissue will be characterised by few cells but with an abundant presence of type III collagen fibers. In the following months, metalloproteinases, synthesised and secreted by fibroblasts, will be responsible for the degradation of collagen III and, at the same time, its progressive replacement with more resistant collagen I. The accumulation of these fibers will activate metalloproteinase inhibitors (TIMPs) and stop the progressive degradation of collagen fibers (Visse et al., 2003; Caley et al., 2015).

1.4. Hematopoiesis

Hematopoiesis is a regulated and controlled process of proliferation, self-renewal and differentiation of Hematopoietic Stem Cells (HSCs). This process, every day, allows the constant and continuous production of 10^12 blood cells by the adult bone marrow. However, hematopoiesis is not only involved in cell turnover but also allows a rapid response to stress situations or injuries. HSCs are identifiable from the early stages of embryonic development throughout the life of the organism. In particular, at the embryonic development, hematopoiesis occurs in different anatomical sites: the yolk sac, the mesonephros gonad-aorta region, the placenta and the fetal liver. Instead, in adults, HSCs are located in the stemness niches present within the bone marrow. The stemness niche represents a dynamic microenvironment formed by: cellular component, matrix glycoproteins and 3D-space organization. The molecular interaction of these elements results in a fine regulation that has direct effects on HSCs but also physical stimuli that influence oxygen concentration, ionic concentration and temperature. However, the stemness niche is also able to respond to external events such as stimuli from the nervous system, from the metabolic activity of tissues, from paracrine and endocrine secretions (Scadden DT, Nature 2006).

The cellular component present in the stemness niche, with effects on HSCs, is formed by different cytotypes: perivascular stromal cells, endothelial cells, macrophages, orthosympathetic neurons, Schwann cells and abundant reticular cells (CAR cells), but also osteoblasts, osteoclasts and adipocytes (Mendelson A & Frenette PS, Nat Med 2014). Since the discovery of the clonal nature of murine bone marrow cells in 1963 (Becker et al.), today we know that HSCs are clonogenic cells characterized by

unlimited self-renewal and able to give rise to oligopotent progenitors that produce a progeny with specific differentiation capacities (Weissman, Cell 2000).

Hematopoiesis (Figure 15) represents a process of progressive differentiation of multipotent HSCs. The HSC can give rise to two primitive progenitor cells: the common lymphoid progenitor (CLP) and the common myeloid progenitor (CMP). These cells undergo further maturation producing progenitors for T cells and natural killer cells (TNKs), granulocytes and macrophages (GMs) or megakaryocytes (MKs) and erythroid cells (MEPs). Finally these progenitors with a higher degree of differentiation will produce monopotent cells for the genesis of B lymphocytes (BCPs), NK cells (NKPs), T lymphocytes (TCPs), granulocytes (GPs), monocytes (MPs), red blood cells (EPs) and megakaryocytes (MKs) (Kaushansky K, N Engl J Med 2006).

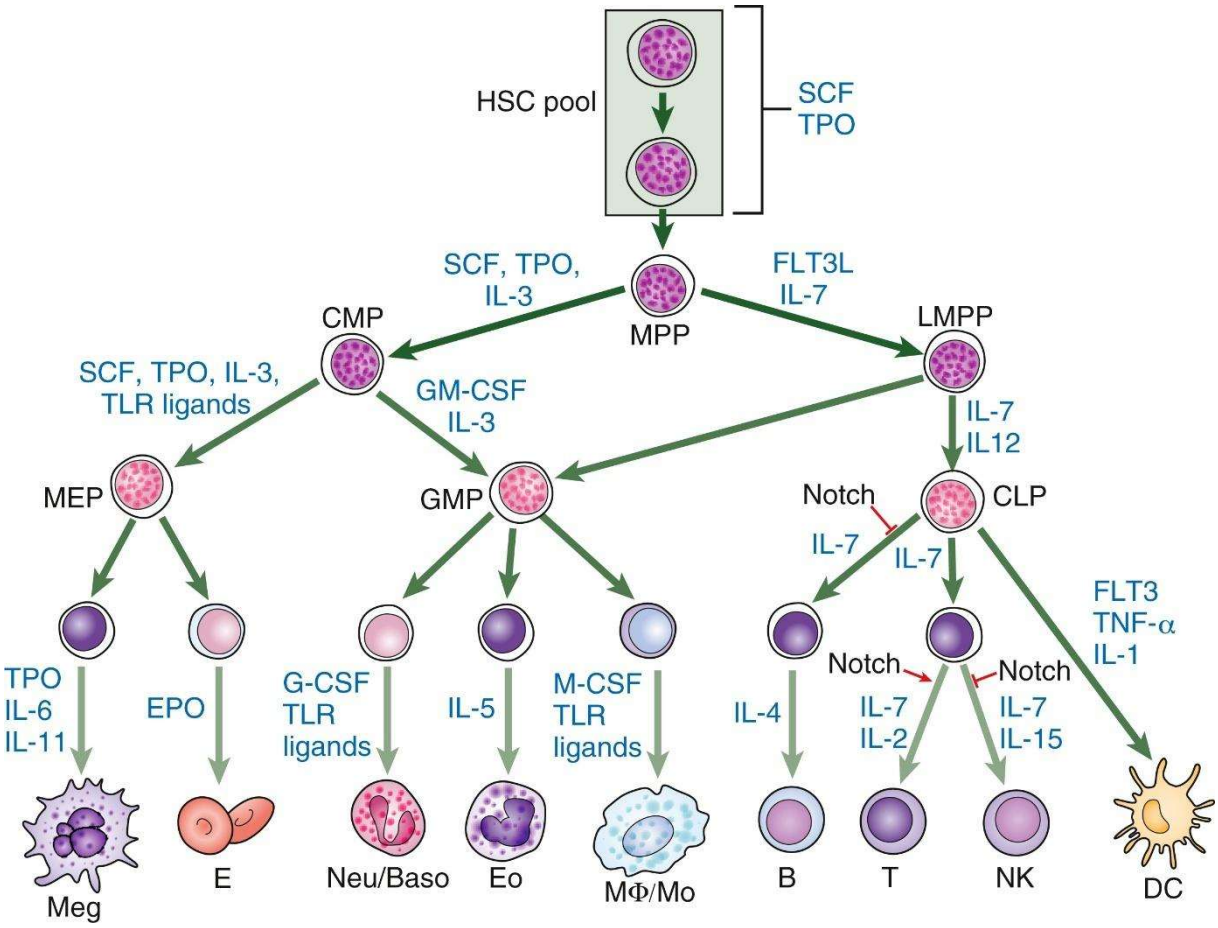

Figure 15 - Growth factors and cytokines responsible for cell survival and proliferation in hematopoietic development. HSC, hematopoietic stem cells; CMP, common myeloid progenitor; LMPP, lymphoid-primed multipotent progenitor; GMP, granulocyte-macrophage progenitor; CLP, common lymphoid progenitor; Meg, megakaryocyte; E, erythrocyte; Neu/Baso, neutrophil/basophil; Neu, neutrophil; Baso, basophil; Eo, eosinophil; MΦ/Mo, macrophage/monocyte; B, B cell; T, T cell; NK, natural killer cell; DC, dendritic cell; FLT, TATA-binding protein-like factor; SCF, stem cell factor; TLR, toll-like receptor; IL, interleukin TPO, thrombopoietin; EPO, erythropoietin; G-CSF, granulocyte colony-stimulating factor; GM-CSF, granulocyte-macrophage colony-stimulating; TNF, tumor necrosis factor. (https://oncohemakey.com)

1.4.1. Cytokines and interleukins in hematopoiesis

The regulatory system of hematopoiesis, in physiological and emergency conditions (non-physiological stimuli), is characterized by the interaction between cytokines, which can have a pleiotropic effect or act on cells of the same lineage, and different receptors, for example: tyrosine kinase receptors (RTKs), receptors for tumor growth factor-beta (TGF-ß), receptors for tumor necrosis factor (TNF-α) and G protein-coupled receptors (GPCRs). The ligand-receptor interaction activates signal transduction at the intracellular level with the aim of modulating gene expression that determines an exclusive and irreversible differentiation of a progenitor towards a specific hematopoietic lineage (Robb, 2007; Endele et al, 2014).

However, the causes that influence the differentiation process are still being studied but, at the moment, two hypotheses have been proposed:

1) factors action inside the cell (for example transcriptional factors);
2) cytokines action that induces a particular differentiation through a lineage-specific transcriptional program.

In particular, in the second case, two models have been proposed:

a) “instructional”, in which extrinsic factors could directly influence lineage choice (Figure 16);
b) “permissive/selective”, in which extrinsic factors allow viability and proliferation of cells while lineage choice is independent of this process (Figure 16) (Endele et al, 2014).

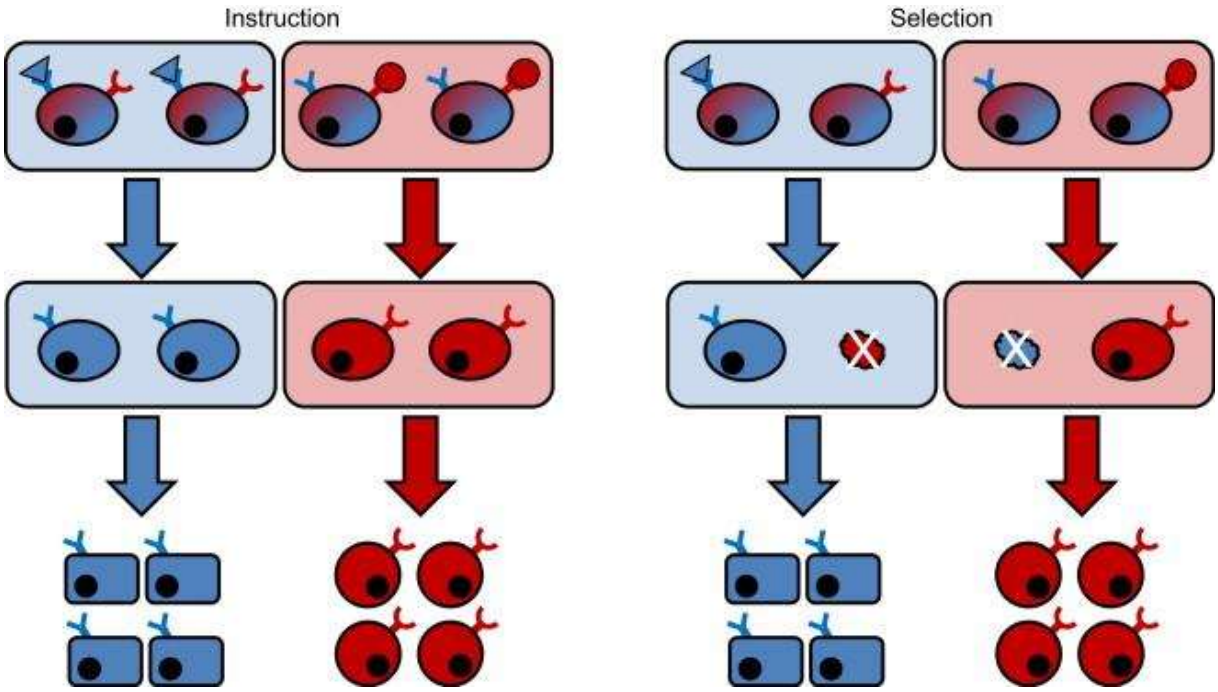

Figure 16 - The instructive versus the permissive/selective model of lineage choice (Endele et al, 2014)

The stemness niche hosts HSCs, but the progenitors of megakaryocytes (MKs) also, whose differentiation process is influenced by cytokines that have the ability to act on both cell types. In the murine model, it has been observed that the migration of megakaryocytes is influenced by CXCL-12 and by Angiopoietic 1 (ANGPT1). However, CXCL-12 acts positively on the quiescence state and on the self-renewal capacity of HSCs; while ANGPT1 as well as ANGPT2, acts in an autocrine mode stimulating the differentiation process of megakaryocytes but inducing the quiescence of HSCs (Psaila et al., J Thromb Haemost 2012; Anthony et al., Trends Immunol 2014).

1.4.2. Thrombopoietin (TPO)

Until a few years ago, the researchers said that thrombopoietin was the only cytokine necessary to megakaryocytes to maintain the number of platelets constant (Kaushansky, K, J. Clin. Invest 2005) but recent studies have shown that the action of IL-3, IL-6 and IL-11 is important for the development of megakaryocytes (Caux et al., 2022). Thrombopoietin is a polypeptide molecule of 353 amino acids, highly glycosylated and with a weight of 70 kda. In particular, the N-terminal region contains the bond domain (RDB) indispensable for interaction with its receptor and the consequent pro-proliferative effect, while the C-terminal region increases the secretion of the protein but also its half-life. The synthesis of this protein occurs mainly in the liver, but also in the kidneys and skeletal muscles. Furthermore, the concentration of thrombopoietin is inversely proportional to the number of platelets in the blood and megakaryocytes in the bone marrow. This regulation occurs with a negative feedback mechanism (Sun et al., 2024). Thrombopoietin not only acts in the proliferation and differentiation of megakaryocytes but also plays a role in hematopoietic stem cells by modulating the localization of some transcription factors, promoting their proliferation as well as differentiation. In fact, in patients affected by congenital amegakaryocytic thrombocytopenia, the deficiency of the thrombopoietin receptor is also associated with the development of an aplastic anemia characterized by a progressive decrease in the number of stem cells. This pathological condition has confirmed the effect of Thrombopoietin on HSCs.

Since the discovery in 1994 of the thrombopoietin receptor, called c-Mpl, and the subsequent advances in molecular biology, researchers have studied and identified its molecular mechanisms (Figure 17). The thrombopoietin binding to its receptor determines its homodimerization and the recruitment of other signal molecules that

activate different pathways such as PI3K, Akt, MAPK, ERK1/ERK2. Furthermore, thrombopoietin promotes the viability and proliferation of megakaryocytes by an increase to cyclin-D and Bcl-XI with antiapoptotic function and the p27 suppression, an inhibitor protein of cell cycle.

Finally, as previously highlighted, platelets express on their surface the receptor for thrombopoietin, showing an inverse proportionality between the number of platelets and the concentration of this molecule.

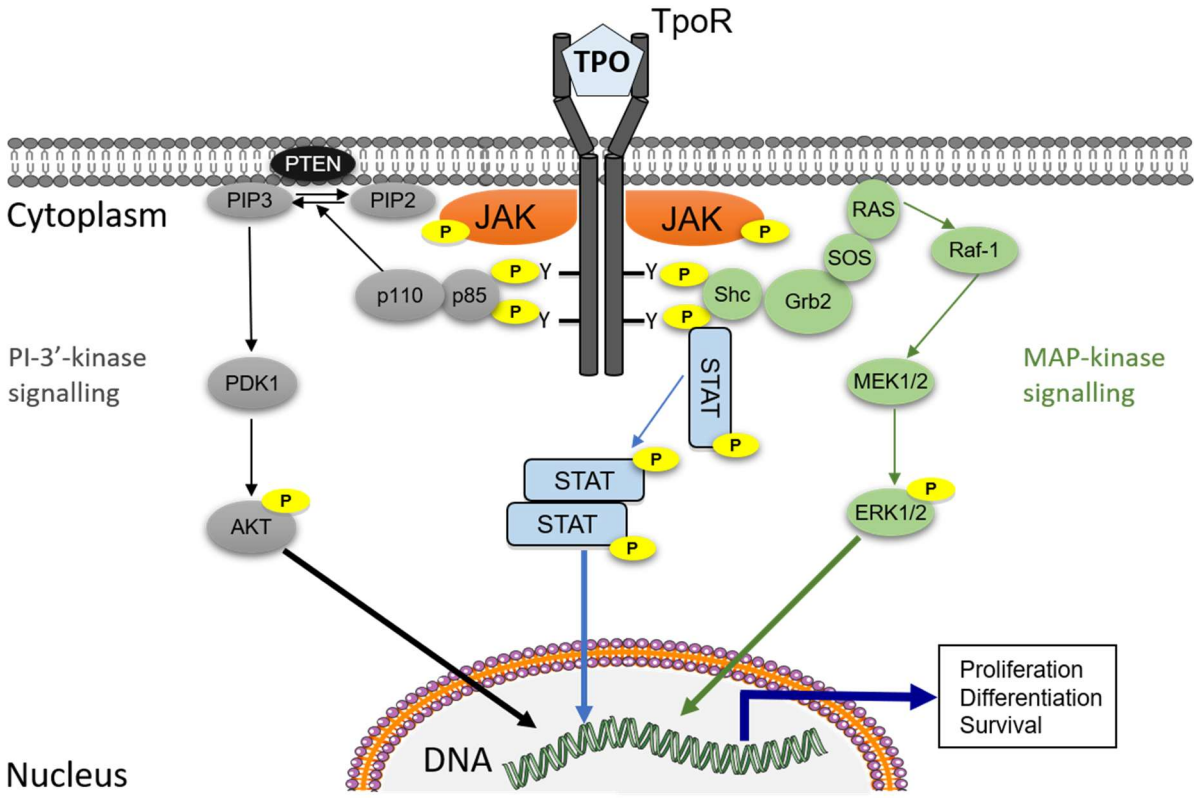

Figure 17 - c-Mpl/TPO signaling pathway (ludwig.ox.ac.uk/ - Constantinescu group)

1.5. Megakaryocytopoiesis

Megakaryocytes are 1% of the myeloid lineage and are mainly located in the bone marrow; however, they can also be found in the lung and peripheral blood (Ogawa M, Blood 1993). Megakaryocytes, erythrocytes, monocytes and granulocytes show a common precursor: the Common Myeloid Progenitor (CMP). The differentiation of CMPs gives rise to Megakaryocyte–erythroid progenitor cells (MEPs), the common progenitors for erythrocytes and megakaryocytes. These cells have a limited proliferative capacity and in the second case differentiate into promegakaryoblasts and subsequently into megakaryocytes. These cells are highly specialized and their function is to form and release platelets to maintain a constant number in the blood circulation and ensure, in case of injury to the blood vessels, the minimization of blood loss. In the human species the differentiation process time of a megakaryocyte lasts 5 days while in the rat it is 2/3 days. (Odell TT Jr & Jackson CW, Blood 1968).

Hematopoietic progenitors are positive for CD34 and CD41 but later cells committed to the megakaryocytic lineage also express CD61 and increase the expression of CD41 (Fackler MJ et al., Blood 1995).

However, CD41 and CD61 markers are receptors for several adhesion molecules, for example, fibrinogen and von Willebrand factor and although CD41 is considered a specific marker of platelets, clonogenicity studies have shown that this molecule can be considered a marker of the early phases of hematopoietic differentiation (MitjavilaGarcia MT, Development 2002). Furthermore, during the differentiation process other receptors are up-regulated, while receptors present in HSCs, such as CD117 (c-kit - receptor for SCF), CD45 (Leukocyte Common Antigen) and Tie-2 (Angiopoietin I receptor) are down-regulated. Up- and down-regulation of these receptors depends on some transcription factors: GATA-1, Fli-1, c-Myb, Pu.1, GATA-

2, Runx1/AML-1 (Freson K et al., Blood 2001 98:85-92; Nichols KE et al., Nat Genet 2000). (Nutt SL et al., . J Exp Med. 2005). (Metcalf D et al., Blood, 2005; Deutsch VR & Tomer A, Br J Haematol. 2006). Finally, microRNAs, such as miR-150, miR-155 and miR-154, can also modulate protein expression by interfering with mRNA and promoting its degradation (Edelstein LC & Bray PF, Blood 2011).

1.5.1. Polyploidy

The polyploidy process is also called endomitosis and it is essential for correct platelet synthesis. At the end of the proliferative phase (S phase), the mononuclear megakaryocytic precursor performs repeated cycles of DNA replication without division cell (no M phase) and with an increase in the chromosomal structure from 4n to 128n. This process allows an amplification of gene expression with an increase in protein synthesis and cell size.

The nuclear membrane of the megakaryocytic precursor dissolves and the microtubules organize themselves to form the mitotic spindle and bind to the kinetochores of the chromatids. Subsequently the chromatids move towards the cell poles but at this stage the process stops and the nuclear membrane is reconstituted forming a nucleus of larger dimensions than the previous one. Consequently, the telophase and cytokinesis process do not happen but it directly enters a new G1 phase (Figure 18) (Zhang Y et al., J. Biol. Chem. 1996; Gao Y et al., Dev. Cell. 2012).

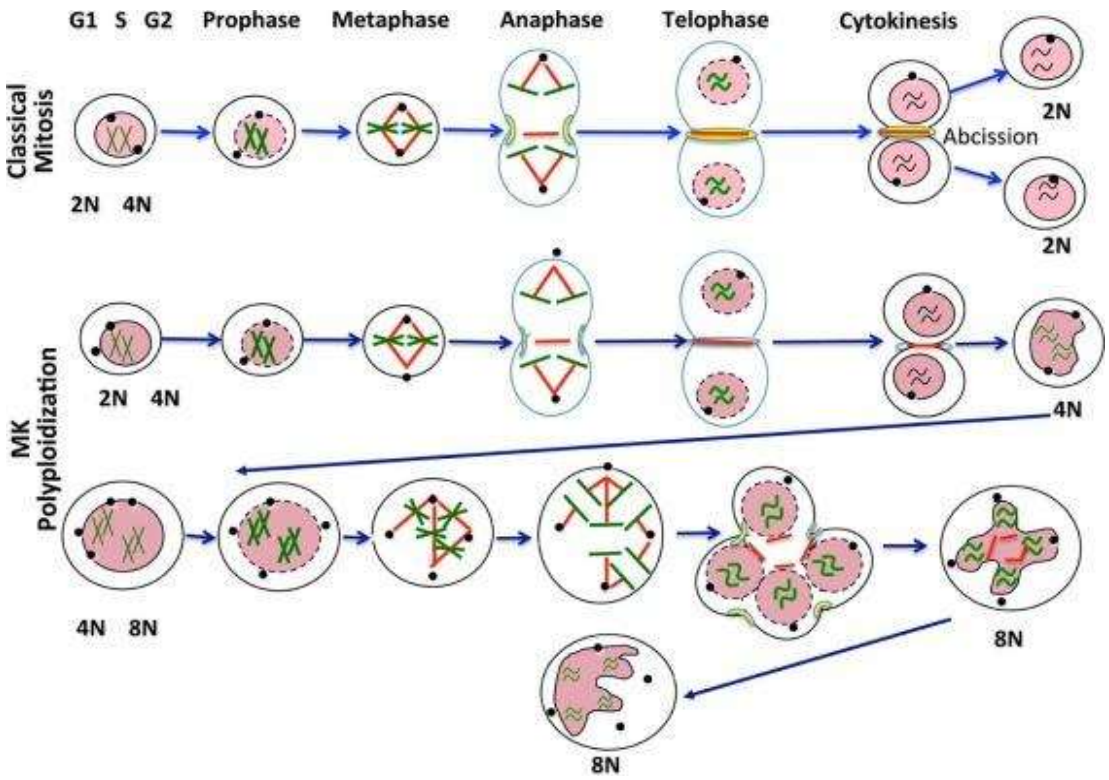

Figure 18 - Schematic comparison of mitosis with MK endomitosis (Mazzi et al., 2018)

By cytological analysis, the first megakaryocytic precursor in the bone marrow is the promegakaryoblast that differentiates into megakaryoblast. This cell has a diameter of 10-50 µm, an oval nucleus with a 4n chromosomal structure and a nucleus/cytoplasm ratio in favor of the first. The cytoplasm is strongly basophilic due to the presence of many ribosomes but few granules. The next differential step is that of promegakaryocytes. This cell has a diameter of 20-80 µm, an oval nucleus and a polycromed cytoplasm because the presence of granules are highlighted. At the end of the endomitosis process of the megakaryocyte is observed the Demarcation Membrane System (DMS) formation. The DMS is a network of cisterns and tubules in continuity with the plasma membrane. Its function is to constitute a reserve of membranes for the subsequent formation of proplatelets.

Finally, other specialized structures that are formed in the maturation phase are: the dense tubular system and the open gully system (OCS). These structures play an important role in the granules formation process (Figure 19).

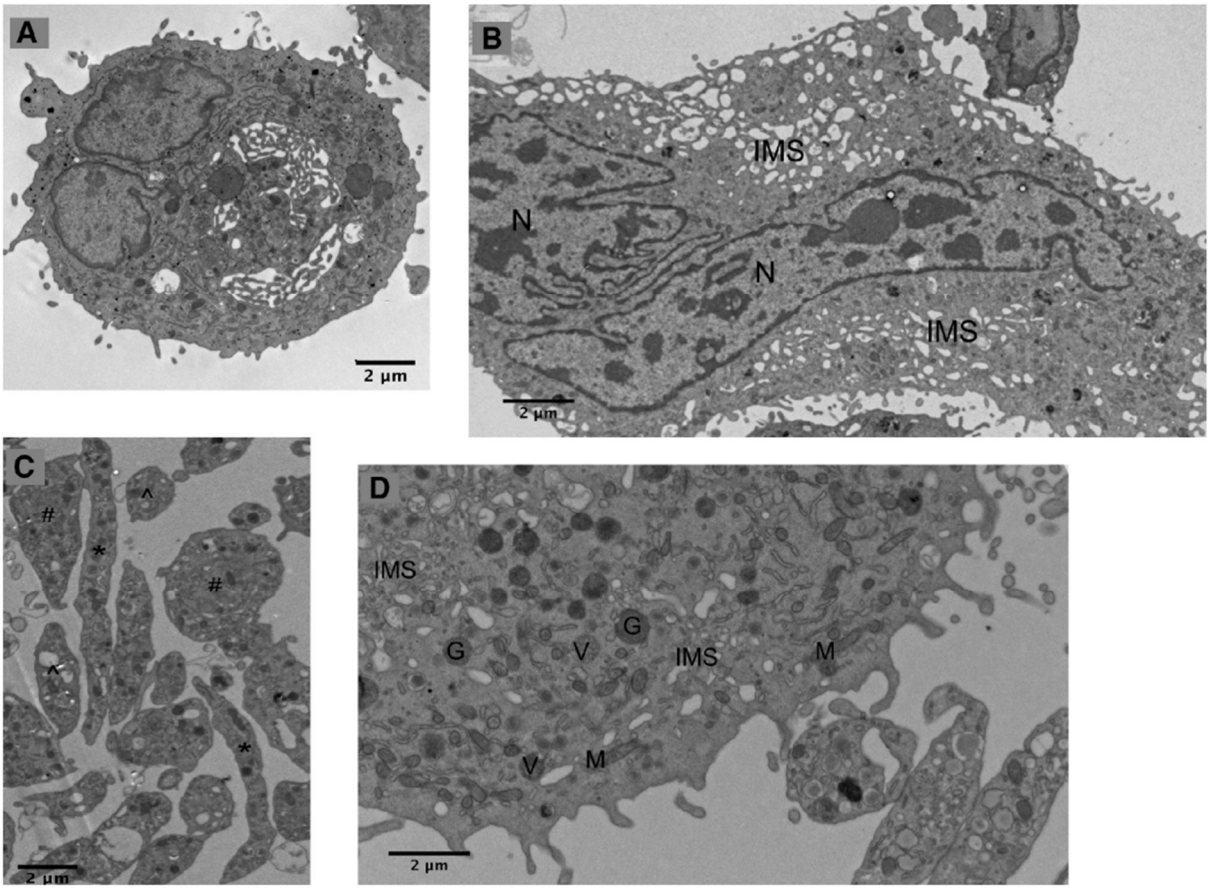

Figure 19 - Transmission electron micrographs of murine MKs and derivatives. (A) Overview of one MK showing multilobulated nucleus. (B) MK with a highly developed IMS. (C) Released preplatelets (#), proplatelets (*), and platelets (^). (D) Detailed view of platelets (bottom right) and an MK, highlighting its contents. N, nucleus; IMS, invaginated membrane system; G, granule; M, mitochondria; V, multivesicular body. (Machlus et al., 2013)

1.6. Platelet genesis

Although several models have been proposed to explain megakaryokinesis, the research conducted by Becker et al. (1976) represents the most accredited model. They say that long and thin structures (2-4 μm) are projected from the megakaryocyte and subsequently these structures undergo branching and folding.

This process originates an anastomosed network of proplatelets surrounding the nucleus (Italiano J. et al, 1999). An essential element for the formation of proplatelets is the reorganization of the cytoskeleton. In particular, the main proteins involved in this process are:

- β1 tubulin and Dynein for the rearrangement of the cytoskeleton;
- F-actin for the folding of the cytoplasmic tubules.

In the distal region of the proplatelet, the long protein molecules form a loop and they become the site of accumulation of granules that are transported by microtubules (Patel et al, 2005; Patel-Hett et al, 2011).

The differentiated megakaryocyte shows a polarization toward the sinusoidal blood vessels of the bone marrow. This polarization is due to the presence of sphingosine-1-phosphate (S1P) in the bloodstream.

In addition, the megakaryocyte presents on its surface structures called podosomes that degrade the extracellular matrix. This process, consequently, allows the proplatelets to cross the basal membrane of the vessels and bind the sphingosine-1-phosphate (S1P). Finally, the proplatelets undergo another fragmentation into platelets and the nucleus goes through an apoptotic process (Schachtner et al, 2013).

Platelets are the smallest blood cells, typically around 2 μm in diameter and anucleated, with an average life of 7-10 days in humans.

Cytologically we can identify three regions:

- the *peripheral zone*, in which the membrane is composed of a phospholipid bilayer that is activated by the exposure on the surface of phosphatidylethanolamine, phosphatidylcholine and phosphatidylserine that bind thrombin. The interaction between these molecules activates the clot formation process.

  Furthermore, the surface of the platelet presents several invaginations that determine an increase in the surface area. It is also possible to identify the open canalicular system (OCS) that allows the exposure of molecules that would otherwise be compartmentalized within the cell. Finally, there is an abundant glycocalyx that performs a barrier function and facilitates the platelet adhesion process;
- *Sol Gel zone*, which is a matrix formed by a fibrous network and its polymerization degree influences the morphology of the platelet and blocks the vesicles and organelles. In particular, in the submembrane region there are thin protein filaments, such as filamin, calmodulin, myosin and short actin filaments, which interact with the cytosolic domain of the glycocalyx, allowing the translocation of molecules on the surface of the cell membrane and modulating signaling.

  Microtubules form the cytoskeleton together with the actin-myosin filaments allow morphological changes and contraction of the platelet plug. Instead, the microfilament system is influenced by the activation/non-activation state of the platelet. In the inactive platelet, the actin/myosin microfilaments maintain the organelles and vesicles separated while its activation promotes: contractile

action, migration and fusion of the granules to the open canalicular system (OCS) for secretion;

- the *membrane system*, which is formed by the open canalicular system (OCS) in continuity with the plasma membrane, and has the function to increase the surface exposed to the plasma. This structure acts in platelet activation through the release of some substances;
- the *organelles*: mitochondria, granular endoplasmic reticulum and in particular the granules (Lentz BR, 2003).

Ultrastructural cytological studies of platelets have highlighted the presence of three types of granules: alpha-granules, beta-granules and lysosomes.

Alpha granules (α-granules) are the most abundant and important in platelets. These granules show a spherical/ovoidal shape of about 200-500 nm, are synthesized during megakaryocyte maturation and are secreted in response to platelet activation (Manole et al., 2023). Proteomic and mass spectrometry studies have identified many soluble and specific proteins, such as: inhibitory proteins (plasminogen inhibitor-1 (PAI-1)), factors involved in coagulation (factor V, XI and XII) and factors involved in the modulation of the inflammatory response (P-selectin or chemokines (CXCL1, CXCL4, CXCL7) (Blair et al., 2010). These granules also contain some matrix metalloproteinases (MMP-1, MMP-2 and MMP-9). Finally, molecules within these granules are growth factors involved in cell proliferation and in the migration process (Yuanying et al., 2018) (Table 3).

Growth factor in α-granules	Functions
Epidermal growth factor (EGF)	● Stimulates the proliferation of epidermal and epithelial cells and fibroblasts ● Chemoattractant for fibroblasts and epithelial cells ● Stimulates re-epithelialization ● Stimulates angiogenesis ● Influences the synthesis and turn-over of extracellular matrix
Platelet derived growth factor (PDGF)	● A and B isoforms are strong mitogenes for fibroblasts, arterial smooth muscle cells, epithelial and endothelial cells ● Strong chemoattractant for fibroblasts ● Stimulates chemotaxis toward a gradient of PDFD ● Stimulates neutrophils and macrophages, collagen activity and synthesis
Transforming growth factor α (TGF- α)	● Similar EGF, binds to the same receptor ● Stimulates epithelial and endothelial cell growth
Transforming growth factor β1 (TGF- β1)	● Stimulates fibroblast chemotaxis and proliferation ● Stimulates collagen synthesis ● Decreases dermal scarring ● Growth inhibitor for endothelial cells, fibroblasts and keratinocytes ● Antagonizes the biological activities of EGF, PDGF, aFGF and bFGF
Keratinocyte growth factor (KGF or FGF-7)	● Plays a role in tissue repair following skin injuries ● Promotes wound healing by proliferation, differentiation, angiogenesis and cell migration ● Mitogen for keratinocytes
Fibroblast growth factor, acidic (aFGF-1)	● Participates in proliferation, differentiation, angiogenesis and cell migration ● Mitogen for keratinocytes, dermal fibroblasts and endothelial cells
Fibroblast growth factor, basic (bFGF-2)	● Stimulates the growth of fibroblasts, endothelial cells and keratinocytes ● Stimulates angiogenesis, collagen and matrix synthesis, wound contraction, epithelialization and KGF production
Vascular endothelial growth factor (VEGF)	● A strong angiogenic protein ● Induces neovascularisation by stimulating the proliferation of macrovascular endothelial cells

	● Induces the synthesis of metalloproteinase, which degrades interstitial collagen type 1, 2 and 3
Connective tissue growth factor (CTGF)	● Induces the proliferation, migration and tube formation of vascular endothelial cells and angiogenesis
Granulocyte/Macrophage colony-stimulating factor (GM-CDF or CSF α)	● Strong chemoattractant for neutrophils and macrophages
Insulin-like growth factor (IGF)	● Promotes the synthesis of collagenase and prostaglandin E2 in fibroblasts ● Stimulates the growth of fibroblasts
Tumor necrosis factor α (TNF- α)	● Stimulates the growth of fibroblasts ● Stimulates angiogenesis
Interleukin 1β (IL-1β)	● Inhibits the growth of endothelial cells ● Enhances inflammatory reactions and collagenase activity
Interleukin 8 (IL-8)	● Supports angiogenesis ● Mitogenic for epidermal cells

Table 3 - : platelet growth factors in α-granules (Rozman et al., 2007)

Dense granules (δ-granules) are smaller than alpha granules. These granules have a spherical shape of about 150-300 nm, they are synthesized during the megakaryocyte differentiation and secreted in response to platelet activation. These organelles contain small molecules, such as calcium ions (Ca^{2+}), Serotonin, Histamine and Adenosine triphosphate or biphosphate (ATP or ADP) and their function is to amplify and modulate the platelet response but also vasoconstriction (Manole et al., 2023) (Table 4).

Molecules in δ-granules	Functions
Calcium ions (Ca^{2+})	● Enzyme cofactor in the coagulation cascade and in degranulation
Histamine	● Stimulates vasodilation ● Increases vascular permeability
Serotonin	● Stimulates blood vessel contraction ● Promotes clot stabilization
Adenosin trifosfato (ATP) o Adenosin bifosfato (ADP)	● Strong platelet aggregating agents ● Stimulates platelet aggregation and the formation of platelet plug

Table 4 - Molecules in α-granules δ-granules (Rozman et al., 2007)

Lysosomes are smaller than alpha and dense granules. These organelles have a spherical shape of about 100-300 nm and are synthesized in the Golgi apparatus during megakaryocyte differentiation (Manole et al., 2023). The lysosomal membrane displays proton ATPases (V-ATPases) to maintain an acidic pH inside it and it's essential for the activity of acid hydrolases, such as proteases, lipases, glycosidases and nucleases (Table 5).

Molecules in platelet lysosomes	Functions
Proteases (cathepsin B, D, L)	● Degrade unnecessary and nonfunctional proteins
Lipases	● Hydrolyze triglycerides into glycerol and fatty acids for energy or structural purposes
Glycosidases	● Degrade complex carbohydrates for energy purposes
Nucleases	● Degrade excess nucleic acids for reuse, or the damaged ones

Table 5 - Molecules in platelet lysosomes (Rozman et al., 2007)

1.7. Blood-derived biomaterials: fibrin glue and Platelet-Rich Plasma

Blood tissue is a good source of cellular elements and protein molecules: some of these components, such as fibrin glue, fibrinogen and platelet-derived growth factors, are used in clinics. In addition, the scientific progress observed in the last 30 years has led to an improvement in the production and clinical use of these products in regenerative medicine (Burnouf et al., 2013).

Fibrin glue, discovered and used since the second half of the last century, is an adhesive material used in plastic and reconstructive surgery (Stuart et al., 1990; Currie et al., 2001). Fibrin glue is composed of fibrinogen and thrombin; subsequently calcium chloride is added to accelerate the polymerization process of the fibrin molecules and promote the formation of a clot that in clinical application adheres to the tissue. Fibrin glue function has been studied in the skin explant model, and has demonstrated a haemostatic effect, an increase in the probability of explant attachment and an antimicrobial action (Currie et al., 2001).

Furthermore, fibrinogen and fibronectin, together with the extracellular matrix, collagen and elastin, are ideal components for the fabrication of scaffolds and biomaterials. These elements form polymeric structures that provide mechanical support, flexibility, and promote the regeneration of injured or pathologically abnormal tissues, through cellular signals that influence cell adhesion, proliferation and differentiation. These protein scaffolds are not immunogenic and thrombogenic, and they can be structurally modified through lytic enzymes (Burnouf et al., 2013).

In 1970, thanks to scientific progress, a fibrin glue-like product was formulated: Platelet Rich Plasma (PRP). This product highlighted a regenerative component of platelet

origin through the attraction, proliferation and transformation of cells involved in tissue repair/regeneration.

In blood, the platelet concentration is 150,000–300,000/μL, but the term PRP refers to a standard volume of autologous plasma with a platelet concentration higher than baseline. Indeed, in 5 mL of plasma volume, the concentration is 1,000,000 platelets per μL (Marx, 2001).

The platelets function as a reservoir of growth factors was discovered at the end of the 20th century and it found application in orthopedics, through the increase of bone formation, in oral and maxillofacial surgery and finally in soft tissues and in wound healing processes (Alsousou et al., 2013). PRP's action derives from the release of growth factors and cytokines contained in alpha and beta granules. Specifically, the secretion process occurs within 10 minutes of clot formation or contact with the basement membrane. In this first phase, 70% of the total growth factors are released; subsequently 95% of the remaining growth factors are released within an hour (Eppley et al., 2004; Cole et al., 2010). Consequently, in clinical practice, PRP must be obtained in an anticoagulated form and applied within 10 minutes from the start of the coagulation process. Finally, it has been observed that after the initial degranulation, platelets continue to release growth factors for approximately 7/8 days, but with a progressive reduction in their quantity (Marx et al., 2001; Marx et al., 2004). Currently, the most widely used anticoagulant is citrate dextrose-A, which promotes increased platelet vitality. The interaction of growth factors through membrane receptors promotes signal transduction, the activation of intracellular second messengers, and finally, gene activation/silencing. This interaction suggests that these molecules do not diffuse into cells and therefore do not cause tumor transformation. PRP contains three proteins: fibrin, fibronectin, and vitronectin, which are present in

high concentrations in the blood. These protein molecules interact with growth factors and they play an important role in tissue regeneration, by promoting adhesion, cell proliferation and collagen synthesis. In particular, fibrin has a dual function (Marx, 2004; Kawase, 2015):

- *in-vivo* - it acts as a scaffold at the regeneration site, promoting adhesion cell, stabilizing growth factors and their bioactivity;
- *in-vitro* - it promotes proliferation cell.

Instead, the ratio between fibrinogen and thrombin affects the mechanical and chemical properties of PRP clot. Indeed, if the thrombin concentration increases, fibrin filaments are: thinner, more branched and compact, while at low concentrations, they are larger, with fewer branches but with larger interfibrillar spaces. For this reason, the diameter of fibrin filaments influences the size of micropores, which play an important role in proliferation, migration, and differentiation of cells, as well as in the delivery of growth factors. Finally, crosslinking between fibrin filaments stabilises its three-dimensional structure and simultaneously limits the fibrinolytic action of plasmin (Kawase, 2015).

1.7.1. PRP preparation techniques: advantages and disadvantages

Today, clinical PRP preparations can be derived from allogeneic PRP and autologous PRP (Figure 20). Allogeneic PRP is derived from selected donors, therefore it is a pharmaceutical product. Its use reduces but does not eliminate the risk of infections, pathologies or other side effects, such as allergic and anaphylactic reactions. Furthermore, in addition to increasing production costs, researchers have observed that the time required for optimal results with allogeneic PRP is longer than with autologous PRP.

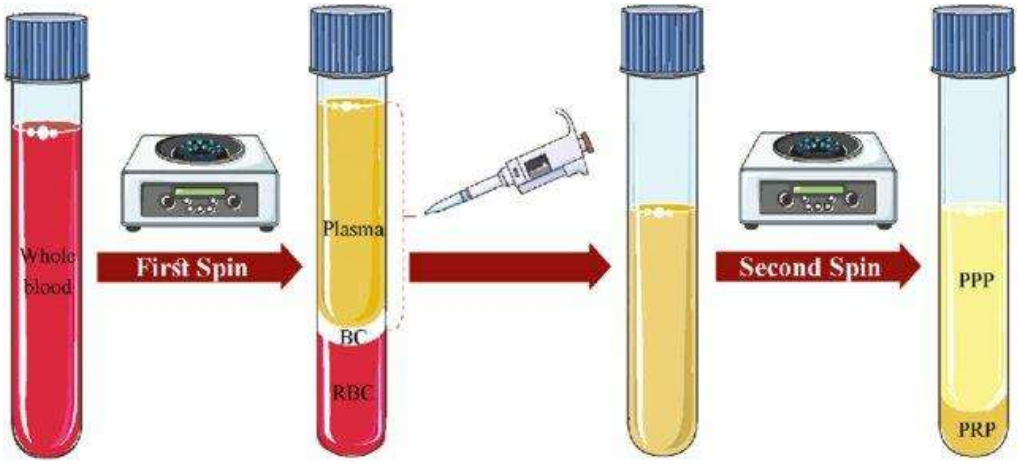

Figure 20 - Guideline for obtaining PRP (Mehdipour et al., 2024)

Clinically, PRP offers several advantages:

- maintains tissue homeostasis, promoting a "controlled" regeneration process;
- preparation is quick and can be performed in surgery room;
- autologous PRP is safer than allogeneic PRP;
- cost-benefit ratio is good as compared to the combination of biomaterials and recombinant growth factors.

The disadvantages are:

- the use of bovine thrombin to prepare PRP from liquid to gel;

- the product quality due to the technique used;
- the time factor, about 30 minutes, which could be frustrating for some medical doctors.

However, scientific progress such as the development of automated systems, the standardization of the preparation method and the use of autologous human thrombin have allowed to overcome several disadvantages (Alsousou et al., 2013; Kawase, 2015).

There are various techniques for obtaining PRP, differing in the anticoagulant, speed, number, and time of centrifugation (Table 6). The first standardized techniques are:

- *Curasan PRP kit:* collect 8.5 mL of blood in a tube containing citrate phosphate dextrose adenine (CDPA), centrifuge at 2400 rpm for 10 minutes, transfer the plasma to a tube and centrifuge at 3600 rpm for 15 minutes, and resuspend the pellet in 0.4 mL of supernatant (Weibrich et al., 2002);
- *Platelet Concentrate Collection System kit (PCCS):* collect 60 mL of blood in a polyvinyl-chloride bottle containing acid citrate dextrose, centrifuge at 3200 rpm for 3 minutes and 45 seconds, open a valve to pass the plasma with the platelets into another compartment, centrifuge at 3000 rpm for 13 minutes, transfer the Platelet Poor Plasma (PPP) with an air jet and resuspend the pellet in the residual plasma volume (Weibrich et al., 2002);
- *Okuda technique:* collect 17 mL of blood into a tube containing acid citrate dextrose, centrifuge at 2400 rpm for 10 minutes, transfer the plasma into a new tube, centrifuge at 3600 rpm for 15 minutes to separate the PRP from the PPP (Okuda et al, 2003).

Kawase's study showed that the best technique for obtaining the largest quantity and best-quality platelet concentrate is the Okuda technique.

However, in subsequent years, two other methods have been proposed:

- Masuki technique: Collect 11.5 mL of blood into a conical-bottom tube, centrifuge at 3200 rpm for 4 minutes, remove the buffy coat and erythrocytes, and centrifuge at 3200 rpm for 4 minutes (Masuki et al., 2016);
- Gentile technique: Collect 8 mL of blood into a tube containing acid citrate dextrose, and centrifuge at 3000 rpm for 10 minutes (Gentile et al., 2016).

	Curasan PRP kit	**PCCS Kit**	**Okuda technique**	**Masuki technique**	**Gentile technique**
Anti-coagulant	citrate phosphate dextrose adenine	acid citrate dextrose	acid citrate dextrose	acid citrate dextrose	acid citrate dextrose
Spin number	2	2	2	2	1
Spin speed (rpm)	2400 3600	3200 3000	2400 3600	3200 3200	3000
Time (min:sec)	10:00 15:00	3:45 15:00	10:00 15:00	4:00 4:00	10:00

Table 6 - Different methods for PRP preparation

1.8. Experimental models of skin and its derivatives

The evolution of different experimental models studying human skin was necessary to understand the dynamics of events occurring in both healthy and injured skin, but also to find an alternative to animal testing. Research conducted on healthy skin has been crucial in understanding both anatomy and physiology, but it also provides a model for testing cosmetic products and topical pharmacological molecules (Lebonvallet et al., 2010). Instead, research focused on damaged skin has improved our understanding of the biological mechanisms of scarring or regeneration (Ud-din and Bayat, 2016).

In scientific research, both the cosmetological and the pharmacological, the experimental models used are: *in-vitro*, *in-vivo*, *in-silico*, *in-virtuo* and *ex-vivo*.

The *in-vitro model* includes monocellular cultures and co-cultures. In monocellular cultures, keratinocytes and fibroblasts are isolated individually and their expansion process is correlated with the use of a specific culture medium. In co-cultures, at least two types of cells are grown together using culture media suitable for both cell types. These models are easily reproducible but do not represent the complex three-dimensional structure of the skin, so the results obtained are not comparable to real life.

The *in-vivo model* involves the human and/or animal organism. The animal *in-vivo* model allows for extensive analysis of tissue regeneration mechanisms, but it has numerous ethical and legal implications that require the approval of an ethics committee for each experimental project. Instead, the human *in-vivo* model allows observation of the body's response to the administration of new drug molecules in patients with skin diseases. In the cosmetics sector, these experiments can only be

performed on healthy volunteers, but the high costs and ethical implications are a limiting factor.

The *in-silico model* represents the best computational method for digitally reproducing biological processes. This model can represent theories and explain physiological processes of the skin, but being a virtual system, it can not completely replicate all the physical and mechanical characteristics of human skin (Ud-Din and Bayat, 2017).

A model currently in development, supported in part by progress in artificial intelligence, is the *in-virtuo model*, which uses advanced software that integrates all the scientific data available on Information Technology platforms. This model aims to eliminate *in-vivo* study methods. However, the available data are not yet completing enough to consider this model an alternative to experimentation on organisms (Lebonvallet et al., 2010).

Today, the *ex-vivo model* is the preferred experimental solution because it can replicate the anatomical architecture and physiological functions of tissue, both native and engineered. Engineered skin comprises two elements: the epidermis and a biocompatible connective tissue scaffold acting as a skin substitute. This substitute can be a scaffold or sponge of natural, synthetic or semi-synthetic origin. To obtain the epidermis, keratinocytes isolated from the biopsy are seeded onto the scaffold; then begin a process of replication and differentiation that will lead to the formation of a three-dimensional construct. This model has some disadvantages: a long procedural process and the support of a cell bank, with a consequent economic impact. For these reasons, knowledge of skin physiology derives from full-thickness explants. This model, surgically collected, maintains all its cellular components and morphology but it is deprived of the vascular perfusion process and nerve endings. Although these last

two aspects are limiting factors, this model is the best for studying skin pathophysiological processes and allows for testing pharmacological or cosmetic molecules.

1.9. Experimental models of *ex-vivo* culture of injured skin

The study of injured skin obtained by surgical resection and maintained using *ex vivo* models can derive from a healthy individual, with a fragment subsequently injured in the laboratory, or from an individual affected by skin lesions or diseases (Ud-Din and Bayat, 2017).

Several studies confirm that using this model allows for a better understanding of physiological and pathological mechanisms, both known and unknown, involved in skin injuries and in their healing process (Figure 21) (Tomic-Canic et al., 2007; Xu et al., 2012; Ud-Din and Bayat, 2017).

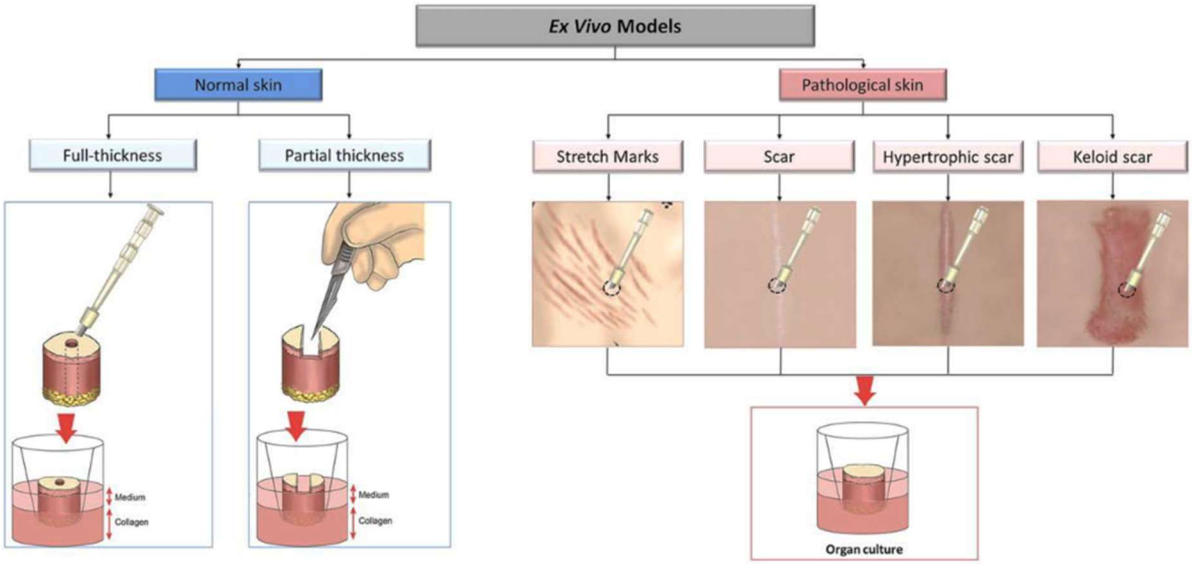

Figure 21: Ex vivo models (Ud-Din and Bayat, 2017)

However, a study conducted by Mendoza-Garcia et al. (2015) highlighted the absence of standardisation in the *ex-vivo* model. This limiting factor is related to three fundamental aspects:

- the type of lesion performed on the biopsy fragment;
- the culture conditions;
- the tests to determine quality and viability of tissue over time.

The study by Mendoza-Garcia et al. (2015) looked to find the best conditions for the *ex vivo* model to survive over time. Specifically, this research focused on three factors: the type of injury, the physical support of the explant, and the culture medium (Figure 22).

After its removal, the skin was cut into biopsy fragments and two types of wounds were made on each sample:

- *partial lesion*: removal of the epidermis and upper part of the dermis;
- *full-thickness lesion*: complete removal of the epidermis and dermis using a circular punch (with diameters of 1, 2 and 3 mm).

In addition, two methods were tested to maintain the samples during culture:

- *transwell system*: the samples were located inside an insert whose base is a membrane that allows the dermis to come into contact with the medium while epidermis was exposed to air (air-liquid interface);
- *collagen gel*: the dermis was inserted into a rat tail type I collagen gel scaffold while the epidermis was exposed to air.

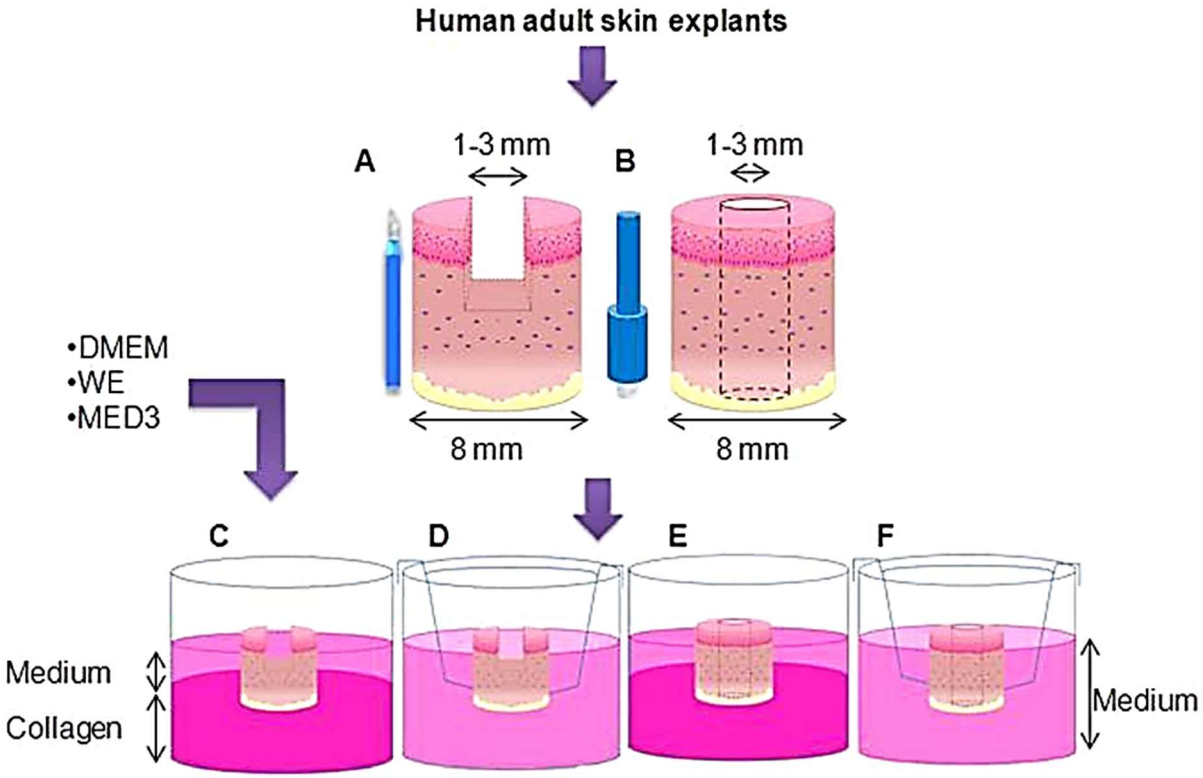

Figure 22: *Ex-vivo* models: partial wound (A) and full thickness wound (B). Biopsies were supported in collagen scaffold (C and E) or introduced in well chamber inserts (D and F) and maintained with DMEM, WE or MED3 medium. All biopsies were exposed to air–liquid interface (Mendoza-Garcia et al., 2015)

Finally, the study compared three culture media: DMEM, William's E, and MED3. Although DMEM and William's E consisted of a common base supplemented with fetal bovine serum, insulin, hydrocortisone, L-glutamine, and antibiotics. MED3 was composed of DMEM, Ham's F12 and Epilife enriched with EpiLife Defined Growth Supplement.

At the end of the experiment (day 14), the team assessed vitality, structural integrity and skin regeneration. Analysis of these parameters allowed the ideal ex vivo model for studying damaged skin to be identified. Specifically, the sample had to be made of by a fragment of skin with a full-thickness lesion with a diameter of 1.5 mm and a scaffold that reproduces the hypodermic structure and maintenance of the epidermis at the air-liquid interface.

CHAPTER 2

AIM OF THE WORK

The PhD project was conducted within the Interuniversity Center for the Promotion of the Principles of the 3Rs:

- *reduction:* reduction in the number of animals used for a specific study;
- *refinement:* improvement of experimental designs to reduce stress and suffering to animals;
- *replacement:* replacement (even partial) of animal testing with alternative methods of comparable validity.

The 3Rs are at the basis of the Directive 2010/63/EU of the European Union on the protection of animals used for scientific purposes which has been implemented in Italy through the Legislative Decree of 4 March 2014, n. 26.

The project was conducted in collaboration between the General Surgery Unit of the Broni-Stradella Unified Hospital of the ASST of Pavia (Italy), the Experimental Surgery Laboratory of the Department of Clinical-Surgical Diagnostic and Pediatric Sciences of the University of Pavia (Italy) and the Pathological Anatomy Laboratory of the IRCCS Ospedale Galeazzi - S. Ambrogio of Milan (Italy).

The study was conducted in accordance with the 1975 Declaration of Helsinki. All patients have signed an informed written consent and the protocol has been presented and approved by the Ethics Committee of the IRCCS Policlinico San Matteo Foundation of Pavia (Italy) (project identification code, 0046911/22).

The endpoint of this project is the validation of a laboratory biotechnological protocol to increase the vitality and the regeneration process of *ex-vivo* human wounded skin culture in dynamic condition, by adding autologous Platelet Rich Plasma (PRP) to a conventional Dulbecco's medium (DMEM).

The protocol validation will be obtained by specific histochemical tests: Hematoxylin-Eosin, Masson Trichrome and Weigert Staining with the aim of analyzing, at a microscopic level, the collagen and elastic fibers, the lymphoplasmacytic and fibroblastic infiltrate at the dermal layer. The re-epithelialization capacity will be evaluated with Hematoxylin-Eosin and Ki-67 immunohistochemical tests. The analysis of the results of samples maintained in *ex-vivo* culture in DMEM will be carried out by comparing samples maintained in DMEM enriched with autologous PRP with similar cultures maintained in conventional DMEM inside the injury.

CHAPTER 3

MATERIALS AND METHODS

The PhD project was conducted in collaboration between the General Surgery Unit of the Broni-Stradella Unified Hospital of the ASST of Pavia (Italy), the Experimental Surgery Laboratory of the Department of Clinical-Surgical Diagnostic and Pediatric Sciences of the University of Pavia (Italy) and the Pathological Anatomy Laboratory of the IRCCS Galeazzi – S. Ambrogio of Milano (Italy).

The study was conducted in accordance with the 1975 Declaration of Helsinki. All patients have signed an informed written consent and the protocol has been presented and approved by the Ethics Committee of the IRCCS Policlinico San Matteo Foundation of Pavia (Italy) (project identification code, 0046911/22).

3.1. Human Skin Specimen Collection

Human skin samples were collected in the Operating Rooms of the General Surgery Unit of the Broni-Stradella Unified Hospital. The samples were obtained from anatomical specimens harvested during sessions of reduction mammoplasty and abdominoplasty, performed on 5 healthy female patients. The inclusion criteria were:

- age range of 30-60 years old;
- healthy patient;
- absence of hormonal therapies;
- absence of allergies;
- no-smokers.

The specimens were sampled by a surgeon in 8 x 8 cm fragments, placed and stored in sterile containers filled with sterile saline solution (S.A.L.F. SpA, Cenate Sotto, Bergamo, Italy) supplemented with 1% penicillin (10,000 U/ml) and streptomycin (10 mg/ml) (Sigma-Aldrich; Merck KGaA, Darmstadt, Germany). Finally, the samples were

kept on ice and transported to the Experimental Surgery Laboratory for further processing. The time lag between tissue harvesting and start of the laboratory procedures was approximately 45 min.

3.2. PRP Preparation

The Tissue Regeneration Kit (New Technologies Supplies, Latina, Italy) was used for preparation of PRP according to the Okuda protocol (Okuda et al., 2003). The kit was equipped with a vacutainer tool and a 12 ml tube provided with sodium citrate anticoagulant and a magnetic polymer separator gel. One hour before the surgical procedure, 10 ml of blood was aspirated from the patient's peripheral vein in the dedicated tube. The tube was gently shaken 5 times and then centrifuged at 1500 G for 5 min, thus obtaining 4 phases: platelet-poor plasma, buffy coat (enriched platelets), separator gel and blood cells. The tube was then gently inverted for 20 s to re-suspend the platelets. Eventually, ~6 ml of pure platelet suspension (PRP) was aspirated with a syringe, kept on ice, and transported to the laboratory (Nicoletti et al., 2019).

3.3. Human Skin Specimen Processing

The human skin sample container, before being opened, was disinfected with absolute ethyl alcohol and placed in a sterile environment provided with a second-class laminar flow hood. Each sample was then taken, washed in sterile saline solution (S.A.L.F. SpA, Cenate Sotto, Bergamo, Italy), placed on a cutting board (Figure 23) and fixed with sterile Backhaus-type clamps.

Figure 23 - Human skin samples obtained from anatomical specimens harvested during sessions of abdominoplasty

Each specimen was divided into multiple 1 cm^2 full thickness punch biopsies that in turn were injured in their central portion with a sterile 3 mm circular punch (Blife, Casale sul Sile, Treviso, Italy), in order to create a standard split thickness skin loss involving the epidermis and the superficial dermis (Figure 24) (Nicoletti et al., 2019; Nicoletti et al., 2023).

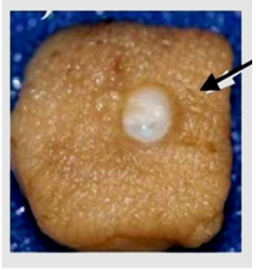

Figure 24 – Experimental human skin model (Edited image – Peramo, 2010)

3.4. Human Skin Specimen Processing in dynamic condition

Each injured sample was placed in a cell culture chamber called LiveBox2 (IV-Tech, Massarosa, LU, Italy) modified to hold a skin sample on the membrane (pore size, 0.40 µm) between the two chambers. The upper chamber was in contact with air while the lower chamber was in contact with the medium, thus each sample was interposed on an air-liquid surface.

The medium, 8 mL, added into the mixing chamber of the bioreactor, was connected in series to a peristaltic pump called LiveFlow (IV-Tech, Massarosa, LU, Italy) and lower chamber of Livebox2. A flow rate of 100 µL/min was applied (Figure 25-26).

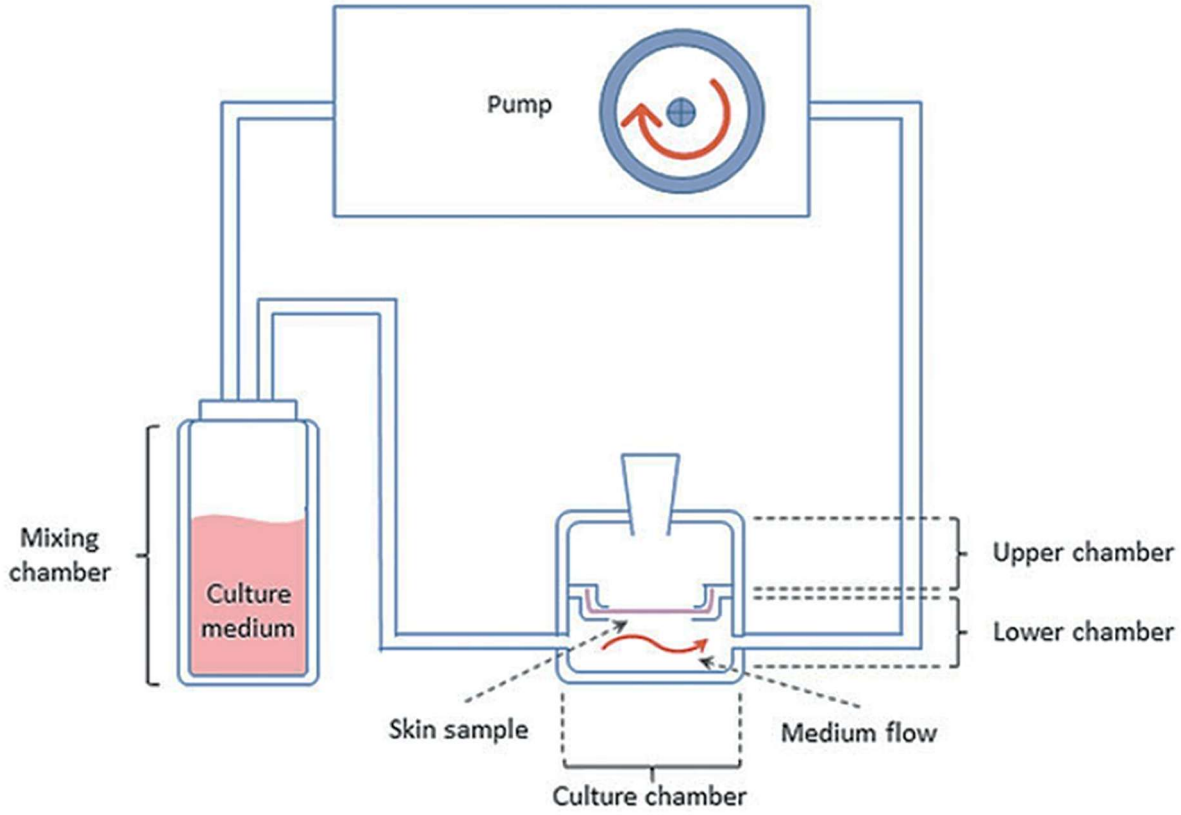

Figure 25 - Structure of the bioreactor: mixing chamber provides the culture medium, a peristaltic pump promotes dynamic flow and culture chamber. The sample is placed between the lower and the upper chamber (Cappellozza et al., 2021)

Figure 26 – Experimental human skin mode in dynamic condiction. The skin sample was cultured in culture chamber. The epidermis and wound area was exposed to the air

3.5. Study Design

The skin specimens, obtained from 5 patients, allowed for the preparation of paired control and experimental samples for each donor. The culture media were prepared according to the Nicoletti protocol (Nicoletti et al., 2017; Nicoletti et al., 2019).

The control samples (D) were cultured in Dulbecco's Modified Eagle's Medium powder with 4,500 mg/l glucose, 0.584 g/l L-glutamine and 0.11 g/l sodium pyruvate (DMEM) (Sigma-Aldrich), reconstituted with distilled water (Milli-Q, Merck-Millipore, Darmastadt, Germany) and enriched with 3.7 g/l sodium bicarbonate, 10% fetal bovine serum (FBS), 1% (10,000 U/ml) penicillin and streptomycin (10 mg/ml) (all from Sigma-Aldrich); the central skin loss region was treated with a constant volume (20 µl) of the same DMEM solution.

The experimental samples (DP) were cultured in DMEM reconstituted with distilled water (Milli-Q, Merck-Millipore, Darmastadt, Germany), enriched with 3.7 g/l sodium bicarbonate, 10% FBS, 1% (10000 U/ml) penicillin and streptomycin (10 mg/ml) (all from Sigma-Aldrich); a constant volume (20 µl) of 2.5% autologous Platelet Rich Plasma (PRP) added culture medium was applied in the central skin loss region, too.

The control and the experimental culture media were changed every seven days. Instead, 20 µl of DMEM and DMEM plus PRP were added daily into the central injury (Figure 27). Both control and treated samples were incubated in an atmosphere of 95% humidified air with 5% CO2 at 37◦C for 28 days. Each 7 days a control and treated sample was fixed in 10% neutral buffered formalin (Bio-Optica, Milan, IT) (Table 7).

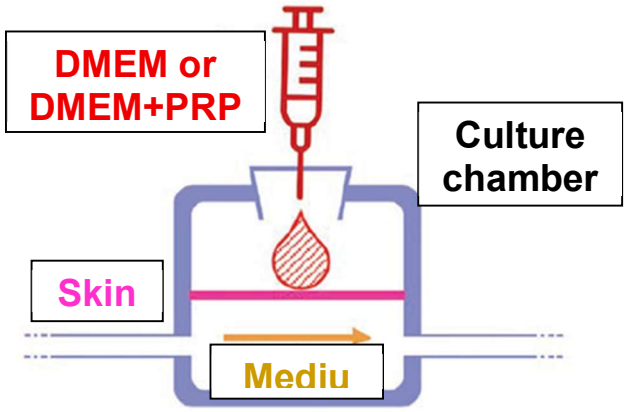

Figure 27 - Administration mode of the control (DMEM) and experimental (DMEM+PRP) solution in dynamic conditions (Edited images – Cappellozza et al., 2022)

3.6. Assessment Modalities

3.6.1. Morphological Analysis

Morphological analysis of the samples was performed by three independent operators at 0 h (T0) to identify the histological features of the untreated skin and subsequently to identify the characteristics of skin in different experimental conditions, following the time scan reported in Table 7.

Day	0	7	14	21	28
Time	T0	T7	T14	T21	T28

Table 7 – Time planning of experimental human skin model.

The skin biopsy fragments were fixed with 10% neutral buffered formalin (pH 7.2) (Bio-Optica, Milan, Italy) for 24 h at room temperature and then they were transported to the Pathological Anatomy Laboratory of the IRCCS Galeazzi – S. Ambrogio of Milano. The samples were loaded into the Donatello series 3 SDSDT9000 instrument (DiaPath SpA, Martinengo, Bergamo, Italy) and automatically dehydrated through graded concentrations of ethanol. Subsequently, they were loaded into Dante Inclusion System SDSDC9000 (DiaPath) and embedded in paraffin. Finally, 3 μm specimens sections were obtained with HistoCore AUTOCUT 149AUTO00C1 (Leica Biosystems Srl, Buccinasco, Milan, Italy), rehydrated and processed with the following different specific staining methods.

3.6.2. Hematoxylin and Eosin Staining protocol

The Hematoxylin and Eosin Staining protocol were used accordingly with the indications provided by the Leica Biosystems.

Following rehydration, the sections were loaded into the HistoCore SPECTRA ST-14051254354 instrument (Leica Biosystems) automated staining instrument and stained with Harry's Hematoxylin (Leica Biosystems) for 5 min and Spectra Eosin (Leica Biosystems) for 2 min at room temperature. Subsequently, the sections automatically passed inside the HistoCore SPECTRA CV-14051454200 instrument (Leica Biosystems) to be dehydrated and mounted. Finally, the stained sections were observed with a Zeiss Axiophot optical microscope (Carl Zeiss AG, Oberkochen, Germany) and photographed by DS-5M Nikon Digital Sight (Nikon Corporation, Tokyo, Japan).

3.6.3. Masson's Trichrome Staining protocol

The Masson's Trichrome Staining protocol was used accordingly with the indications provided by the Bio-Optica company and the bibliographic data of Nicoletti et al. (2019). Following rehydration, the staining was carried out manually by the operator at room temperature. The sections were treated with 6 drops of Weigert's Iron Hematoxylin Solution (reagent A) and 6 drops of Weigert's Iron Hematoxylin Solution (reagent B) for 10 min. After removing the A and B reagents, the sections were treated with 10 drops of Picric Acid Alcoholic Solution (reagent C) for 4 min. Subsequently, after a fast washing with distilled water, 10 drops of Ponceau Acid Fuchsin according to Mallory (reagent D) were added for 4 min. After a further washing, the sections were treated with 10 drops of Phosphomolybdic Acid Solution (reagent E) for 10 min and, after draining the slide, 10 drops of Masson Aniline Blue (reagent F) were added for 5 min (all reagents from Bio-Optica). Subsequently, after a rinse quickly in distilled water the sections were loaded on the HistoCore SPECTRA CV-14051454200 instrument (Leica Biosystems) to be dehydrated and mounted. Finally, the stained sections were observed with a Zeiss Axiophot optical microscope (Carl Zeiss AG) in bright field and photographed by DS-5M Nikon Digital Sight (Nikon Corporation).

3.6.4. Weigert Staining protocol

The Weigert Staining protocol was used accordingly with the indications provided by the Bio-Optica company and the bibliographic data of Nicoletti et al. (2019). Following rehydration, the staining was carried out manually by the operator at room temperature. Following rehydration, the sections were treated with 5 drops of Potassium Permanganate Solution (reagent A) and 5 drops of Acid Activation Buffer (reagent B) for 5 min. After washing with distilled water, 10 drops of Oxalic Acid Solution (reagent C) were added for 5 min and then the sections were placed in a box with Weigert's Resorcin-Fuchsin Solution (reagent D) and left overnight at room temperature. Following washing, the sections were treated with 10 drops of Acid Differentiation Buffer (reagent E) for 10 min (all reagents from Bio-Optica). Subsequently, after a rinse quickly in distilled water the sections were loaded on the HistoCore SPECTRA CV-14051454200 instrument (Leica Biosystems) to be dehydrated and mounted. Finally, the stained sections were observed with a Zeiss Axiophot optical microscope (Carl Zeiss AG) in bright field and photographed by DS-5M Nikon Digital Sight (Nikon Corporation).

3.6.5. Ki-67 Immunostaining protocol

The Ki-67 Staining protocol was used accordingly with the indications provided by the Bio-Optica company and the bibliographic data of Nicoletti et al. (2019).

Staining for Ki-67 was performed using the Bench Mark XT ICH/ISH system (Ventana Medical System, Roche, Arizona, USA). The specific protocol is selected by a special software connected to the instrument. Each slide is placed on a "thermopad" equipped with an independent sensor for the temperature. The sections were warmed up to 75°C, dewaxed by using EZ PREP buffer (Roche) and after washing with a reaction buffer for 8, 20, and 36 min, the sections were treated with fixative for 20 min. Subsequently, the temperature was raised to 95°C and the sections were treated with a UV inhibitor for 30 min, to block endogenous peroxidase activity. The samples were then incubated with 2 µg/ml primary rabbit monoclonal antibody (catalog number 790-4286) for 12 min at 37°C. Subsequently, the sections were washed with distilled water, treated with UltraView Universal DAB, further washed with distilled water for 4 min and eventually stained with Harry's Hematoxylin (Leica Biosystems) for 5 min. Subsequently, the sections were loaded on the HistoCore SPECTRA CV-14051454200 instrument (Leica Biosystems) to be dehydrated and mounted. Finally, the stained sections were observed with a Zeiss Axiophot optical microscope (Carl Zeiss AG) in bright field and photographed by DS-5M Nikon Digital Sight (Nikon Corporation).

CHAPTER 4

RESULTS

4.1. Haematoxylin and Eosin staining

The Haematoxylin and Eosin staining results of both control (C) and experimental (DP) samples are comprehensively summarised in Table 8 and Figure 28.

Control samples (C)

Re-epithelialisation: at T7, the re-epithelialisation process was in its early stages but with modest stratification. In particular, moderate stratification was observed near the edge of the lesion compared to the central portion of the wound. At T14, the re-epithelialisation process was similar at T7, but the degree of stratification was complete. In particular, the spinous layer and granular layer were mature, while the stratum corneum was absent. At T21, the re-epithelialisation process was advanced but not complete, while the degree of stratification was similar to that at T14. At T28, the re-epithelialisation process was complete, but the stratification was similar at T14 and T21. In particular, a primitive stratum corneum was observable at the margins of the injury.

Cellular infiltration: at T7, T14, T21 and T28, there was a limited presence of lymphoplasmacytic infiltrate, even if with different tissue distribution. In particular, at T7 the cells were located in the deeper layers of the dermis, while at T14 a minimal tendency to increase was observed in the superficial layers of the dermis. At T21 and T28, although the presence of lymph-plasma-cells minimal, greater localisation was observed in superficial dermis. At T7, T14 and T21, there was a limited presence of fibroblasts, with greater localisation in the deepest region of the dermis, while at T28, although the presence of fibroblasts was ever minimal, greater localisation was observed in the superficial dermis.

Vascularization: at T7, T14, T21 and T28, dermal vascularisation was minimal and the structures identified were capillaries. In particular, at T7, capillaries were located at the borders of the wound. At T14, T21 and T28, however, some capillaries were visible in the previously injured region.

Experimental samples (DP)

Re-epithelialisation: at T7, the re-epithelialisation process was advanced, but the degree of stratification was complete. In particular, the spinous layer and granular layer were mature. At T14, the re-epithelialisation process and stratification were similar to T7. However, a primitive transition to the stratum corneum was appreciated at the margins of the injury. At T21, the re-epithelialisation process was complete, but the stratification of the epithelium was similar at T7 and T14. However, the stratum corneum was more mature at the margins of the lesion than at the centre of the injury. At T28, the re-epithelialisation process was similar to that at T21, while the degree of stratification was complete and mature. In particular, the basal layer showed weak brown pigmentation, while there was a constant presence of the stratum corneum on the newly formed tissue limb.

Cellular infiltration: at T1, lymphoplasmacytic infiltrate was minimal with a homogeneous distribution in the dermis. At T14, an abundant presence of cells was observed in the perivascular sites but with a tendency to decrease and a more homogeneous distribution in the dermal tissue. At T21, a modest number of cells were present a homogeneous distribution only in the deeper dermal regions. At T28, a minimal presence of cells was observed in the perivascular sites and in the loose subepithelial regions. At T7, T14 and T21, there was a moderate presence of

fibroblasts, even if with a different tissue distribution. In particular, at T7, a greater number of cells was observed in the sub-epithelial regions, while at T14 and T21, they were located in the deep dermis, with a progressive decrease observed at T28.

Vascularization: at T7, T14, T21 and T28, the vascular structures identified were capillaries but with a different location. In particular, at T7, of capillaries were observed in minimal quantity, and they were located at the borders of the injury but also in the central portion of the lesion. At T14, there was a moderate presence of capillaries but with a similar location to T7. At T21 and T28, the quantity of capillaries was similar to T7 but with a location similar to T14 and T21.

Table 8 - Semi-quantitative analysis of tissue and cellular characteristics

		T7	T14	T21	T28
C	Epithelial cell advancement front	+	+	++	+++
	Multi-layered re-epithelialization	+	++	++	++
	Ki-67-positive nuclei at the margins	+	+	+	0
	Ki-67-positive nuclei in the wound	++	++	+	0
	Lymph-plasma-cell infiltration	+	+	+	+
	Fibroblast infiltration	+	+	+	+
	Vascularization	+	+	+	+
DP	Epithelial cell advancement front	++	++	+++	+++
	Multi-layered re-epithelialization	++	++	++	+++
	Ki-67-positive nuclei at the margins	+++	+	+	0
	Ki-67-positive nuclei in the wound	+++	++	++	0
	Lymph-plasma-cell infiltration	+	+++	++	+
	Fibroblast infiltration	+	++	++	+
	Vascularization	+	++	+	+

Epithelial cell advancement front: 0 = absent, + = initial, ++ = advanced, +++ = complete
Multi-layered re-epithelialization: 0 = absent, + = low, ++ = good, +++ = mature
Ki-67-positive nuclei at the margins: 0 = absent, + = minimum, ++ = moderate, +++ = abundant
Ki-67-positive nuclei in the wound: 0 = absent, + = diffuse but minimal, ++ = diffuse and moderate, +++ = diffuse and abundant
Lymph-plasma-cell infiltration: + = minimum, ++ = moderate, +++ = abundant
Fibroblast infiltration: + = minimum, ++ = moderate, +++ = abundant
Vascularization: + = poor, ++ = discrete, +++ = abundant

Figure 28 - Haematoxylin and Eosin staining

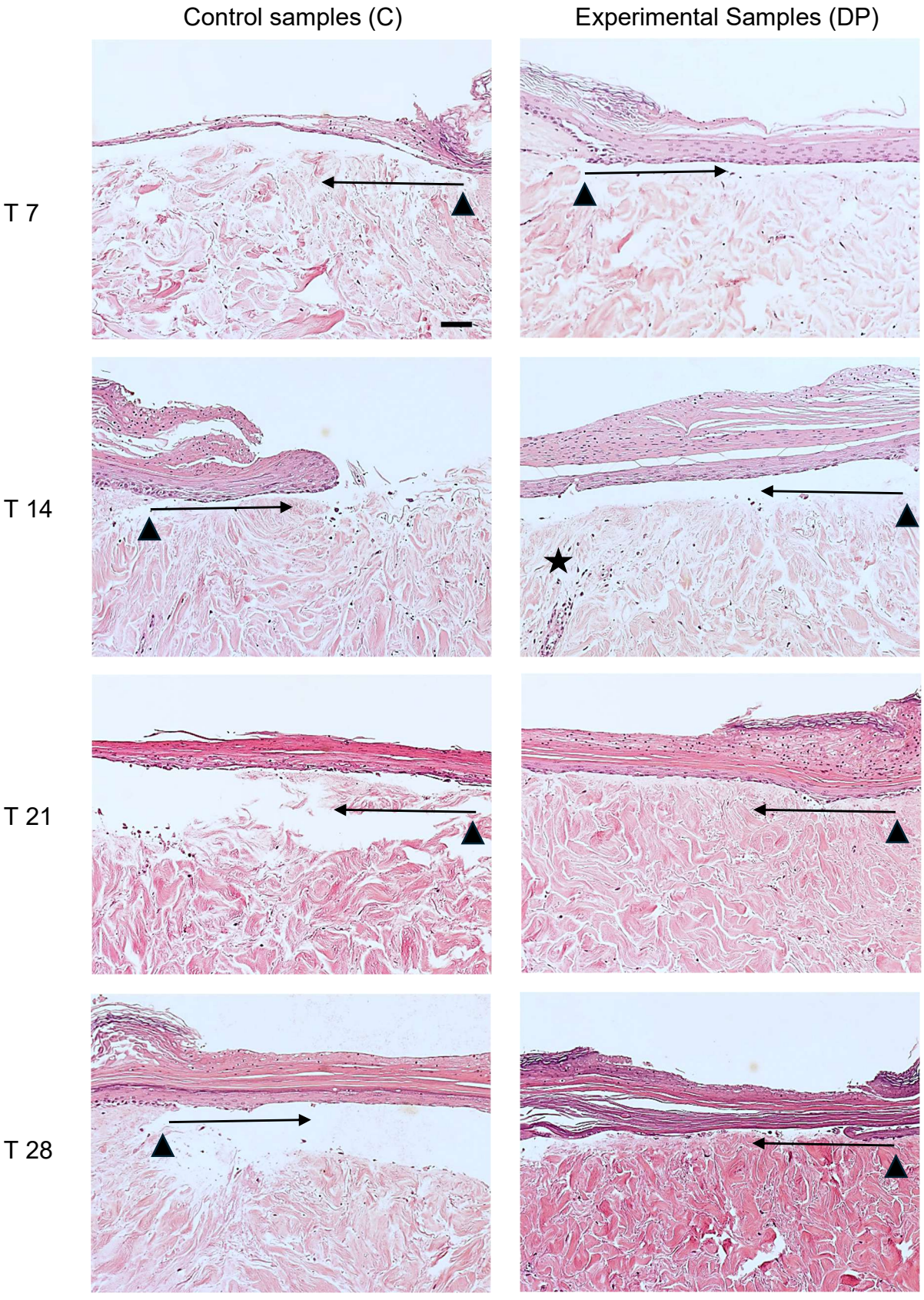

Figure 28 - Hematoxylin and Eosin staining staining in the different culture conditions at the different time points. Control (C): sample maintained with a flow of DMEM and DMEM within the lesion. Experimental sample (DP): sample maintained with a flow of DMEM and DMEM enriched with PRP within the lesion. DMEM: Dubecco's Modified Eagle Medium; PRP, Platelet Rich Plasma. Sample maintenance time: T7 – T28.
Magnification: 10x. Scale bar: 100 μm. Black triangle = wound margins; black arrow = re-epithelialization; black star = lymph-plasma-cell infiltration

4.2. Masson's Trichrome staining

The Masson's Trichrome staining results of both control (C) and experimental (DP) samples are comprehensively summarised in Table 9 and Figure 29.

Control samples (C)

At T7, the papillary dermis showed initial development, while the reticular dermis was very loose with large interfibrillar spaces. Thick and thin collagen fibres were observable but with a different distribution in the tissue; in particular, the thick fibres were more concentrated in the deep regions of the dermis, while the thin ones were located in the superficial portion of the injury. In addition, some thick collagen fibres in the deeper regions were red in the centre of the fibre and blue in the peripheral portions, compared to some thin but more structured fibres in the superficial portion, which showed a homogeneous red colouration. The orientation was disorganised.

At T14, the papillary and reticular dermis were similar to T7. Thick and thin collagen fibres were observed, but with a different distribution compared to T7. In particular, thick fibres tended to be distributed from the deep regions of the dermis towards the superficial injured region, while the distribution of thin fibres was homogeneous. In addition, some thick collagen fibres, both in the deep and superficial regions, were red in the centre of the fibre and blue in the peripheral portions, compared to some thin fibres that showed a homogeneous red colouration. The orientation was perpendicular to the borders of the injury, while in the central portion it was similar to T7.

At T21 and T28, the newly formed papillary dermis was at a more advanced phase than at T7, while the reticular dermis showed a tendency towards a progressive decrease in interfibrillary spaces compared to T7 and T14. The thick fibres showed a homogeneous distribution in the dermis, while the thin fibres showed a progressive

tendency towards greater structuring compared to T14. There weren't observed red fibres or portions of them. The orientation was perpendicular to the margins of the lesion, while in the central portion it was parallel.

Experimental samples (DP)

At T7, the papillary dermis showed initial development, while the reticular dermis was slightly loose. Thick and thin collagen fibres were observable but with a different distribution in the tissue; in particular, the thick fibres were more concentrated at the wound margin and in the deep regions of the dermis, at the site of the lesion, while the thin fibres were located in the superficial region. In addition, some thick collagen fibres at the margins of the injury were red in the centre of the fibre and blue in the peripheral portions, compared to some thin fibres located in the central portion of the wound which showed a homogeneous blue colouration. The orientation was generally disorganised but perpendicular to the margins of the lesion.

At T14, the papillary and reticular dermis were similar to T7. Thick and thin collagen fibres were observable but with a different distribution compared to T7. In particular, the thick fibres tended to be distributed from the margins of the lesion towards the central portion of the wound and were also located in the deep central part. The distribution of thin fibres was generally homogeneous, although slightly greater in the superficial region. In addition, some thick collagen fibres in the deep regions were red in the centre of the fibre and blue in the peripheral portions, compared to other thin but more structured fibres, which showed a homogeneous red colouration. The orientation of the fibres was perpendicular to the surface.

At T21, the papillary dermis was mature and the reticular dermis was compact, with a progressive decrease in interfibrillar spaces, compared to T14. The thick fibres showed a homogeneous distribution in the dermis and the deep and superficial thin fibres were also more structured. There were no red fibres or portions of them. Fibres were oriented perpendicular to the surface.

At T28, the structure of the papillary and reticular dermis was similar to that at T21. The thick fibres showed a homogeneous distribution in the dermis similar to that at T21, although they were more structured, while there were no thin fibres. There were no red fibres or portions of them. Fibres' orientation was generally parallel to the surface.

Table 9 - Semi-quantitative analysis of tissue and cellular characteristics

		T7	T14	T21	T28
C	Papillary dermis	+	+	++	++
	Reticular dermis	+	+	++	++
	Masson's trichrome blue stained collagen fibers' thickness	++	++	+++	+++
	Masson's trichrome red stained collagen fibers' thickness	++	++	0	0
	Reticular collagen fibers' orientation	+	++	+++	+++
DP	Papillary dermis	++	++	+++	+++
	Reticular dermis	++	++	+++	+++
	Masson's trichrome blue stained collagen fibers' thickness	++	++	++	+++
	Masson's trichrome red stained collagen fibers' thickness	+++	+++	0	0
	Reticular collagen fibers' orientation	+	++	++	+++

Papillary dermis: 0 = absent, + = initial, ++ = advanced, +++ = mature
Reticular dermis: + = very loose, ++ = partially loose, + + + = thick, ++++ = hypertrophic
Masson's trichrome blue stained collagen fibers' thickness: + = thin fibers, ++ = blended thin and thick fibers, +++ = thick fibers, ++++ = very thick fibers
Masson's trichrome red stained collagen fibers' thickness: 0 = absent, + = thin fibers, ++ = blended thin and thick fibers, +++ = thick fibers, ++++ = very thick fibers
Reticular collagen fibers' orientation: + = chaotic, ++ = perpendicular to the skin surface, +++ = parallel to the skin surface

Figure 29 - Masson's Trichrome staining

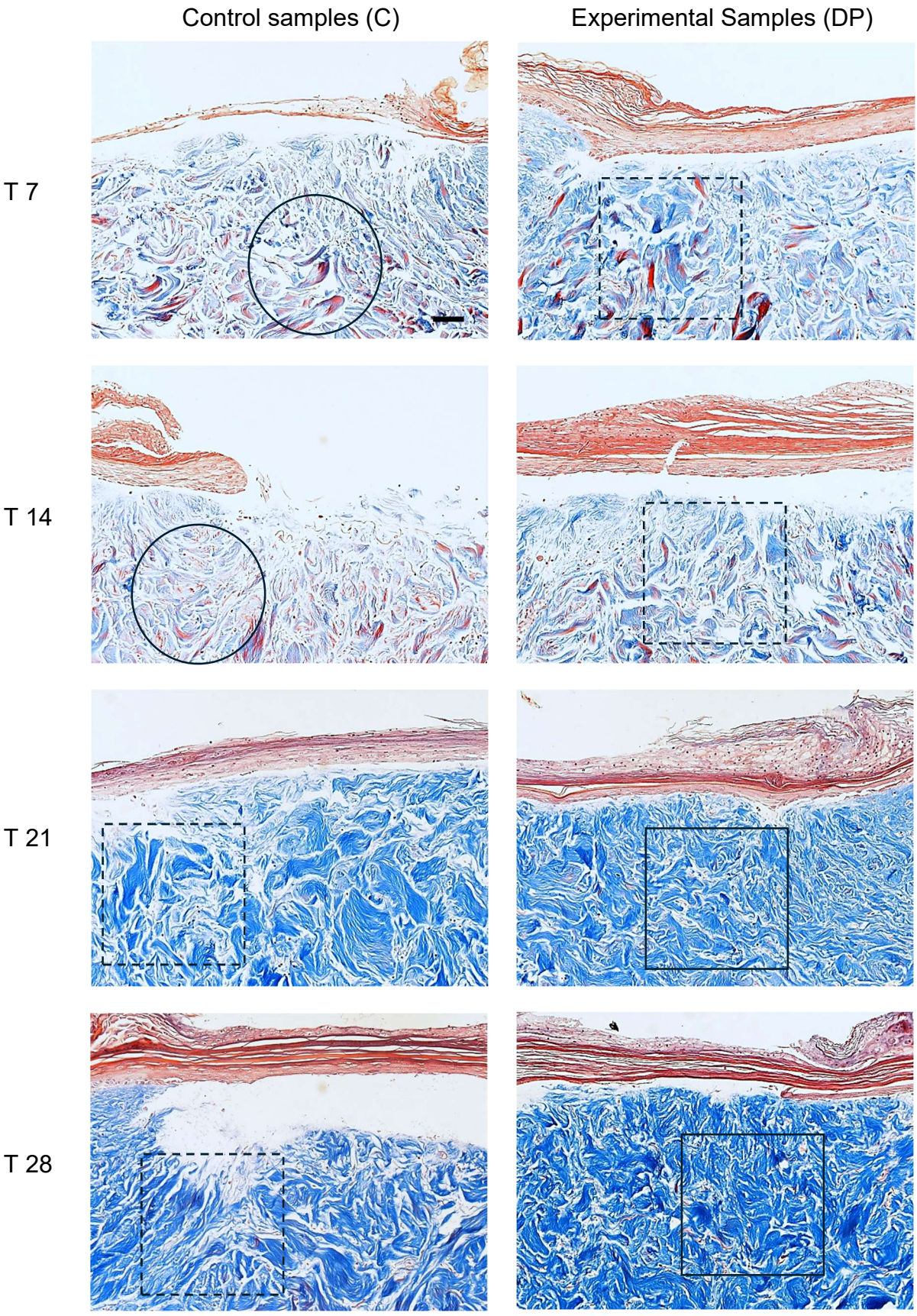

Figure 29 - Masson's trichrome staining in the different culture conditions at the different time points. Control (C): sample maintained with a flow of DMEM and DMEM within the lesion. Experimental sample (DP): sample maintained with a flow of DMEM and DMEM enriched with PRP within the lesion. DMEM: Dubecco's Modified Eagle Medium; PRP, Platelet Rich Plasma. Sample maintenance time: T7 – T28.
Magnification: 10x. Scale bar: 100 μm. Black circle = chaotic reticular collagen fibers' orientation; square = parallel reticular collagen fibers' orientation; dotted line square = perpendicular reticular collagen fibers' orientation.

4.3. Weigert staining

The Weigert staining results of both control (C) and experimental (DP) samples are comprehensively summarised in Table 10 and Figure 30.

Control samples (C)

At T7, T14, T21 and T28, there was a modest presence of elastic fibres and the coexistence of fragmented and long fibres was observable, although their distribution was different. In particular, long elastic fibres were observed in the most superficial portion of the dermis at the site of the lesion. On the other hand, fragmented elastic fibres, also at the site of the lesion, were distributed evenly. The orientation of the elastic fibres at the site of the injury was parallel to the surface at T7, T14, T21 and T28, although at T7 the orientation at the margins of the injury was perpendicular.

Experimental samples (DP)

At T7 and T14,there was a limited presence of elastic fibres, with an increasing tendency at T21 and subsequently at T28. At T7, the co-existence of fragmented and long elastic fibres showed a different distribution. In particular, structured fibres were observed at the borders of the injury and in the deeper portions of the dermis at the site of injury, while fragmented fibres were found in greater quantities in the superficial portion of the wound. At T14, fragmented elastic fibres were located in the superficial portion of the dermis, while structured elastic fibres were present in greater quantities and tended to be more uniformly distributed in the dermal tissue. At T21 and T28, fragmented elastic fibres tended to decrease, while structured elastic fibres showed an increasingly uniform distribution in the dermal tissue. In contrast, the orientation of the elastic fibres at T7 was perpendicular to the margins of the injury, and parallel to the

surface at the site of the injury. At T14, the orientation was perpendicular, then assumed to be parallel to the surface at T21 and T28.

Table 10 - Semi-quantitative analysis of tissue and cellular characteristics.

		T7	T14	T21	T28
C	Elastic fibers' amount	++	++	++	++
	Elastic fibers' integrity	++	++	++	++
	Elastic fibers' orientation	++	++	++	+++
DP	Elastic fibers' amount	++	++	+++	+++
	Elastic fibers' integrity	++	+++	++	++
	Elastic fibers' orientation	+++	++	+++	+++

Elastic fibers' amount: + = minimal, ++ = moderate, +++ = abundant
Elastic fibers' integrity: + = fragmented fibers, ++ = blended fragmented and long fibers, +++ = long fibers
Elastic fibers' orientation: + = poorly organized, ++ = perpendicular to the skin surface, +++ = parallel to the skin surface

Figure 30 - Weigert staining

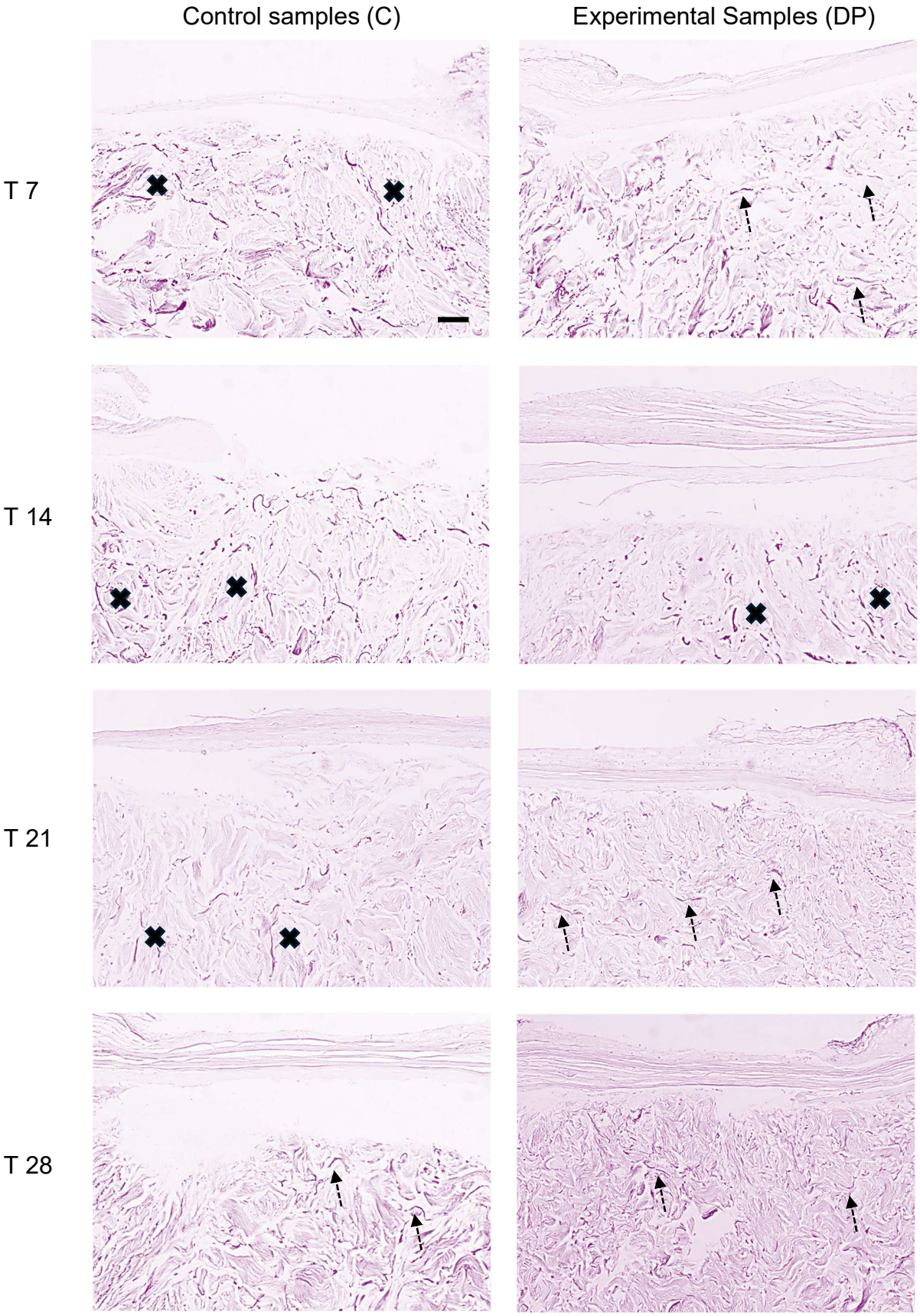

Figure 30 - Weigert staining in the different culture conditions at the different time points. Control (C): sample maintained with a flow of DMEM and DMEM within the lesion. Experimental sample (DP): sample maintained with a flow of DMEM and DMEM enriched with PRP within the lesion. DMEM: Dubecco's Modified Eagle Medium; PRP, Platelet Rich Plasma. Sample maintenance time: T7 – T28.
Black asterisk = poorly organized elastic fibers; black cross = parallel elastic fibers' orientation; dotted arrow = perpendicular elastic fibers' orientation.

4.4. Ki-67 immunostaining

The ki-67 immunostaining results of both control (C) and experimental (DP) samples are comprehensively summarised in Table 8 and Figure 31. The regenerative re-epithelialization process was demonstrated by the Ki-67 positive nuclei.

Control samples (D)

At T7, T14 and T21, nuclear positivity was minimal at the margins of the injury, with a progressive tendency to decrease until to become zero at T28. The newly formed epithelial cell front showed nuclear positivity at moderate extent at T7 and T14. However, the progressive epithelial cell advancement front and stratification showed a decrease in nuclear positivity at T21, and no positivity at T28.

Experimental samples (DP)

At T7, nuclear positivity was abundant at the margins of the injury, with a tendency to decrease at T14 and T21, while no positivity was observed at T28. The newly formed epithelial cell front showed abundant nuclear positivity at T7. However, the progressive epithelial cell front advancement and stratification showed a decrease in nuclear positivity at T14 and T21, and no positivity at T28.

Figure 31 - Ki-67 immunostaining

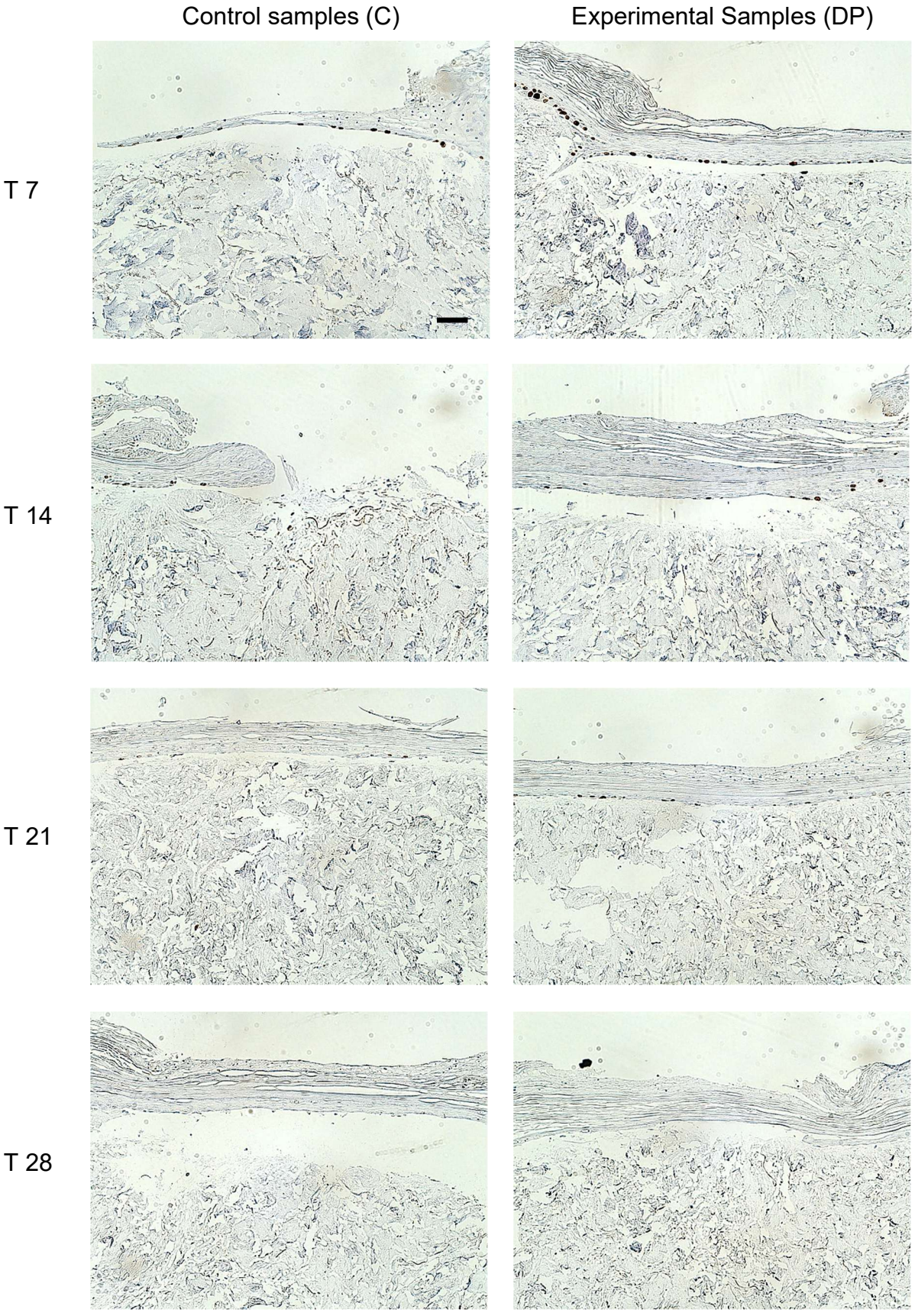

Figure 31 - Ki-67 immunostaining in the different culture conditions at the different time points. Control (C): sample maintained with a flow of DMEM and DMEM within the lesion. Experimental sample (DP): sample maintained with a flow of DMEM and DMEM enriched with PRP within the lesion. DMEM: Dubecco's Modified Eagle Medium; PRP, Platelet Rich Plasma. Sample maintenance time: T7 – T28. In brown color the Ki-67-positive nuclei.

CHAPTER 5

DISCUSSION

The research project is aligned with the objectives of the 3R Centre which, together with European Directive No. 63/2010, represent the fundamental ethical principles of scientific research. These objectives are: reducing the number of animals used in experiments, refining experimental procedures to reduce stress and suffering in the animals involved, and replacing animals in experiments with new experimental models. Although some of these objectives have not yet been completely achieved, continuous progress in biomedical research has allowed the development of new techniques and experimental models. In particular, in recent decades, Regenerative Medicine, born as a new branch of Medical Sciences, has emerged and developed with the aim of regenerating damaged body structures and restoring their functions.

In recent years there has been a growing number of therapeutic applications able to stimulate tissue regeneration processes. The progressive reduction in the use of animal testing and the advent of regenerative solutions that overcome the limits of healing by repair also in humans has led to a synergic development of ethically and functionally valid experimental models allowing the demonstration of regenerative processes in the human species. In particular, Platelet Rich Plasma (PRP), an excellent reservoir of growth factors, is a key element in regenerative medicine and inductive surgery. Although this new revolutionary approach represents a transition from the traditional concept of healing through scarring to an innovative concept of healing through tissue regeneration, this new vision of medicine still requires numerous extensive studies (Hersant et al., 2017; Phoebe et al., 2024; Mert et al., 2025).

This research project involved the use of PRP, with a twofold aim: the increase in the useful viability of the experimental wound model on *ex-vivo* human skin culture and the demonstration of its regenerative efficacy in the experimental wound healing process. The concentration of PRP was derived from data in literature (Okuda et al., 2003;

Masuki et al., 2016) and from our laboratory experience with *ex-vivo* cultures on human skin fragments (Nicoletti et al., 2019). The ideal experimental model for studying regenerative processes and, consequently, wound healing, is represented by the fragment of damaged skin. Over the years, several studies have been conducted using this model, involving the use of substances with regenerative properties (Nicoletti et al., 2017; Nicoletti et al., 2019; Nicoletti et al., 2023). The latest evolution of this experimental wound model on ex vivo human skin culture in a continuous peristaltic perfusion system represents, at present, the best approximation to the physiological conditions of living human skin for the study of the wound healing process and for the potential development of tissue regeneration in humans. Additionally, the use of this experimental model required a level of cooperation and organisation between different entities: Azienda Socio-Sanitaria Territoriale (ASST) of Pavia, the Experimental Surgery Laboratory of the Department of Clinical-Surgical Diagnostic and Pediatric Sciences of the University of Pavia and the Pathological Anatomy Laboratory of the IRCCS Galeazzi – S. Ambrogio of Milano. The synergistic action adopted between apparently different structures has become a key strength in the medical-biological and biotechnological context, elevating the quality of basic research.

In literature, a study conducted by Cipriani Frade et al. (2015) demonstrated the viability of skin samples for up to 75 days. In this study, tissue explants, standardised in 1.0 cm^2 fragments, were maintained in *ex vivo* culture on metal supports inside multiwells, guaranteeing the dermal interface with DMEM supplemented with Fetal Bovine Serum (10%), L-glutamine (1%) and antibiotics and antifungals (1%) and incubated under controlled conditions (37 °C, 5% CO_2 in a humidified atmosphere). The primary objective of this study is to validate an innovative experimental biotechnological protocol for *ex vivo* culture of damaged skin. This protocol differs from

current static models thanks to the integration of a fluid-dynamic culture medium system, aimed at simulating the physiological turnover of the medium. Cell viability and histological integrity of samples were weekly monitored, extending the observation up to a maximum of 28 days. Macroscopic analysis conducted systematically during the experimental process has not revealed areas of tissue necrosis in any of the samples analysed for its entire lenght. This clinical evidence was supported by microscopic analysis, which documented the maintenance of cell viability and histological architecture up to day 28.

The secondary objective was to compare the effects of DMEM added to PRP with those of DMEM alone in the wound healing process. The action of PRP within the lesion not only has favoured the healing process but has also increased the vitality of the skin samples. In particular, macroscopic analysis conducted during the experiments has shown that a bright pink colour remained until day 14, while in the control samples this characteristic was maintained up to a maximum of 7 days with a tendency towards yellowing but without tissue necrosis.

Microscopic analysis showed that PRP has stimulated and promoted the wound re-epithelialisation process. Although the dynamic mechanisms of re-epithelialisation are currently under investigation, the sliding and rolling models proposed by Usui et al. (2005) appear to be equally involved. Furthermore, PRP seems to promote fibroblast proliferation and lymphoplasmacytic infiltrate. A progressive increase was observed within 15 days, followed by a gradual decrease. The minimal presence of cellular elements was comparable to the control samples, whose parameters did not change in time. Immune stimulation seems to play an important role in regeneration mechanisms through controlled anti-inflammatory action. The experimental samples showed progressive and regular organization of the dermis compared to the control,

both in the interfibrillar spaces and in the size of the collagen fibres. However, the coexistence of thick and thin collagen fibres was consistently observed, but with a tendency towards thick fibres observable on day 28 compared to the control, in which this characteristic was highlighted in previous experimental times.

Through Masson's trichrome staining, a peculiar characteristic was observed in some thin and thick collagen fibres. In particular, on days 7 and 14, the control and experimental samples showed red staining in some fibres. The cause could be a reduction in the permeability of collagen fibres due to the action of metalloproteinases (Bancroft and Stevens, 1982) or other as yet unknown factors involved in a process of fibre maturation or degradation. Furthermore, a different spatial distribution of collagen fibres was observed. In the samples treated with PRP, the fibres were chaotically distributed on day 7, then oriented perpendicular to the surface on days 14 and 21, and finally parallel on day 28. In contrast, the fibres' orientation in the control samples was the same as in the experimental samples on days 7 and 14, while an orientation parallel to the surface was obtained on day 21. This possible spatial difference in collagen fibres could be due to the action of type 1 metalloproteinases involved in degradation and remodelling processes, but slowed by the presence and modulatory action of PRP.

The experimental samples showed a small increase in the quantity of elastic fibres on days 21 and 28, compared to the controls, while integrity remained constant over time in both experimental conditions. The orientation has shown a different distribution compared to collagen fibres. In particular, the experimental samples showed a constant parallel orientation to the surface on days 7, 21 and 28, while on day 14 the fibres assumed a perpendicular orientation. In the control samples, the perpendicular orientation of the elastic fibres was maintained until day 21, subsequently the fibres

assumed an orientation parallel to the surface. A possible explanation could be the action of elastase in the dermis, which is slowed by PRP, while in the control samples, the increased activity of this enzyme could promote progressive disorganisation of the elastic fibers.

CHAPTER 6

CONCLUSION

The experimental *ex-vivo* culture model included in a dynamic fluidic circuit confirmed its validity in maintaining the viability of human skin samples for up to 28 days after explantation. PRP added to conventional DMEM within the wound has shown good ability to accelerate the tissue regeneration process. It also has stimulated and modulated fibroblasts and lymphoplasmacytic infiltrate. Although further studies are required, PRP appears to act on the collagen fibers reorganisation process, also promoting elastic fibers orientation similar to their physiological conditions.

Comparative studies will be necessary to evaluate the effectiveness of the dynamic model validated in this study compared to conventional static culture protocols. The future objective will be to determine if the implementation of the fluid dynamic circuit is able to extend the tissue viability of the explants beyond the 75 days currently documented for static models.

Finally, this developed protocol can be considered the closest possible reproduction of human skin in living beings' conditions, allowing for greater efficacy and accuracy than in the experimental animal models for testing pharmacological molecules, reducing the use of animals and cosmetic substances for which animal testing is prohibited, and a virtuous use of animal models.

REFERENCES AND WEBSITES

Abraham J., Mathew S. *Merkel Cells: A Collective Review of Current Concepts*. International Journal of Applied Basic Medical Research. 2019; 9: 9-13, doi: 10.4103/ijabmr.IJABMR_34_18

Akbarzadeh S., McKenzie M.B., Rahman M. *Allogeneic Platelet-Rich Plasma: Is It Safe and Effective for Wound Repair?.* European Surgery Research. 2021; 62: 1-9, doi: 10.1159/000514223

Alsousou J., Ali A., WIllet K., Harrison P. *The role of platelet rich plasma in tissue regeneration.* Platelets. 2013; 24: 173-182, doi: 10.3109/09537104.2012.684730

Anthonu B., Link D. *Regulation of hematopoietic stem cells by bone marrow stromal cells.* Trends in Immunology. 2014; 35: 32-37, doi: 10.1016/j.it.2013.10.002

Armulik A., Genové G., Betsholtz C. *Pericytes: developmental, physiological, and pathological perspectives, problems, and promises.* Developmental Cell. 2011; 21: 193-215, doi: 10.1016/j.devcel.2011.07.001

Bancroft J. and Stevens, A. *Theory and Practice of Histotechnology*. 1982; 2nd Ed. New York, NY: Churchill-Livingston

Barbosa F., Chaurasia S., Cutler A., Asosingh K., Kaur H., de Medeiros F., Agrawal V., Wilson S. *Corneal myofibroblast generation from bone marrow-derived cells.* Experimental Eye Research Journal. 2010; 91: 92-96, doi: 10.1016/j.exer.2010.04.007

Barletta M. *Animal testing in Europe: the incidence of directive 2010/63 eu among Member States and its role in the development of the covid-19 vaccine.* BioLaw Journal. 2021; doi: 10.15168/2284-4503-808

Biga L.M., Bronson S., Dawson S., Harwell A., Hopkins R., Kaufmann J., LeMaster M., Matern P., Morrison-Graham K., Oja K., Quick D., Runyeon J. *Anatomy & Physiology.* 2019; 1st edition, OpenStax

Blair P., Faumenhaft R.. *Platelet α–granules: Basic biology and clinical correlates.* Blood Reviews. 2010; 23: 177-189, doi: 10.1016/j.blre.2009.04.001

Blanco R., Gerhardt H. *VEGF and Notch in Tip and Stalk Cell Selection.* Cold Spring Harbor Perspectives in Medicine Journal. 2013; 3: a006569, doi: 10.1101/cshperspect.a006569

Bodnar R. *Chemokine regulation of angiogenesis during wound healing.* Advances in wound care (New Rochelle). 2015; 4: 641-650, doi: 10.1089/wound.2014.0594

Blanpain C., Fuchs E. *Stem cell plasticity. Plasticity of epithelial stem cells in tissue regeneration.* Science. 2014; 344: 1242281, doi: 10.1126/science.1242281

Bonham C.A., Kuehlmann B, Gurtner GC. *Impaired neovascularization in aging*. Advances in Wound Care. 2020; 9: 111−126, doi: 10.1089/wound.2018.0912

Borregaard N., Cowland J.B. *Granules of the human neutrophilic polymorphonuclear leukocyte.* Blood. 1997; 89: 3503-3521

Bos J.D., Teunissen M.B., Cairo I., Krieg S.R., Kapsenberg M.L., Das P.K., Borst J. T-*cell receptor gamma delta bearing cells in normal human skin.* Journal Investigative Dermatology. 1990; 94: 37-42, doi: 10.1111/1523-1747.ep12873333

Burnouf T., Goubran H.A., Chen T., Ou K., El-Ekiaby, M., Radosevic, M. *Blood-derived biomaterials and platelet growth factors in regenerative medicine.* Blood Reviews. 2013; 27: 77-89, doi: 10.1016/j.blre.2013.02.001

Caley M.P., Martins V.L., O'Toole E.A. *Metalloproteinases and Wound Healing.* Advances in wound care (New Rochelle). 2015; 4: 225–234, doi: 10.1089/wound.2014.0581

Cappellozza E., Boschi F., Sguizzato M, Esposito E, Cortesi R., Malatesta M., Calderan L. *A spectrofluorometric analysis to evaluate transcutaneous biodistribution*

of fluorescent nanoparticulate gel formulations. European Journal of Histochemistry. 2022; 66: 3321

Cappellozza E, Zanzoni S., Malatesta M., Calderan L. *Integrated Microscopy and Metabolomics to Test an Innovative Fluid Dynamic System for Skin Explants In-Vitro.* Microscopy and Microanalysis. 2021; 27: 923–934, doi: 10.1017/S1431927621012010

Caux M., Mansour R., Xuereb J., Chicanne G., Viaud J., Vauclard A., Boal F., Payrastre B., Tronchère H., Severin S. *PIKfyve-dependent Phosphoinisitide dynamics in megakaryocyte/platelet granule integrity and platelet functions.* Arteriosclerosis Thrombosis and Vascular Biology. 2022; 8: 987-1004, doi 10.1161/ATVBAHA.122.317559

Chen Y., Yuan Y., Li W.. *Sorting machineries: how platelet-dense granules differ from α-granules.* Bioscencie Reports. 2018; 38: BSR20180458, DOI: 10.1042/BSR20180458

Chodaczek G., Papanna V., Zal M.A., Zal T. *Body barrier surveillance by epidermal gammadelta TCR.* Nature Immunology. 2012; 13: 272-282, doi: 10.1038/ni.2240

Cipriani Frade M.A., Moretti de Andrade T.A., Aguiar A.F., Guedes F.A., Leite M., Rodrigues Passos W., Barbosa Coelho E., Kummar Das P. *Prolonged viability of human organotypic skin explant in culture method (hOSEC).* Anais Brasileiros de Dermatologia. 2015; 90: 347-350, doi: 10.1590/abd1806-4841.20153645

Cole B.J., Seroyer S.T., Filardo G., Bajai S., Fortier L.A. *Platelet-Rich Plasma: Where Are We Now and Where Are We Going?*. Sports Health. 2010; 2: 203-210, doi: 10.1177/1941738110366385

Costin G.E., Hearing V.J. *Human skin pigmentation: melanocytes modulate skin color in response to stress.* Federation of American Societies for Experimental Biology Journal. 2007; 21: 976–994, doi: 10.1096/fj.06-6649rev

Crisan M., Yap S., Casteilla L., Che C.W., Corselli M., Soon Park T., Andriolo G., Sun B., Zheng B., Zhang L., Norotte C., Teng P.N., Traas J., Schugar R., Deasy B., Badylak S., Buhring H.J., Giacobino J.P., Lazzari L., Huard J., Péault B. *A perivascular origin for mesenchymal stem cells in multiple human organs.* Cell Stem Cell. 2008; 3: 301-313, doi: 10.1016/j.stem.2008.07.003

Currie L.J., Sharpe J.R., Martin R. *The use of fibrin glue in skin grafts and tissue-engineered skin replacements: a review.* Plastic and Reconstructive Surgery, 2001; 108: 1713-1726, doi: 10.1097/00006534-200111000-00045

desJardins-Park H.E., Foster D.S., Longaker M.T. *Fibroblasts and wound healing: an update.* Regenerative Medicine. 2018; 13: 491-495, doi: 10.2217/rme-2018-0073

Deutsch V.R., Tomer A. *Megakaryocyte development and platelet production. British Journal of Haematology*. 2006; 134: 453-466, doi: 10.1111/j.1365-2141.2006.06215.x

Doupé D.P., Jones P.H. *Interfollicular epidermal homeostasis: dicing with differentiation.* Experimental Dermatology. 2012; 21: 249-253, doi: 10.1111/j.1600-0625.2012.01447.x

Driskell R., Lichtenberger B., Hoste E., Kretzschmar K., Simons B., Charalambous M., Ferron S., Herault Y., Pavlovic G., Ferguson-Smith A., Watt F. *Distinct fibroblast lineages determine dermal architecture in skin development and repair.* Nature. 2013; 504: 277-281, doi: 10.1038/nature12783

Du R.; Lei T. Effects of Autologous Platelet-rich *Plasma Injections on Facial Skin Rejuvenation.* Experimental and Therapeutic Medicine. 2020; 19: 3024–3030, doi: 10.3892/etm.2020.8531

Edelstein L.C., Bray P.F. *MicroRNAs in platelet production and activation.* Blood. 2011; 117: 5289-5296, doi: 10.1182/blood-2011-01-292011

Endele M., Etzrodt M., Schroeder T. *Instruction of hematopoietic lineage choice by cytokine signaling.* Experimental Cell Research. 2014; 329: 207-213. doi: 10.1016/j.yexcr.2014.07.011

Eppley B. L., Woodell J. E., Higgins J. B.S. *Platelet Quantification and Growth Factor Analysis from Platelet-Rich Plasma: Implications for Wound Healing.* Plastic and Reconstructive Surgery. 2004; 114: 1502-1508, doi: 10.1097/01.PRS.0000138251.07040.51

Fackler M.J., Krause D.S., Smith O.M., Civin C.I., May W.S. *Full-length but not truncated CD34 inhibits hematopoietic cell differentiation of M1 cells.* Blood. 1995; 85: 3040-3047

Freson K., Devriendt K., Matthijs G., Van Hoof A., De Vos R., Thys C., Minner K., Hoylaerts M.F., Vermylen J., Van Geet C. *Platelet characteristics in patients with X-linked macrothrombocytopenia because of a novel GATA1 mutation.* Blood. 2001; 98: 85-92, doi: 10.1182/blood.v98.1.85

Fujiwara H., Ferreira M., Donati G., Marciano D., Linton J., Sato Y., Hartner A., Sekiguchi K., Reichardt L., Watt F. *The basement membrane of hair follicle stem cells is a muscle cell niche.* Cell. 2011; 18: 577-589, doi: 10.1016/j.cell.2011.01.014

Galli S.J., Borregaard N., Wynn T.A. *Phenotypic and functional plasticity of cells of innate immunity: macrophages, mast cells and neutrophils.* Nature Immunology. 2011; 12: 1035-1044, doi: 10.1038/ni.2109

Galligan C., Fish E. *The role of circulating fibrocytes in inflammation and autoimmunity.* Journal of Leukocyte Biology. 2013; 93: 45-50, doi: 10.1189/jlb.0712365

Gao Y., Smith E., Ker E., Campbell P., Cheng E., Zou S., Lin S., Wang L., Halene S., Krause D.S. *Role of RhoA-specific guanine exchange factors in regulation of endomitosis in megakaryocytes.* Developmental Cell. 2012; 22: 573-584, doi: 10.1016/j.devcel.2011.12.019

Gartner L.P., Hiatt J.M. *Istologia.* 2024; 8th edition, Piccic

Gebhardt T., Whitney P.G., Zaid A., Mackay L.K., Brooks A.G., Heath W.R., Carbone F.R., Mueller S.N. *Different patterns of peripheral migration by memory CD4+ and CD8+ T cells.* Nature. 2011; 477: 216-219, doi: 10.1038/nature10339

Gentile P., De Angelis B., Agovino A., Orlandi F., Migner A., Di Pasquali C., Cervelli V., *Uso of Platelet Rich Plasma and Hyaluronic Acid in the treatment of complications of Achilles tendon reconstruction.* World Journal of Plastic Surgery. 2016; 5: 124-132

Gerhardt H., Goldin M., Fruttiger M., Ruhrberg C., Lundkvist A., Abramsson A., Jeltsch M., Mitchell C., Alitalo K., Shima D., Betsholtz C. *VEGF guides angiogenic sprouting utilizing endothelial tip cell filopodia.* Journal of Cell Biology. 2003; 161: 1163-1177, doi: 10.1083/jcb.200302047

Gilaberte Y., Prieto-Torres I., Pastushenko I., Juarranz Á. *Anatomy and Function of the Skin.* Nanoscience in Dermatology. 2016; pp 1-14, doi: 10.1016/B978-0-12-802926-8.00001-X

Godo S., Shimokawa H. *Endothelial functions.* Arteriosclerosis, Thrombosis, and Vascular Biology. 2017; 37: e108-e114, doi: 10.1161/ATVBAHA.117.309813

Goldberg M.T., Han Y.P., Yan C., Shaw M.C., Garner W.L. *TNF-alpha suppresses alphasmooth muscle actin expression in human dermal fibroblasts: an implication for abnormal wound healing.* Journal of Investigative Dermatology. 2007; 127: 2645-2655, doi: 10.1038/sj.jid.5700890

Golebiewska E., Poole A. *Platelet secretion: From haemostasis to wound healing and beyond*. Blood Reviews. 2015; 29: 153-162, doi: 10.1016/j.blre.2014.10.003

Gurtner G., Werner S., Barrandon Y., Longaker M. *Wound repair and regeneration*. Nature. 2008; 456: 314-321, doi: 10.1038/nature07039

Hajar R. *Animal testing and medicine*. Heart Views. 2011; 12, p 42, doi: 10.4103/1995-705X.81548

Harper R.A., Grove G. *Human skin fibroblasts derived from papillary and reticular dermis: differences in growth potential in vitro*. Science. 1979; 204: 526-527, doi: 10.1126/science.432659

Havran W.L., Jameson J.M. *Epidermal T Cells and Wound Healing*. The Journal of Immunology. 2011; 15: 5423-5428, doi: 10.4049/jimmunol.0902733

Heath W.R., Carbone F.R. *The skin-resident and migratory immune system in steady state and memory: innate lymphocytes, dendritic cells and T cells*. Nature Immunology. 2013; 14: 978-985, doi: 10.1038/ni.2680

Hersant B., La Padula S., SidAhmed-Mezi M., Rodriguez A.M., Meningaud J.P. *Use of platelet-rich plasma (PRP) in microsurgery.* Journal of Stomatology Oral and Maxillofacial Surgery. 2017; 118: 236-237, doi: 10.1016/j.jormas.2017.05.009

Italiano J., Lecine P., Shivdasani R., Hartwig J. *Blood platelets are assembled principally at the ends of proplatelet processes produced by differentiated megakaryocytes.* The Journal Cell Biology. 1999; 147: 1299-1312, doi: 10.1083/jcb.147.6.1299

Ito M., Liu Y., Yang Z., Nguyen J., Liang F., Morris R.J., Cotsarelis G. *Stem cells in the hair follicle bulge contribute to wound repair but not to homeostasis of the epidermis*. Nature Medicine. 2005*;* 11: 1351–1354, doi: 10.1038/nm1328

Jameson J., Ugarte K., Chen N., Yachi P., Fuchs E., Boismenu R., Hayran W.L. *A role for skin gammadelta T cells in wound repair.* Scienze. 2002; 296: 747-749, doi: 10.1126/science.1069639

Jones P., Simons B.D. *Epidermal homeostasis: do committed progenitors work while stem cells sleep?.* Nature Reviews Molecular Cell Biology. 2008; 9: 82-88, doi: 10.1038/nrm2292

Jorch S.K., Kubes P*. An emerging role for neutrophil extracellular traps in noninfectious disease*. Nature Medicine. 2017, 23: 279-287, doi: 10.1038/nm.4294

Kaushansky K. *Lineage-specific hematopoietic growth factors*. The New England Journal Medicine. 2006; 354: 2034-2045, doi: 10.1056/NEJMra052706

Kaushansky K. *The molecular mechanisms that control thrombopoiesis*. The Journal Clinical Investigation. 2005; 115: 3339-3347, doi: 10.1172/JCI26674

Kawase T. *Platelet-rich plasma and its derivatives as promising bioactive materials for regenerative medicine: basic principles and concepts underlying recent advances*. Odontology. 2015; 103: 126–135, 10.1007/s10266-015-0209-2

Keyes B.E., Liu S., Asare A., Naik S., Levorse J., Polak L., Lu C.P., Nikolova M., Pasolli H.A., Fuchs E. *Impaired Epidermal to Dendritic T Cell Signaling Slows Wound Repair in Aged Skin*. Cell. 2016; 167: 1323-1338.e14, doi: 10.1016/j.cell.2016.10.052

Korosec A., Frech S., Gesslbauer B., Vierhapper M., Radtke C., Petzelbauer P., Lichtenberger B.M. *Lineage Identity and Location within the Dermis Determine the Function of Papillary and Reticular Fibroblasts in Human Skin*. Journal of Investigative Dermatology. 2019; 139: 342-351, doi: 10.1016/j.jid.2018.07.033

Leask A. *Potential therapeutic targets for cardiac fibrosis: TGFbeta, angiotensin, endothelin, CCN2, and PDGF, partners in fibroblast activation.* Circulation Research. 2010; 106: 1675–1680, doi: 10.1161/CIRCRESAHA.110.217737

Lebonvallet, N., Jeanmaire, C., Danoux, L., Sibille, P., Pauly, G., and Misery, L. *The evolution and use of skin explants: Potential and limitations for dermatological research.* European Journal of Dermatology. 2010; 20: 671–684, doi: 10.1684/ejd.2010.1054

Lech M., Anders H.J. *Macrophages and fibrosis: how resident and infiltrating mononuclear phagocytes orchestrate all phases of tissue injury and repair*. Biochimica et Biophysica Acta (BBA) - Molecular Basis of Disease. 2013, 7: 989-997, doi: 10.1016/j.bbadis.2012.12.001

Lentz B. *Exposure of platelet membrane phosphatidylserine regulates blood coagulation.* Progress in Lipid Research. 2003; 42: 423-438, doi: 10.1016/s0163-7827(03)00025-0

Lotfollahi Z. *The anatomy, physiology and function of all skin layers and the impact of ageing on the skin*. Wound Practice and Research. 2024; 32: 6-10, doi: 10.33235/wpr.32.1.6-10

Machlus K.,Italiano J. *The incredible journey: From megakaryocyte development to platelet formation.* Journal Cell Biology. 2013; 201: 785-796, doi.org/10.1083/jcb.201304054

Mackenzie I.C. *Relationship between mitosis and the ordered structure of the stratum corneum in mouse epidermis*. Nature. 1970; 226: 653–655, doi: 10.1038/226653a0

Manole C.G., Soare C., Ceafalan L.C., Voiculescu V.M. *Platelet rich plasma in dermatology: new insights on the cellular mechanism of skin repair and regeenration*. Life. 2023; 14: 40, doi: 10.3390/life14010040

Marx, R.E. *Platelet Rich Plasma: evidence to support its use*. Journal of Oral Maxillofacial Surgery. 2004; 62: 489-496, doi: 10.1016/j.joms.2003.12.003

Mascré G., Dekoninck S., Drogat B., Youssef K.K., Broheé S., Sotiropoulou P.A., Simons B.D., Blanpain C. *Distinct contribution of stem and progenitor cells to epidermal maintenance.* Nature. 2012; 489: 257–262, doi: 10.1038/nature11393

Masuki H., Okudera T., Watanebe T., Suzuki M., Nishiyama K., Okudera H., Nakata K., Uematsu K., Su C., Kawase T. *Growth factor and proinflammatory cytokine contents in plateletrich plasma (PRP), plasma rich in growth factors (PRGF), advanced*

plateletrich fibrin (A-PRF), and concentrated growth factors (CGF). The International Journal of Implant Dentistry. 2016; 2:19, doi: 10.1186/s40729-016-0052-4

Matins-Green M., Petreaca M., Wang L. *Chemokines and Their Receptors Are Key Players in the Orchestra That Regulates Wound Healing*. Advances in Wound Care (New Rochelle). 2013; 2: 327-347, doi: 10.1089/wound.2012.0380

Mazzi S., Lordier L., Debili N., Raslova H., Vainchenker W. *Megakaryocyte and polyploidization.* Experimental Hematology. 2018; 57: 1-13, doi: 10.1016/j.exphem.2017.10.001

Mehdipour K., Enderami S.E., Mansour R.N., Hasanzadeh E., Mahabadi, Mohamadfoad Abazari J.A., Asadi P., Hojjat A. *Applications of blood plasma derivatives for cutaneous wound healing: A mini-review of clinical studies*. Regenerative Therapy. 2024; 27: 251-258, doi: 10.1016/j.reth.2024.02.011

Mendelson A., Frenette P. *Hematopoietic stem cell niche maintenance during homeostasis and regeneration.* Nature Medicine. 2014; 20: 833-846, doi: 10.1038/nm.3647

Mendoza-Garcia J., Sebastian A., Alonso-Rasgado T., Bayat A. *Optimization of an ex vivo wound healing model in the adult human skin: functional evaluation using photodynamic therapy.* Wound Repair and regeneration. 2015; 100: 685-702, doi: 10.1111/wrr.12325

Mert A., Keles A.I., Aydin M., Erol H.S., Sonmez O.F. *The role of PRP in the healing of disc degeneration and the effect of local anesthetics on PRP*. Frontiers in Bioengineering and Biotechnology. 2025; 13: 1613148, doi: 10.3389/fbioe.2025.1613148

Mine S., Fortunel N.O., Pageon H., Asselineau D. *Aging Alters Functionally Human Dermal Papillary Fibroblasts but Not Reticular Fibroblasts: A New View of Skin Morphogenesis and Aging.* PLoS One. 2008, 3: e4066, doi: 10.1371/journal.pone.0004066

Mirastschijski U., Haaksma C.J., Tomasek J.J., Agren M.S. *Matrix metalloproteinase inhibitor GM 6001 attenuates keratinocyte migration, contraction and myofibroblast formation in skin wounds.* Experimental Cell Research. 2004; 299: 465-475, doi: 10.1016/j.yexcr.2004.06.007

Mitiavila Garcia M.T., Cailleret M., Godin I., Nogueira M.M., Cohen Solal K., Schiavon V., Lecluse Y., Le Pesteur F., Lagrue A.H., Vainchenker W. *Expression of CD41 on hematopoietic progenitors derived from embryonic hematopoietic cells*. Development. 2002; 129: 2003-2013, doi: 10.1242/dev.129.8.2003

Nagaoka T., Kaburagi Y., Hamaguchi Y., Hasegaea M., Takehara K., Steeber D., Tedder T., Sato S. *Delayed wound healing in the absence of intercellular adhesion molecule-1 or L-selectin expression*. The American Journal of Pathology. 2000; 157: 237-247, doi: 10.1016/S0002-9440(10)64534-8

Napolitano F., Postiglione L., Mormile I., Barrella V., De Paulis A., Montuori N., Rossi F.W. *Water from Nitrodi's springs induces dermal fibroblast and keratinocyte activation, thus promoting wound repair in the skin: an in vitro study*. International Journal of Molecular Sciences. 2023; 24, p 5357, doi: 10.3390/ijms24065357

Neagu M., Constantin C., Jugulete G., Cauni V., Dubrac S., Gabor Szollosi A., Zurac S. *Langerhans Cells—Revising Their Role in Skin Pathologies*. Journal Personalized Medicine. 2022; 12: p 2072, doi: 10.3390/jpm12122072

Nichols K.E., Crispino J.D., Poncz M., White J.G., Orkin S.H., Maris J.M., Weiss M.J. *Familial dyserythropoietic anaemia and thrombocytopenia due to an inherited mutation in GATA1*. Nature Genetics. 2000; 24: 266-270, doi: 10.1038/73480

Nicoletti G., Saler M., Pellegatta T., Tresoldi M.M., Bonfanti V., Malovini A., Faga A., Riva F. *Ex-vivo regenerative effects of a spring water.* Biomedical Reports. 2017; 7: 508-514, doi: 10.3892/br.2017.1002

Nicoletti G., Saler M., Tresoldi M.M., Scevola S., Faga A. *Unrecognized cell torpidity as a risk factor in elective plastic surgery.* Plastic and Reconstructive Surgery—Global Open. 2018; 6: e1727, doi: 10.1097/GOX.0000000000001727

Nicoletti G., Saler M., Tresoldi M.M., Villani L., Tottoli E.M., Jousson O., Faga A. *Effects of Comano spring water-derived bacterial lysates on skin regeneration: an ex-vivo study.* In Vivo. 2023; 37: 2498-2509, doi: 10.21873/invivo.13357

Nicoletti G., Saler M., Villani L., Rumolo A., Tresoldi M.M., Faga A. *Platelet Rich Plasma enhancement of skin regeneration in an ex-vivo human experimental model*. Frontiers in Bioengineering and Biotechnology. 2019; 7: 2, doi: 10.3389/fbioe.2019.00002

Noran H.M., Morsy A.A., Doaa A.H., Heba M.A. *Comparative Study on the Effect of Injectable Platelet Rich Plasma versus its Topical Application in the Treatment of Thermal Burn in Adult Male Albino Rat: Histological and Immunohistochemical Study.* The Egyptian Journal of Histology. 2021; 45: 125-135, doi: 10.21608/ejh.2021.58480.1420

Odell T.T., Jackson C.W. *Polyploidy and maturation of rat megakaryocytes*. Blood. 1968; 32: 102-110

Ogawa M. *Differentiation and proliferation of hematopoietic stem cells*. Blood. 1993; 81: 2844-2853

Okuda K., Kawase T., Momose M., Murata M., Saito Y., Suzuki H., Larry F.W., Yoshie H. *Platelet-rich plasma contains high levels of platelet-derived growth factor and transforming growth factor-β and modulates the proliferation of periodontally related cells in vitro*. Journal Periodontology. 2003; 74, 849–857, doi: 10.1902/jop.2003.74.6.849

Okuda K., Kawase T., Momose M., Murata M., Saito Y., Suzuki H., Wolff L.F., Yoshie, H. *Platelet-Rich Plasma contains high levels of platelet-derived growth factor and transforming growth factor-β and modulates the proliferation of periodontally related*

cells In Vitro. Journal of Periodontology. 2003; 74: 849–857, doi: 10.1902/jop.2003.74.6.849

Oskeritzian C.A. *Mast Cells and Wound Healing.* Advances in Wound Care (New Rochelle). 2012; 1: 23-28, doi: 10.1089/wound.2011.0357

Patel S.R., Richardson J.L., Schulze H., Kahle E., Galiart N., Drabek K., Shiydasani R.A., Hartwig J.H., Italiano J.E. *Differential roles of microtubule assembly and sliding in proplatelet formation by megakaryocytes*. Blood. 2005; 106: 4076-4085, doi: 10.1182/blood-2005-06-2204

Patel-Hett S., Wang H., Begonia A.J., Thon J.N., Alden E.C., Wandersee N.J., An X., Mohandas N., Hartwig J.H., Italiano J.E. *The spectrin-based membrane skeleton stabilizes mouse megakaryocyte membrane systems and is essential for proplatelet and platelet formation.* Blood. 2011; 118: 1641-1652, doi: 10.1182/blood-2011-01-330688

Pastar I., Stojadinovic O., Yin N.C., Ramirez H., Nusbaum A.G., Sawaya A., Patel S.B., Khalid L., Isseroff R.R., Tomic-Canic M. *Epithelialization in Wound Healing: A Comprehensive Review.* Advances in Wound Care. 2014; 3: 445-464, doi: 10.1089/wound.2013.0473

Peramo A. *Autologous cell delivery to the skin-implant interface via the lumen of percutaneous devices in vitro*. Journal of Funciotianl Biomaterials. 2010; 1: 14-21, doi: 10.3390/jfb1010014

Phoebe L.K.W., Lee K.W.A., Chan L.K.W., Hung L.C., Wu R., Wong S., Wan J., Yi K.H. *Use of platelet rich plasma for skin rejuvenation.* Skin Research and Technology. 2024; 30: e13714, doi: 10.1111/srt.13714

Pradhan S., Khatlani T., Nairn A., Vinod Vijayan K. *The heterotrimeric G protein Gβ1 interacts with the catalytic subunit of protein phosphatase 1 and modulates G protein-coupled receptor signaling in platelets.* Journal of Biological Chemistry. 2017; 292: 13133-13142, doi: 10.1074/jbc.M117.796656

Psaila B., Lyden D., Roberts I. *Megakaryocytes, malignancy and bone marrow vascular niches.* Journal of Thrombosis and Haemostasis. 2012; 10: 177-188, doi: 10.1111/j.1538-7836.2011.04571.x

Rinkevich Y., Walmsley G., Hu M., Zeshaan M., Newman A., Drukker M., Januszyk M., Krampitz G., Gurtner G., Lorenz H.P., Weissman I. Longaker M. *Skin fibrosis. Identification and isolation of a dermal lineage with intrinsic fibrogenic potential*. Science. 2015; 348: aaa2151, doi: 10.1126/science.aaa2151

Rippa A.L., Kalabusheva E.P., Vorotelyak E.A. *Regeneration of Dermis: Scarring and Cells Involved*. Cells. 2019; 8: 607, doi: 10.3390/cells8060607

Robb L. *Cytokine receptors and hematopoietic differentiation*. Oncogene. 2007; 15: 6715-6723. doi: 10.1038/sj.onc.1210756

Rodrigues M., Gurtner G. *Black, White, and Gray: Macrophages in Skin Repair and Disease.* Current Pathobiology Reports. 2017; 5: 333-342, doi: 10.1007/s40139-017-0152-8

Rodrigues M., Kosaric N., Bonham C., Gurtner G. *Wound healing: a cellular perspective.* Physiological Reviews - American Journal of Physiology. 2019; 99: 665-706, doi: 10.1152/physrev.00067.2017

Rognoni E., Gomez C., Pisco A., Rawlins E., Simons B., Watt F., Driskell R. *Inhibition of β-catenin signalling in dermal fibroblasts enhances hair follicle regeneration during wound healing*. Development. 2016; 143: 2522-2535, doi: 10.1242/dev.131797

Rompolas P., Mesa K.R., Greco V. *Spatial organization within a niche as a determinant of stem-cell fate*. Nature. 2013; 502: 513–518, doi: 10.1038/nature12602

Rozman P., Bolta Z. *Use of platelet growth factors in treating wounds and soft-tissue injuries.* Acta Dermatovenerologica. 2007; 16: 156-165, doi: 10.15570/actaapa.2025.12

Savagner P., Kusewitt D.F., Carver E.A., Magnino F., Choi C., Gridley T., Hudson L.G. *Developmental transcription factor slug is required for effective re-epithelialization by adult keratinocytes.* Journal of Cellular Physiology. 2005; 202: 858-866, doi: 10.1002/jcp.20188

Scadden D. *The stem-cell niche as an entity of action*. Nature. 2006; 441: 1075-1079. doi: 10.1038/nature04957

Schachtner H., Calaminus D.J., Sinclair A., Monypenny J., Blundell M.P., Leon C., Holyoake T.L., Thrasher A.J., Michie A.M., Vukovic M., Gachet C., Jones G.E., Thomas S.G., Watson S.P., Machesky L.M. *Megakaryocytes assemble podosomes that degrade matrix and protrude through basement membrane*. Blood. 2013; 28:2542-2552, doi: 10.1182/blood-2012-07-443457

Schrimpf C., Duffield J. *Mechanisms of fibrosis: the role of the pericyte*. Current Opinion in Nephrology and Hypertension. 2011; 20: 297-305, doi: 10.1097/MNH.0b013e328344c3d4

Schultz G., Davidson J., Kirsner R., Bornstein P., Herman I. *Dynamic reciprocity in the wound microenvironment*. Wound Repair and Regeneration. 2011; 19: 134-148, doi: 10.1111/j.1524-475X.2011.00673.x

Serini G., Bochaton-Piallat M.L., Ropraz P., Geinoz A., Borsi L., Zardi L., Gabbiani G. *The fibronectin domain ED-A is crucial for myofibroblastic phenotype induction by transforming growth factor-beta1*. Journal of Cell Biology. 1998; 142: 873–881, doi: 10.1083/jcb.142.3.873

Simpson R.M., Meran S., Thomas D., Stephens P., Bowen T., Steadman R., Phillips A.
Age-related changes in pericellular hyaluronan organization leads to impaired dermal fibroblast to myofibroblast differentiation. The American Journal of Pathology. 2009; 175: 1915-1928, doi: 10.2353/ajpath.2009.090045

Sindrilaru A., Scharffetter-Kochanek K. *Disclosure of the Culprits: Macrophages-Versatile Regulators of Wound Healing*. Advances Wound Care (New Rochelle). 2013; 2: 357-368, doi: 10.1089/wound.2012.0407

Slauch J.M. *How does the oxidative burst of macrophages kill bacteria? Still an open question.* Molecular Microbiology. 2011; 80: 580-583, doi: 10.1111/j.1365-2958.2011.07612.x

Smith M.M., Melrose J*. Proteoglycans in normal and healing skin*. Advances in Wound Care (New Rochelle). 2015; 4: 152–173, doi: 10.1089/wound.2013.0464

Sorrentino S., Studt D., Medalia O., Sapra T. *Roll, adhere, spread and contract: Structural mechanics of platelet function*. European Journal of Cell Biology. 2015; 94: 129-138, doi: 10.1016/j.ejcb.2015.01.001.

Strecker-McGraw M., Jones T., Baer D. *Soft tissue wounds and principles of healing*. Emergency Medicine Clinics of North America Journal. 2007; 25: 1-22, doi: 10.1016/j.emc.2006.12.002

Stuart J.D., Morgan R.F., Kenney J.G. *Single donor fibrin glue for hand burns*. Annals of Plastic Surgery. 1990; 24: 524-527, doi: 10.1097/00000637-199006000-00009

Sun Y., Tong H., Chu X., Li Y., Zhang J., Ding Y., Zhang S., Gui X., Chen C., Xu M., Li Z., Gardiner E., Andrews R., Zeng L., Xu K., Qiao J. *Notch1 regulates hepatic thrombopoietin production.* Blood. 2024; 143: 2778-2790, doi: 10.1182/blood.2023023559

Tabib T., Morse C., Wang T., Chen W., Lafyatis R. *SFRP2/DPP4 and FMO1/LSP1 Define Major Fibroblast Populations in Human Skin*. Journal of Investigative Dermatology. 2018; 138: 802-810, doi: 10.1016/j.jid.2017.09.045

Tannenbaum J., Taylor Bennett B. *Russell and Burch's 3Rs Then and Now: The Need for Clarity in Definition and Purpose.* Journal of the American Association for Laboratory Animal Science. 2015; 54: 2, pp. 120–132

Tripoli M., Cordova A., Moschella F. *Update on the role of molecular factors and fibroblasts in the pathogenesis of Dupuytren's disease*. Journal of Cell Communication and Signaling. 2016; 10: 315–330, doi: 10.1007/s12079-016-0331-0

Tomasek J.J., Gabbiani G., Hinz B., Chaponnier C., Brown R.A. *Myofibroblasts and mechano-regulation of connective tissue remodelling.* Nature Reviews Molecular Cell Biology. 2002; 3: 349–363, doi: 10.1038/nrm809

Tomic-Canic M., Mamber S.W., Stojadinovic O., Lee B., Radoja N., McMichael J. *Streptolysin O enhances keratinocyte migration and proliferation and promotes skin organ culture wound healing in vitro.* Wound Repair and Regeneration. 2007; 15, 71‑79, doi: 10.1111/j.1524-475X.2006.00187.x

Ud-Din S., Bayat A. *Non-animal models of wound healing in cutaneous repair: in silico, in vitro, ex vivo, and in vivo models of wounds and scars in human skin*. Wound Repair and Regeneration. 2017; 25, 164-176, doi: 10.1111/wrr.12513

Ud-din S., Bayat A. *Non-invasive objective devices for monitoring the inflammatory, proliferative and remodelling phases of cutaneous wound healing and skin scarring*. Experimental Dermatology. 2016; 25: 579-285, doi: 10.1111/exd.13027

Usui M.L., Underwood R.A., Mansbridge J.N., Muffley L.A., Carter W.G., Olerud, J.E. *Morphological evidence for the role of suprabasal keratinocytes in wound reepithelialization.* Wound Repair and Regeneration. 2005; 13: 468-479, doi: 10.1111/j.1067-1927.2005.00067.x

Van der Veer W.M., Bloemen M.C., Ulrich M.M., Molema G., van Zuijlen P.P., Middelkoop E., Niessen F.B. *Potential cellular and molecular causes of hypertrophic scar formation.* Burns. 2009; 35: 15-29, doi: 10.1016/j.burns.2008.06.020

Visse R., Nagase H. *Matrix metalloproteinases and tissue inhibitors of metalloproteinases: structure, function, and biochemistry.* Circulation Research. 2003; 92: 827–839, doi: 10. 1161/01.RES.0000070112.80711.3D

Weibrich G., Wilfried K.G.K. *Curasan PRP kit vs PCCS PRP system: collection efficiency and platelet counts of two different methods for the preparation of platelet rich plasma.* Clinical Oral Implant Research. 2002; 13: 437-443, doi: 10.1034/j.1600-0501.2002.130413.x

Weibrich G., Wilfried K.G.K, Hafner G. *Growth factor leves in the Platelet-rich Plasma produced by 2 different methods: Curasan-type PRP kit versus PCCS PRP system*. The International Journal of Oral and Maxillofacial Implants. 2002; 17: 184-190

Weissman I. *Stem cells: units of development, units of regeneration, and units in evolution*. Cell. 2000; 100: 157-168, doi: 10.1016/s0092-8674(00)81692-x

Weller K., Foitzik K., Paus R., Syska W., Maurer M. *Mast cells are required for normal healing of skin wounds in mice.* Faseb Journal. 2006; 20: 2366-2368, doi: 10.1096/fj.06-5837fje

Wong V.W., Paterno J., Sorkin M., Glotzbach J.P., Levi K., Januszyk M., Rustad K.C., Longaker M.T., Gurtner G.C. *Mechanical force prolongs acute inflammation via T-cell-dependent pathways during scar formation*. Faseb Journal. 2011; 25: 4498-4510, doi: 10.1096/fj.10-178087

Xiong N., Raulet D.H. *Development and selection of gammadelta T cells*. Immunological Review. 2007; 215: 15-31, doi: 10.1111/j.1600-065X.2006.00478.x

Xu W., Hong S.J., Jia S., Zhao Y., Galiano R.D., Mustoe T.A. *Application of a partial-thickness human ex vivo skin culture model in cutaneous wound healing study*. Laboratory Investigation. 2012; 92, 584‑599, doi: 10.1038/labinvest.2011.184

Yanez D.A., Lacher R.K., Vidyarthi A., Colegio O.R. *The Role of Macrophages in Skin Homeostasis*. Pflugers Archiv: European Journal of Physiology. 2017; 469: 455-463, doi: 10.1007/s00424-017-1953-7

Younan G., Suber F., Xing W., Shi T., Kunori Y., Abrink M., Pejler G., Schlenner S.M., Rodewald H.R., Moore F.D., Stevens R., Adachi R., Austen K.F., Gurish M.F. *The*

inflammatory response after an epidermal burn depends on the activities of mouse mast cell proteases 4 and 5. The Journal of Immunology. 2010; 185: 7681-7690, doi: 10.4049/jimmunol.1002803

Zhang Y., Shang F., Liao D., Li X. *Clinical guidelines for the use of platelet-rich plasma (PRP) for osteoarthritis.* Bone and Arthrosurgery Science. 2025; 3: 1-13, doi: 10.26689/bas.v3i3.10496

Zhu J., Peng T., Johnston C., Phasouk K., Kask A.S., Klock A., Jin L., Diem K., Koelle D.M., Wald A., Robins H., Corey L. *Immune surveillance by CD8αα+ skin-resident T cells in human herpes virus infection*. Nature. 2013; 497: 494-497, doi: 10.1038/nature12110

Zhu Z., Ding J., Ma Z., Iwashina T., Tredget E. *Alternatively activated macrophages derived from THP-1 cells promote the fibrogenic activities of human dermal fibroblasts*. Wound Repair Regeneration. 2017; 25: 377-388, doi: 10.1111/wrr.12532

https://www.altex.org

https://www.centro3r.it

http://eur-lex.europa.eu

https://oncohemakey.com